Regional Velocity-Depth Anomalies, North Sea Chalk: A Record of Overpressure and Neogene Uplift and Erosion[1]

Peter Japsen[2]

ABSTRACT

A normal velocity-depth trend for the Upper Cretaceous–Danian Chalk Group is determined by identifying interval-velocity data that represent maximum burial in areas unaffected by overpressuring; these data are derived from 845 wells throughout the North Sea Basin. Data from pelagic carbonate deposits on a stable plateau constrain the trend for shallow depths. Positive velocity anomalies relative to the trend are mapped along the western and eastern margins of the North Sea Basin, and reflect regional Neogene uplift and erosion of up to 1 km along the present-day limit of the Chalk. A hiatus at the base of the Quaternary increases in magnitude away from the basin center, where a complete Cenozoic succession is found. This hiatus is consistent in size with the missing section estimated from Chalk velocities when allowance is made for the Quaternary reburial of the Chalk. Negative velocity anomalies in the central and southern parts of the basin outline an area within which overpressures in the Chalk exceed 10 MPa, equivalent to a burial anomaly greater than 1 km relative to the normal trend. The Chalk pressure system is primarily dependent on overburden properties because retention of overpressure generated by the load of the upper overburden depends on the thickness and sealing quality of the lower overburden; therefore, the Chalk is considered to represent a regional aquitard, and the hydrodynamic model of long-distance migration within the Chalk is rejected. The Neogene uplift and erosion of the margins of the North Sea Basin and the rapid, late Cenozoic subsidence of its center fit into a pattern of late Cenozoic vertical movements around the North Atlantic.

[1]Manuscript received June 20, 1996; revised manuscript received March 16, 1998; final acceptance April 15, 1998.

[2]Geological Survey of Denmark and Greenland (GEUS), Thoravej 8, DK-2400 Copenhagen NV, Denmark; e-mail: pj@geus.dk

This study was made possible through the generous support of the Carlsberg Foundation and GEUS. Petroleum Information (Erico) is thanked for giving me permission to use Chalk pressure data from its British and Norwegian pressure studies, and for placing the British and most of the Norwegian well velocity data at my disposal; without the backing of Peter Sheil and Stuart Thomas, both Petroleum Information (Erico), this study would not have been possible. Statoil is thanked for giving me access to well data. Christian Hermanrud, Erik Vik, and Lars Wensaas at the Statoil Research Center in Trondheim, Norway, helped me with many basic questions. The Geological Survey of the Netherlands is thanked for giving me access to pressure data. Per Knudsen, National Survey and Cadastre-Denmark, advised me on the kriging technique, and Ida Lind, Danish Technical University, took part in many considerations. I thank colleagues who have supported me in many ways, in particular Torben Bidstrup, Jim Chalmers, Anders Mathiesen, and Jens Jørgen Møller. Jens Clausen, Dopas; Finn Surlyk, University of Copenhagen; and Claus Andersen, Thomas Dons, Jon Ineson, Peter Konradi, and Birger Larsen, all GEUS, provided valuable comments on different parts of the manuscript. Finally, editors and journal referees are thanked for their penetrative and constructive reviews.

TABLE OF CONTENTS

INTRODUCTION

The Upper Cretaceous–Danian Chalk Group forms a coherent body in the North Sea region covering more than 500,000 km^2, with an average thickness of about 500 m (Figures 1, 2). Clastic influx into the North Sea Basin was low during the deposition of the Chalk, which is composed mainly of coccoliths, the debris of planktonic algae (Kennedy, 1987; Ziegler, 1990). Today, the Chalk crops out in most countries in northwest Europe, but is buried at depths greater

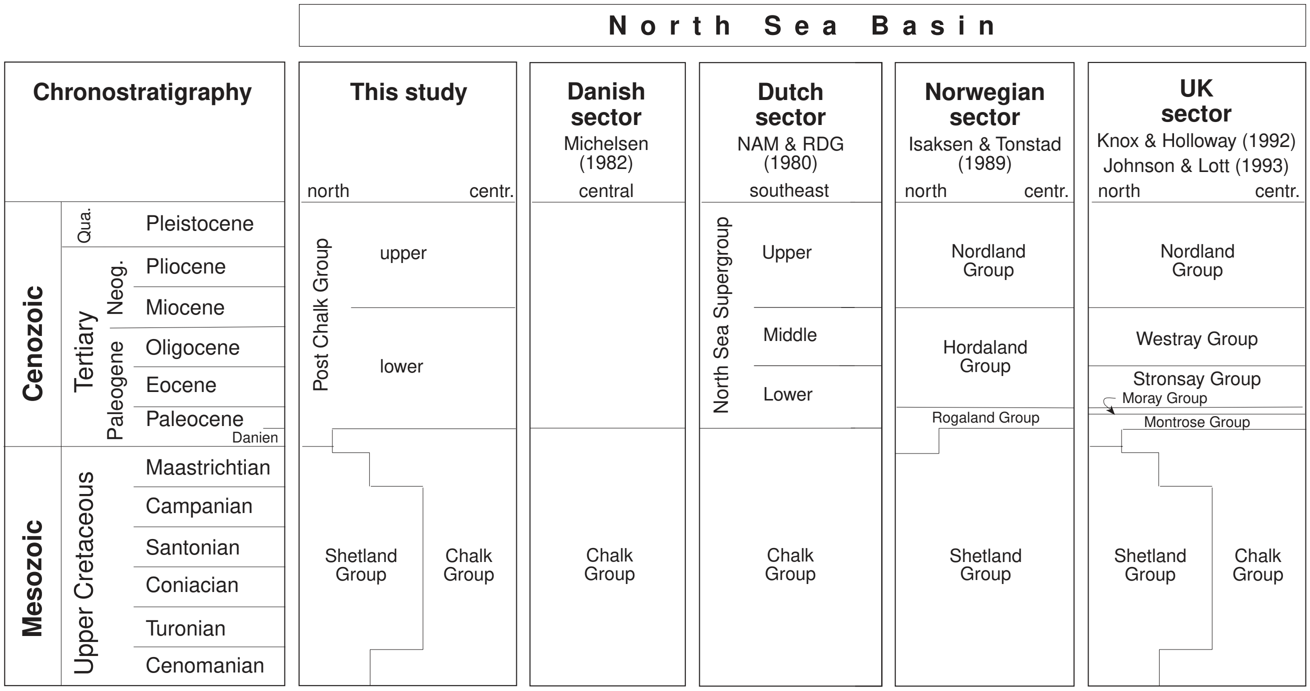

Figure 1—Lithostratigraphic nomenclature for the Upper Cretaceous–Cenozoic in the North Sea Basin. This study follows the nomenclature used in the Danish, Dutch, and United Kingdom sectors by using the term "Chalk Group" to refer to the chalky limestone facies as opposed to the mudstone facies of the Shetland Group (Johnson and Lott, 1993). The Post Chalk Group (Nielsen and Japsen, 1991) is subdivided into an upper and lower part at the mid-Miocene unconformity (Japsen, 1994).

than 3 km in the central North Sea (Figures 3, 4). The Cenozoic North Sea Basin gently bends from its margins to its depocenter, aligned over the mainly Late Jurassic Central and Viking grabens (Figure 2C). Nature thus provides a spectacular laboratory to study the effect of large depth variations on the compaction of the Chalk, and hence on velocity, which varies over a range of 3000 m/s.

The compaction of the Chalk does not everywhere correspond to its present burial depths (Scholle, 1977). Along the margins of the North Sea Basin, the thickness of the Chalk overburden has been reduced. The regional character of this exhumation was recognized only recently, and the magnitude (up to 1 km), timing, and causes of this exhumation are still disputed (e.g., Bulat and Stoker, 1987; Jensen et al., 1992; Japsen, 1993a, 1997; Hillis, 1995a; Rohrman and van der Beek, 1996). In the central North Sea, the Chalk is overpressured (up to 20 MPa at 2600 m depth), mainly due to rapid, late Cenozoic burial (Carstens, 1978; Japsen, 1994). Major commercial interests are related to the porosity of the Chalk because giant hydrocarbon accumulations are trapped in the Chalk in the Norwegian and Danish sectors of the central North Sea (e.g., the Ekofisk and Dan fields).

From the observation that the Chalk over large areas is far from normally compacted, I here present a new normal velocity-depth trend for the Chalk Group based on North Sea data constrained by data from pelagic carbonate deposits on a stable plateau (Shipboard Scientific Party, 1991; Urmos et al., 1993). Normal compaction curves for the Chalk have been suggested by previous workers (Scholle, 1977; Sclater and Christie, 1980; Bulat and Stoker, 1987; Hillis, 1995a). The trend presented here,

Figure 2—Late Cretaceous–Cenozoic geology of the North Sea Basin. The Chalk crops out along the basin margins, but is buried below more than 3000 m of Cenozoic cover in the center of the basin. (A) Isopach of the Post Chalk Group. (B) Isopach of the Chalk Group. (C) Late Cretaceous–Cenozoic structural elements. In (A and B), Edb. (Edinburgh) and Cph. (Copenhagen) mark the location of the depth profile on Figure 3. Modified after Ziegler (1990), with corrections from well data and Andrews et al. (1990), Britze et al. (1995a, b), Cameron et al. (1992), Day et al. (1981), Gatliff et al. (1994), Isaksen and Tonstad (1989), Japsen and Langtofte (1991), Johnson and Lott (1993), Knox and Holloway (1992), Kockel (1988a, b), and Ter-Borch (1990).

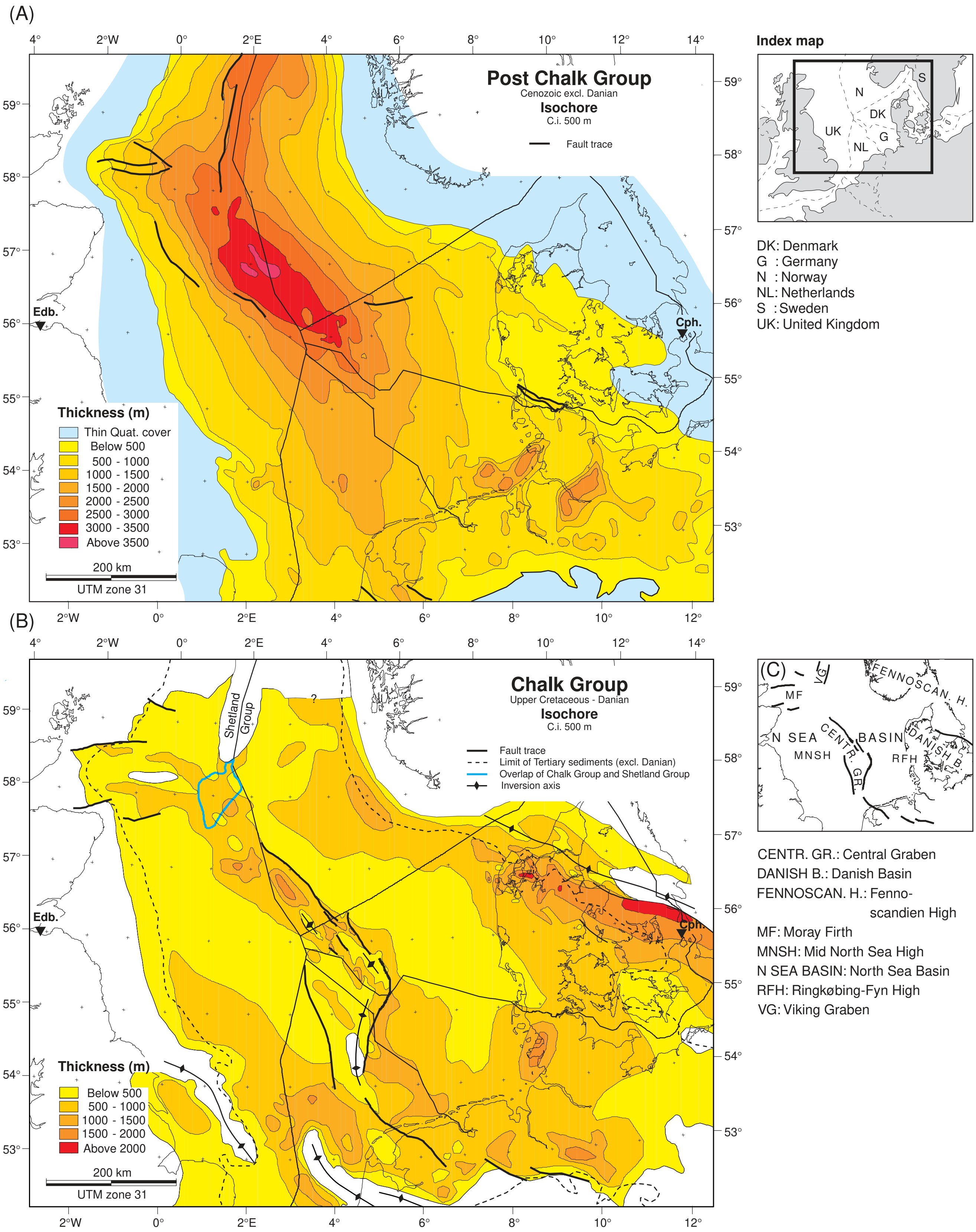
(A)
Index map
Post Chalk Group
Cenozoic excl. Danian
Isochore
C.i. 500 m
Fault trace
Thickness (m)
Thin Quat. cover
Below 500
500 - 1000
1000 - 1500
1500 - 2000
2000 - 2500
2500 - 3000
3000 - 3500
Above 3500
200 km
UTM zone 31
Edb.
Cph.
DK: Denmark
G : Germany
N : Norway
NL: Netherlands
S : Sweden
UK: United Kingdom
(B)
Chalk Group
Upper Cretaceous - Danian
Isochore
C.i. 500 m
Fault trace
Limit of Tertiary sediments (excl. Danian)
Overlap of Chalk Group and Shetland Group
Inversion axis
Shetland Group
Thickness (m)
Below 500
500 - 1000
1000 - 1500
1500 - 2000
Above 2000
200 km
UTM zone 31
(C)
MF
VG
FENNOSCAN. H.
N SEA
BASIN
MNSH
CENTR. GR.
RFH
DANISH B.
CENTR. GR.: Central Graben
DANISH B.: Danish Basin
FENNOSCAN. H.: Fennoscandien High
MF: Moray Firth
MNSH: Mid North Sea High
N SEA BASIN: North Sea Basin
RFH: Ringkøbing-Fyn High
VG: Viking Graben

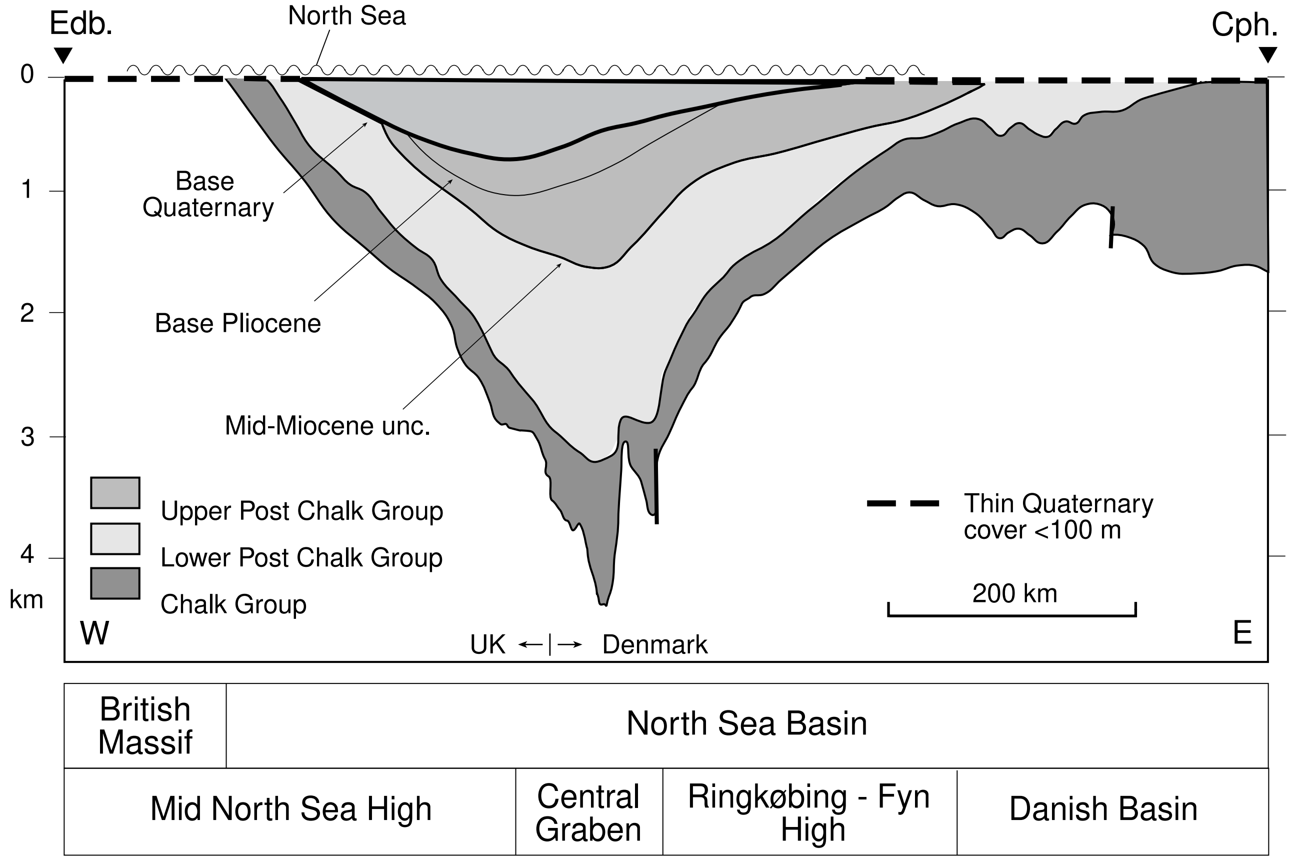

Figure 3—Burial of the Chalk Group across the North Sea with indication of both Mesozoic and Late Cretaceous–Cenozoic structural elements. Depths below sea bed (water depth <50 m). Location of profile from Edinburgh (Ed.b), UK, to Copenhagen (Cp.h), Denmark, is shown on Figure 2A and B. Modified after Ziegler (1990), with corrections from well data and Andrews et al. (1990), Britze et al. (1995a, b), Cameron et al. (1992), Day et al. (1981), Gatliff et al. (1994), Isaksen and Tonstad (1989), Japsen and Langtofte (1991), Johnson and Lott (1993), Knox and Holloway (1992), Kockel (1988a, b), Ter-Borch (1990), and Caston (1977).

however, is the first that is derived from data covering the full depth range and from the full lateral extent of the Chalk. If overpressure and regional erosion are not taken into account, the increase of velocity with depth is underestimated, resulting in erroneous depth conversions. The trend is expressed as four linear segments because a single mathematical function fails to reflect the depth variations in the compaction process.

I interpret velocity anomalies relative to the normal trend (Japsen, 1993a) to be related on a regional scale to the burial history of the Chalk (Japsen, 1993b). Consequently, I introduce the corresponding concept of burial anomaly relative to a normal velocity-depth trend. Estimates of maximum burial based on Chalk velocity anomalies are comparable to estimates based on other methods; furthermore, North Sea pressure data confirm the level of overpressure, as well as the areal extent of the overpressured zone, predicted from Chalk velocities in the central and southern North Sea. Estimates of maximum burial and overpressure frequently have been based on shale data, due to the uniformity of shale over large distances (e.g., Herring, 1973; Carstens, 1978; Magara, 1978; Chiarelli and Duffaud, 1980; Hansen, 1996). The exhumation of the North Sea Basin also has been estimated from Chalk data because the Chalk is widespread and relatively homogeneous (Bulat and Stoker, 1987; Hillis et al., 1994; Hillis, 1995a). Estimates of overpressure based on Chalk data have not previously been presented.

VELOCITY ANOMALY AND BURIAL ANOMALY

The normal velocity-depth trend, $V_N(z)$, for a sedimentary rock expresses the increase of velocity as porosity is reduced during normal compaction, where pore pressure is hydrostatic and the burial

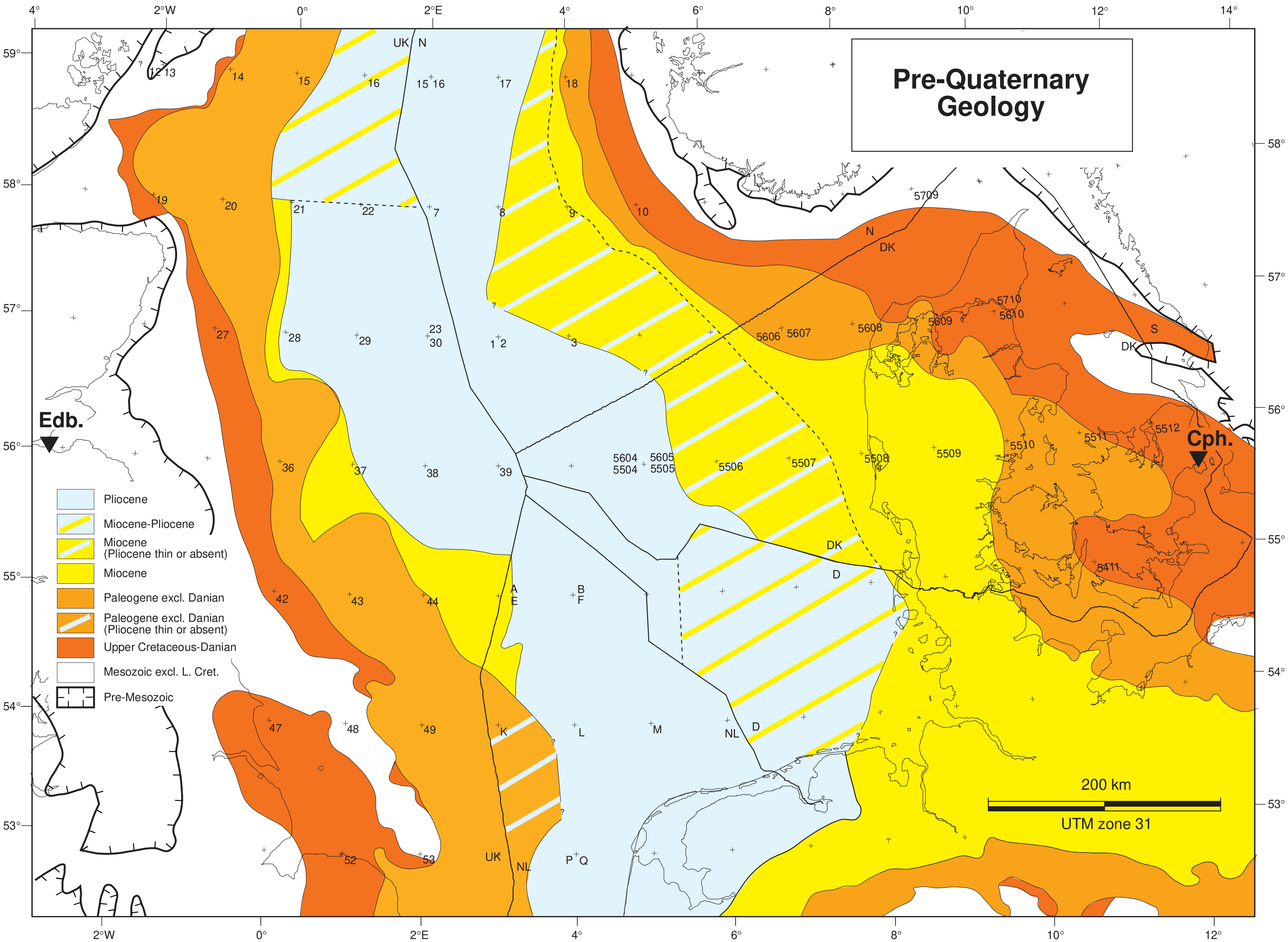

Figure 4—Pre-Quaternary geology of the North Sea Basin. Note the symmetry across the basin. Based on Andrews et al. (1990), Bidstrup (1994), Cameron et al. (1987, (1992), Choubert and Faure-Murat (1976), Gatliff et al. (1994), Håkansson and Pedersen (1992), Johnson et al. (1993), Jordt et al. (1995), Kreizer and Letsch (1963), Michelsen et al. (1996), Sigmond (1993), Sørensen and Michelsen (1995), Vinken et al. (1988), Zagwijn (1989), and Ziegler (1990).

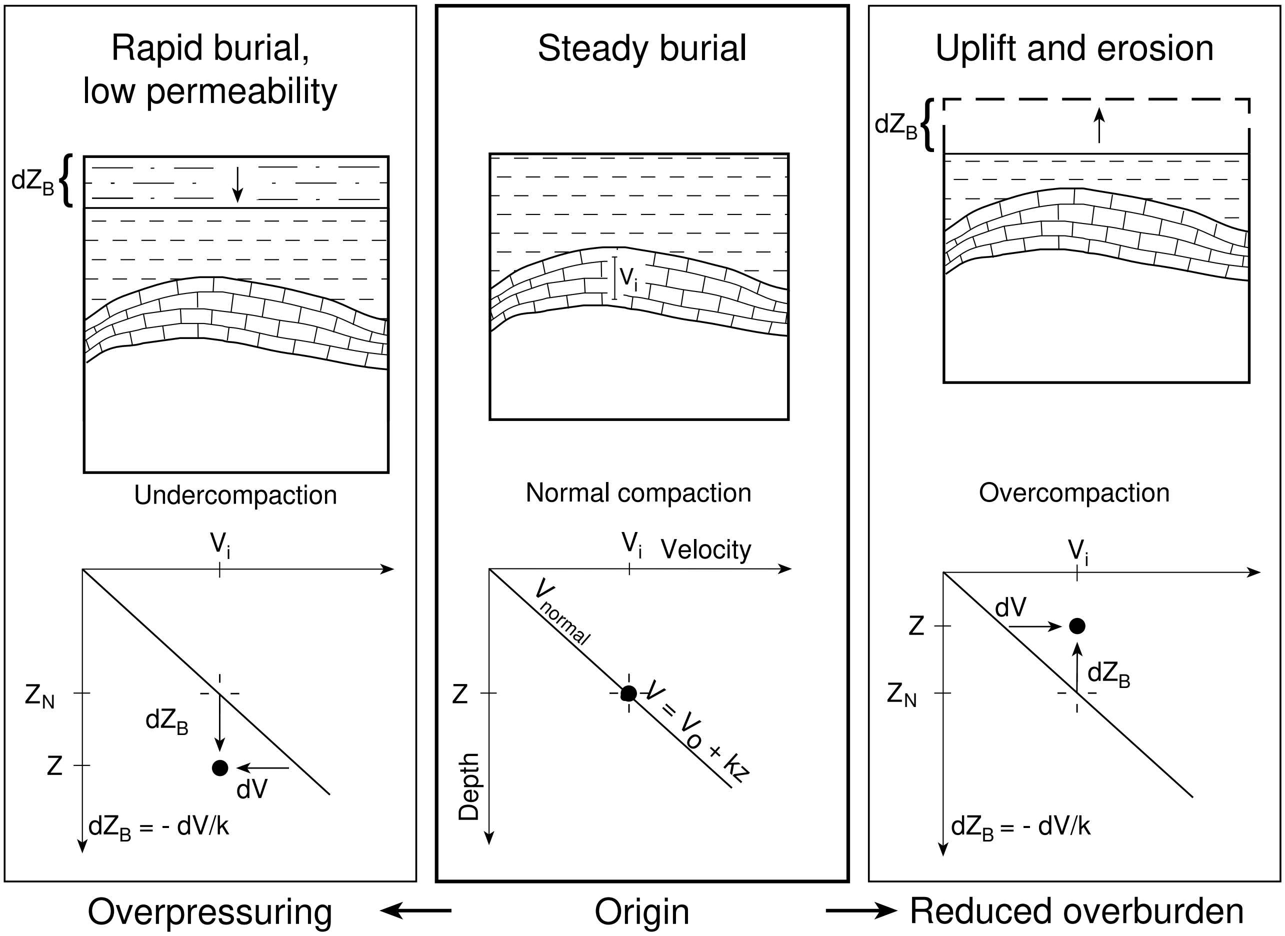

Figure 5—Velocity anomaly (dV) and burial anomaly (dZ_B) as expression of reduced burial and undercompaction due to overpressure (equations 1, 2). Retarded compaction due to rapid burial and low permeability causes overpressure, and hence velocities low relative to depth (negative dV and positive dZ_B) (equation 5). Uplift and erosion may reduce the overburden and cause overcompaction expressed as velocities that are high relative to depth (positive dV and negative dZ_B). The normalized depth, z_N, is the depth corresponding to normal compaction as predicted by the normal velocity-depth trend for the measured velocity.

depth of the rock is not reduced {V = the instantaneous velocity [in meters/second (m/s)] measured over a thin unit at depth z [in meters (m)]; see list of symbols in Appendix 1}. The velocity trend should be constrained by knowledge about the velocity of the rock at the surface and at infinite depth. Let V_N be given by a linear approximation,

$$V_N = V_0 + k \times z$$

where V_0 = the velocity at the surface and k = the velocity-depth gradient [in meters/second/meters (m/s/m)]. Based on this approximation, an expression can be developed for the interval velocity, V_i, measured over a layer of thickness Δz (in meters) and two-way traveltime thickness ΔT [in seconds (s)] (Slotnick, 1936; Japsen, 1993a). The velocity anomaly, dV (m/s), has been defined as a correction to the linear velocity model to calibrate the model to well data (Japsen, 1993a):

$$dV = k\Delta z(e^{k\Delta T/2} - 1)^{-1} - V_0 - kz_t \qquad (1)$$

where Δz, ΔT, and depth to the top of layer, z_t, are well data. Lateral variations of dV are the combined expression of lateral variation in V_0 and k caused by differences in both lithology and pore fluids, and in the burial history of the rock (Figure 5) (Japsen, 1993a, 1994). A velocity-depth model given by linear segments must be defined for intervals of V rather than z because velocity is the irreversible parameter. The velocity anomaly for a segmented model may be approximated by calculating dV relative to the segment given for the actual interval velocity.

The burial anomaly, dZ_B (m), is introduced here as the difference between the present burial of the rock, z, and the normalized depth, z_N, corresponding to normal compaction as predicted by the normal velocity-depth trend for the measured velocity (Figure 5). The velocity-depth gradient, k, expresses the relation between depth and velocity along the linear trend; consequently we get

$$dZ_B = - dV/k \qquad (2)$$

where the minus indicates that a positive velocity anomaly corresponds to a reduction in depth. The term "burial anomaly" is neutral as to what caused the anomaly, and indicates only that the depth of the rock is anomalous relative to a reference trend. Burial anomaly, as well as velocity anomaly, is zero for a normally compacted rock; that is, a rock at maximum burial and hydrostatic pore pressure.

Negative Burial Anomaly Due to Overburden Reduction

A negative burial anomaly may indicate overcompaction due to a reduction in burial depth but, as pointed out by Bulat and Stoker (1987), factors other than burial influence velocity. The term "uplift" [apparent uplift of Bulat and Stoker (1987) or net uplift of Riis and Jensen (1992)] is not used here, as uplift of rocks (relative to the geoid) must be distinguished from exhumation of rocks (relative to the Earth's surface) (England and Molnar, 1990). A geological formation can be considered exhumed only when it has been returned to the surface, not when the overburden has been partially removed; consequently, the term "apparent exhumation" (Hillis, 1995a) is inappropriate (compare Japsen, 1997). The quantity estimated in exhumation studies is thus the reduction in overburden thickness, or the burial anomaly, for a formation. Overburden reduction may be estimated by physical methods based on measurements of velocity, density, vitrinite reflectance, or fission tracks, or by inference from known geology in adjacent areas. All methods require comparison with some absolute standard, which is particularly difficult to establish in the method based on known geology. To infer actual exhumation from velocity data, the geological unit in question should be of relative homogeneous lithology, and should be geographically widespread to determine where normal compaction is present. If a lithologically homogeneous unit is thick and known from many wells, statistical uncertainties are reduced.

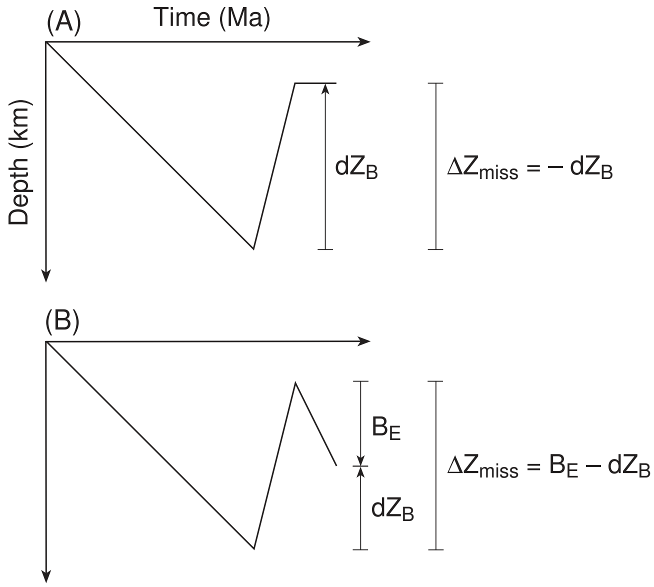

Figure 6—Schematic burial diagrams illustrating that the magnitude of the missing overburden section (Dz_{miss}) will be less than the magnitude of the measured burial anomaly (dZ_B) in the case of post-exhumational burial (B_E) (equation 3). (A) Exhumation followed by no deposition; (B) exhumation followed by burial.

The missing overburden section, Δz_{miss}, removed by erosion only equals the magnitude of the burial anomaly if no burial took place subsequent to exhumation (Figure 6A). Any post-exhumational burial, B_E, will mask the magnitude of the missing section, and we get (Figure 6B) (Hillis, 1995a)

$$\Delta z_{miss} = - dZ_B + B_E \qquad (3)$$

Consequently, a pre-Quaternary erosion of 500 m will be masked by a subsequent Quaternary burial of 500 m. Equation 3 implies that only when the timing of the exhumation is known do we know B_E and are able to infer Δz_{miss}. The timing thus becomes a critical aspect not only for understanding the succession of events, but also for understanding their true magnitude and for identifying the age of the eroded succession.

Positive Burial Anomaly Due to Overpressure

A positive burial anomaly may indicate undercompaction due to overpressure. Overpressure, ΔP [in Pascals (Pa)] (1 MPa = 145 psi), is the difference between the measured formation pressure, P, and the calculated hydrostatic pressure, P_H, at depth z:

$$\Delta P = P - P_H = P - \rho f \times g \times z$$

where ρ_f [in kilograms per cubic meter (kg/m^3)] is the mean pore fluid density of the overburden, and g is the gravitational acceleration (9.807 m/s^2). The lithostatic pressure, S (Pa), at depth z is the stress exerted by the weight of the overburden:

$$s = \rho_b \times g \times z$$

where ρ_b is the mean bulk density (wet). Terzaghi's principle states that the weight of the overburden per unit area, S, is borne partly by the rock matrix and partly by the pore fluid:

$$s = \sigma + P$$

where σ (Pa) is the effective stress that is transmitted through the matrix (Terzaghi and Peck, 1968).

Overpressure is generated by disequilibrium compaction when the weight of the overburden is increased by addition of sediments at the surface, and the pore fluid in the formation is sealed in the formation (Dickinson, 1953; Rubey and Hubbert, 1959; Osborne and Swarbrick, 1997). The rock is unable to compact because the pore fluid cannot escape at the same rate as load is added to the overburden of the rock. Consequently, the additional load is carried by pore fluids, and pressures higher than hydrostatic pressure result. The rock is said to be undercompacted because porosity becomes high relative to depth.

Let the overburden to an overpressured unit (e.g., the North Sea Chalk) be divided into a normally compacted upper unit and an overpressured lower unit, and let the burial rate accelerate during the deposition of the upper unit. The maximum overpressure generated by disequilibrium compaction thus may be approximated by the effective load, σ_{up}, of the upper unit that initiated the overpressure by rapid burial (compare Rubey and Hubbert, 1959):

$$\sigma_{up} = \Delta\rho_{up} \times g \times \Delta z_{up} \quad (4)$$

where $\Delta\rho_{up}$ is the density contrast (wet bulk density minus pore fluid density) in the upper part of the overburden, and Δz_{up} is its thickness. In the central North Sea, $\Delta\rho_{up}$ is slightly above 1×10^3 kg/m^3, so $\sigma_{up} \approx \Delta z_{up}/100$ MPa when Δz_{up} is in meters, meaning that deposition of 1000 m of sediment may generate an overpressure of 10 MPa.

The overpressure of an undercompacted rock, ΔP_{comp}, is proportional to the burial anomaly, dZ_B, if the effective stress is increasing with time (compare Hubbert and Rubey, 1959; Magara, 1978):

$$\Delta P_{comp} = \Delta\rho_{up} \times g \times dZ_B \quad (5)$$

Equation 5 is based on Terzaghi's principle and states that if a rock is shifted to a greater depth by dZ_B without change in the effective stress (indicated by unchanged velocity), the effective stress of the added load is carried by an increase in pore pressure (Figure 5). We get $\Delta P_{comp} \approx dZ_B/100$ MPa if we substitute $\Delta\rho_{up} = 1 \times 10^3$ kg/m^3, and dZ_B is in meters. This means that a burial anomaly of 1000 m reflects overpressure due to undercompaction of 10 MPa.

The effective stress, however, may be reduced with time even during continuous sedimentation. Such unloading may take place if overpressure increases due to transference (redistribution of overpressure) or by buoyancy when brine is substituted by hydrocarbons. Unloading leads to a higher overpressure, ΔP, than the paleo-overpressure, ΔP_{comp}, that prevailed at the time when the effective stress was at maximum. As compaction is largely irreversible, the burial anomaly reflects the paleo-overpressure and not the actual overpressure after unloading.

Net Drainage Capacity

If a rock were completely sealed off when overpressure was induced by rapid burial, the pore fluid of the rock would carry the effective stress of the weight added:

$$\Delta P_{comp} = \sigma_{up}$$

Thus, from equations 4 and 5 we get $\Delta z_{up} = dZ_B$, meaning that the burial anomaly equals the thickness of the load added since the onset of overpressure. The burial anomaly thus is generally a fraction of Δz_{up} depending on the efficiency of the rock to dewater. The net drainage capacity, DC (%), is thus introduced as

$$DC = (1 - dZ_B/\Delta z_{up}) \times 100 \quad (6)$$

The net drainage capacity expresses how close the rock is to compaction equilibrium relative to the rapid, late loading, Δz_{up}. If no drainage, and consequently no compaction, has taken place, $dZ_B = \Delta z_{up}$, and the drainage capacity for the rock is 0%. If the rock is normally compacted, $dZ_B = 0$, and

DC becomes 100%. The drainage capacity does, however, only account for the net drainage if pore fluid is added to the rock from above or below.

The drainage capacity, *DC* (equation 6), depends on the maximum effective stress exerted on the rock and not on the present overpressure. A drainage capacity relative to overpressure, $DC_{\Delta P}$, can be calculated by substituting the burial anomaly, dZ_B, in equation 6 by $\Delta P \times 100$ (ΔP in MPa):

$$DC_{\Delta P} = (1 - 100\Delta P/\Delta z_{up}) \times 100 \quad (7)$$

Because ΔP_{comp} (equation 5) is only part of the total overpressure, we get $DC_{\Delta P} \leq DC$.

DATABASE

Chalk Velocity Data

The database for this study contains interval velocities for the Chalk Group measured in 845 wells that penetrated the Chalk in the British (UK), Danish (DK), Dutch (NL), and Norwegian (N) sectors of the North Sea Basin (Figures 7, 8). Interval velocity is calculated by dividing the thickness of the Chalk by the corresponding transit time determined from calibrated sonic logs. In the Viking Graben, the mudstone facies of the Upper Cretaceous Shetland Group substitutes for the chalky limestone facies of the Chalk Group, whereas the two facies overlap south of the Viking Graben (Johnson and Lott, 1993) (Figures 1, 2B). The range of the depth and velocity data for the Chalk is considerable: The depth to the top of the Chalk ranges from sea level to 3350 m below the sea bed; the Chalk thickness ranges from 50 to 1850 m with a mean of 520 m; and the Chalk interval velocity ranges from 2290 to 5350 m/s (Tables 1, 2).

All logs and reports for Danish wells were available for this study [see Nielsen and Japsen (1991) for a detailed lithostratigraphic subdivision of most of these wells]. The only data available about the Chalk for the remaining wells were time and depth readings to top and base of the Chalk, water depths, and coordinates. The quality of these data thus could be checked only by comparing results from neighboring wells, making the results from isolated wells critical. Eleven wells were considered to have erroneous data and were excluded from the database. Sixty-six wells with thin Chalk sections also were excluded ($\Delta z < 50$ m or $\Delta T < 25$ ms) because the uncertainty on the interval velocity and the velocity anomaly is considerable for a thin unit. Wells drilled on or near salt diapirs are included in the database, however, to emphasize regional trends; data points from recognized diapirs are omitted from the maps. Identification of all errors and diapirs is less important to regional mapping of velocity anomalies and burial anomalies because the ordinary kriging procedure applied in the contouring (see following paragraphs) produces a result with less variance than the data (Figures 8, 9, 10B).

Data from the North Sea Chalk is compared to data obtained from ODP Leg 130, Site 807, on the Ontong Java Plateau (western Pacific Ocean, near the equator) (Shipboard Scientific Party, 1991; Urmos et al., 1993). An almost continuous sequence of pelagic carbonates of Albian–Aptian to Pleistocene age was drilled over 1380 m. The sonic log becomes noisy for depths greater than 980 m below the sea bed, and is only used here above that depth (Figure 11) (Urmos et al., 1993).

Chalk Pressure Data

Chalk formation pressures are available for the study from 126 locations from producing Chalk fields and wells in the British, Danish, Dutch, and Norwegian sectors in the North Sea (Figures 10A, 12; Table 3). The pressure evaluations are based on drill-stem and repeat-formation tests, and are generally from the uppermost part of the Chalk. A few test results indicating high pressure near the base of the Chalk probably are related to the Jurassic–Lower Cretaceous pressure regimes in the Central Graben and are not included in the study. Mud weights are used to give an upper limit for the overpressure where overpressure is below 5 MPa; however, in Dutch waters one formation test for the Chalk is available and, consequently, mud weights are used to outline the area where the overpressure is 5–10 MPa.

Chalk burial anomalies are assigned to nine Norwegian Chalk fields for which pressure was estimated by Caillet et al. (1997), and velocity is known for a well in the field. Corresponding values of formation pressure and interval velocity for the Chalk are thus known in 68 cases. In wells where the depth to the middle Miocene unconformity (called the top overpressure) was not available, a value was determined from a map, because the topography of the unconformity is gentle apart from over some diapirs.

Overburden Densities

Densities are rarely logged in the upper Post Chalk Group in the central North Sea (Figure 1). The mean density of the upper Post Chalk Group is estimated to be 2.05×10^3 kg/m^3, based on a density log

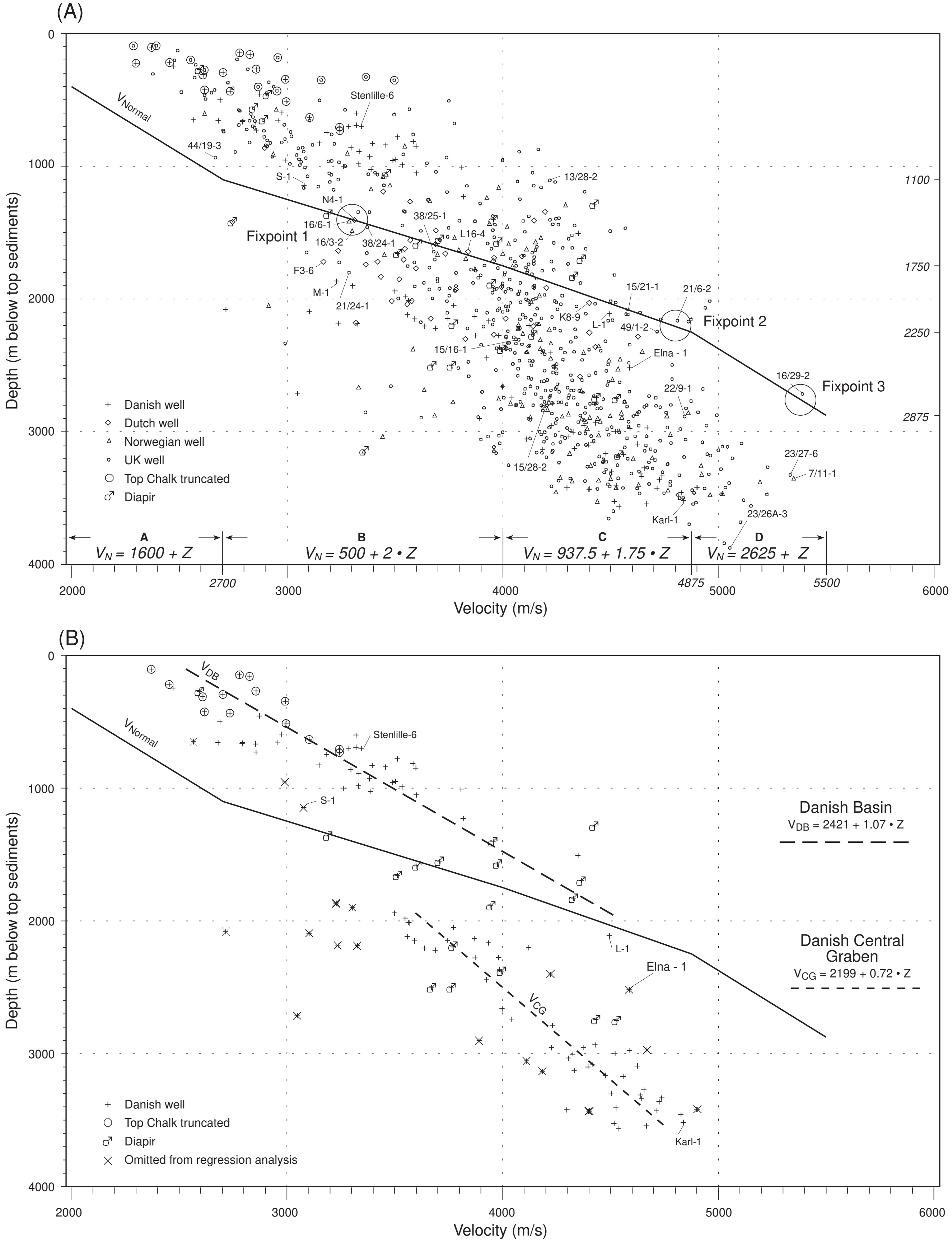

(A)
Depth (m below top sediments)
Velocity (m/s)
0
1000
2000
3000
4000
2000
2700
3000
4000
4875
5000
5500
6000
1100
1750
2250
2875
VNormal
Fixpoint 1
Fixpoint 2
Fixpoint 3
44/19-3
S-1
N4-1
16/6-1
16/3-2
38/24-1
38/25-1
L16-4
F3-6
M-1
21/24-1
Stenlille-6
13/28-2
15/21-1
21/6-2
K8-9
L-1
49/1-2
15/16-1
Elna - 1
16/29-2
22/9-1
15/28-2
23/27-6
7/11-1
Karl-1
23/26A-3
Danish well
Dutch well
Norwegian well
UK well
Top Chalk truncated
Diapir
A
B
C
D
VN = 1600 + Z
VN = 500 + 2 • Z
VN = 937.5 + 1.75 • Z
VN = 2625 + Z
(B)
Depth (m below top sediments)
Velocity (m/s)
0
1000
2000
3000
4000
2000
3000
4000
5000
6000
VDB
VNormal
VCG
Stenlille-6
S-1
L-1
Elna - 1
Karl-1
Danish Basin
VDB = 2421 + 1.07 • Z
Danish Central Graben
VCG = 2199 + 0.72 • Z
Danish well
Top Chalk truncated
Diapir
Omitted from regression analysis

from 50 to 1200 m below the sea bed in the M-10 well, quadrant DK 5505 (Foged et al., 1995). The mean bulk density of the lower Post Chalk Group is taken to be 2.11×10^3 kg/m^3, the mean density calculated for the Post Chalk Group below 1300 m based on 43 density (Formation Density Compensated™) logs in the area (Knudsen, 1993). The mean bulk density for the Post Chalk Group thus becomes 2.08×10^3 kg/m^3, assuming the thicknesses of the upper and lower Post Chalk Group to be 1200 and 1300 m, respectively (Japsen, 1994).

Pore fluid density, ρ_f, equals 1.02×10^3 kg/m^3 at depth in the Viking Graben (Chiarelli and Duffaud, 1980). This value is also applied to this study due to the similar evolution of the Viking Graben and Central Graben areas during the Cenozoic, and is supported by the trend of pressures vs. depth for normally compacted Chalk (Figure 12). The mean density contrast (difference between bulk density and pore fluid density) for the upper part of the overburden, $\Delta\rho_{up}$, thus equals 1.03×10^3 kg/m^3 for the upper Post Chalk Group.

Pre-Quaternary Geology

The pre-Quaternary geology is well known in areas where Mesozoic and older rocks subcrop the Quaternary, because these areas are mainly onshore (Figure 4) (Ziegler, 1990). The Tertiary geology, however, appears to be less well known for the younger sediments (Vinken et al., 1988) because the Neogene depocenter is situated offshore and is divided by the five national sectors. The Neogene depocenter, furthermore, is of little direct commercial interest. My mapping of the transnational pre-Quaternary geology is based on publications from the national sectors of the North Sea: the British sector (Andrews et al., 1990; Cameron et al., 1992; Johnson et al., 1993; Gatliff et al., 1994), the Dutch sector and parts of the German sector (Kreizer and Letsch, 1963; Choubert and Faure-Murat, 1976; Cameron et al., 1987; Zagwijn, 1989), the Danish sector and parts of the German sector (Håkansson and Pedersen, 1992; Bidstrup, 1994; Sørensen and Michelsen, 1995; Michelsen et al., 1996), and the Norwegian sector (Sigmond, 1993; Jordt et al., 1995). In the Dutch part of the mapped area, thin Pliocene deposits extend far southward (Choubert and Faure-Murat, 1976; Cameron et al., 1987; Zagwijn, 1989). The Miocene, or its upper part, is missing in Dutch offshore and onshore areas below the Pliocene–Pleistocene cover (Kreizer and Letsch, 1963; Cameron et al., 1987).

In the North Sea Basin, the base of the Pleistocene generally is placed at approximately 2.4 Ma, at the first indication of cold climate (Zagwijn, 1989; Cameron et al., 1993). This practice is followed likewise by the British and Dutch geological surveys (Gatliff et al., 1994), even though the boundary is at 1.6 Ma, according to Haq et al. (1987).

DERIVATION OF THE NORMAL VELOCITY-DEPTH TREND

A normal velocity-depth trend for the Chalk, V_N, is derived here to describe how velocity of Chalk with average composition increases during normal compaction. The normal trend is defined qualitatively by identifying data that represent maximum burial in areas unaffected by overpressure, and by constraining the trend by likely values near the surface (Figure 7A). The curved path of the normal trend is expressed in linear segments because a single mathematical function fails to account for depth variations in the compaction process. To arrive at a smooth normal trend, the final choice of linear parameters is confined to a narrow interval, where round figures are preferred because the trend is only a model of the complex geological reality.

Segment A, $V < 2700$ m/s

For the shallow data points, the smaller velocities for a given depth are closest to normal compaction, whereas the higher velocities in general reflect increasing burial anomalies (Figure 7A). The principal question, however, is whether the North Sea Chalk at shallow depths anywhere is found at maximum burial. An envelope of minimum velocity for each depth can be traced from zero burial to a depth of around 1400 m. At this maximum depth, the present burial of the Chalk must be closest to maximum burial. Fixpoint 1 for

Figure 7—Interval velocity vs. midpoint depth for the Chalk Group, and the normal velocity-depth trend, V_N (equation 8; Table 2). Shallow data points reveal high velocities relative to V_N due to overburden reduction. Deeper data reveal low velocities relative to V_N due to undercompaction and overpressure. See text for discussion of derivation of fixpoints and the normal velocity-depth trend. (A) Plot of 845 wells in the North Sea Basin. A, B, C, and D (along bottom) indicate the four segments of V_N. (B) Plot of 135 Danish wells and two semiregional trends with low apparent velocity-depth gradients.

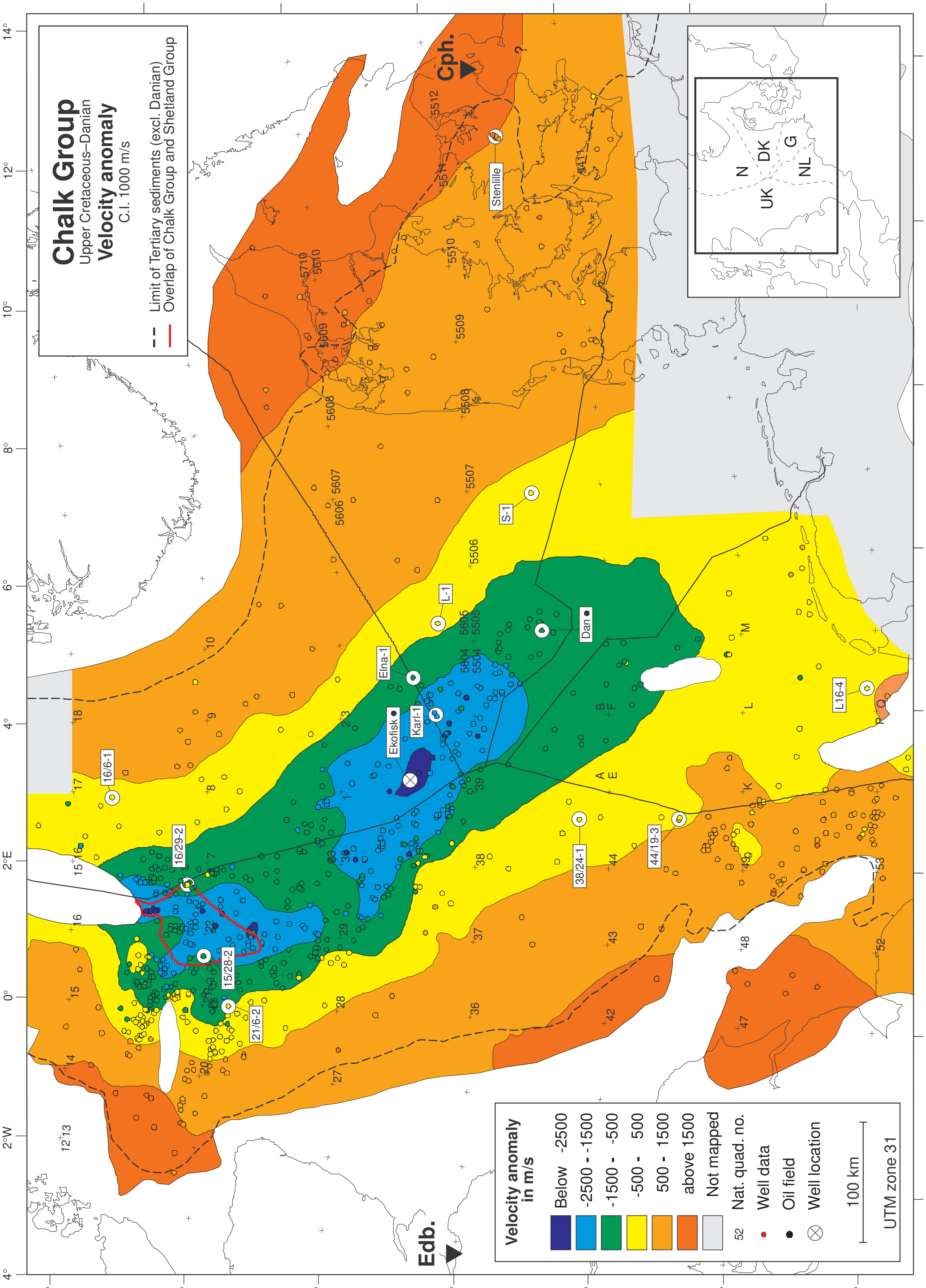

Figure 8—Velocity anomaly for the Chalk Group in the North Sea Basin relative to V_N (equations 1, 8; Table 2). Negative Chalk velocity anomalies in the central North Sea are caused by undercompaction due to overpressure. Positive anomalies along the basin margin indicate reduced burial of the Chalk. Contouring from kriged estimates. On inset, UK = United Kingdom, N = Norway, DK = Denmark, G = Germany, and NL = Holland.

Table 1. Statistics for the Well-Velocity Database*

Chalk Group Penetrated	No. Wells	V_i (m/s) mean	std.	min.	max.	z_t (m) min.	max.	z_b (m) max.	Δz (m) mean	max.	Sediment Top (m) min.	max.
Denmark	135	3708	678	2299	4903	2	3067	4139	572	1854	−73	72
Holland	41	3742	421	2746	4627	540	2360	3111	716	1651	7	51
Norway	104	4135	516	2618	5349	213	3129	4004	429	992	37	149
UK	565	4043	605	2288	5333	0	3347	4403	503	1142	16	169
All wells	845	4074	615	2288	5349	0	3347	4403	515	1854	−73	169

*See Appendix 1 for list of symbols. This table does not include 66 wells penetrating thin Chalk (Δz < 50 m or ΔT < 25 ms) and 11 wells with erroneous velocity data. Top of sediments indicates ground level/sea bed relative to mean sea level.

the normal trend is taken as the group of wells at 1400 m depth, where interval velocity is around 3300 m/s (all from areas of normally pressured Chalk). Below fixpoint 1, the first wells from areas affected by overpressure are indicated by a shift to smaller velocities.

Rather than extrapolating the diffuse data trend above fixpoint 1 to the surface, segment A of V_N is estimated as $V = 1600 + z$ based on sonic logs down to 980 m below the sea bed, obtained from pelagic carbonates, ODP Leg 130, Site 807 (Urmos et al., 1993) (Figure 11). Segment A is slightly below the data point for well UK 44/19-3, which thus places a tight upper limit on normal Chalk velocities for depths around 1 km, indicating a close agreement between normal compaction for chalk in the North Sea and those drilled at ODP Site 807.

Segment B, 2700 < *V* < 4000 m/s, and Segment C, 4000 < *V* < 4875 m/s

In the deep parts of the North Sea Basin, the Chalk is at maximum burial (except over diapirs) but frequently is overpressured. The overpressure causes porosity preservation (e.g., Scholle, 1977; D'Heur, 1986; Maliva and Dickson, 1992) and hence low velocities. For the deep data points, the higher velocities for a given depth are interpreted to represent normal compaction. The velocity level for normal compacted Chalk is thus defined by the clear trend of data points below 2000 m marking maximum velocities (4000–4900 m/s). Fixpoint 2 for the normal trend is taken to be 4800 m/s at a depth of 2200 m, and the velocity-depth gradient between fixpoints 1 and 2 becomes 1.9 m/s/m. The velocity gradient, however, is reduced with depth as the rock is compacted, and the velocity gradient is set to 2 m/s/m around 3300 m/s (fixpoint 1), and to 1.75 m/s/m for 4000 < V < 4875 m/s, as indicated by the data trend near fixpoint 2. Segment B becomes $V = 500 + 2 \times z$, which crosses segment A for V = 2700 m/s. Segment C becomes $V = 937.5 + 1.75 \times z$, which crosses segment B for V = 4000 m/s and passes close to fixpoint 2.

Segment D, 4875 < *V* < 5500 m/s

At great depth the upper velocity level is defined by a single well, UK 16/29-2. Fixpoint 3 is taken to be 5375 m/s at 2750 m, and Segment D becomes $V_N = 2625 + z$ (4875 < V < 5500) where the velocity-depth gradient is reduced to 1 m/s/m. Above this velocity interval there are no data to indicate a further approximation of Chalk velocity to the matrix velocity of calcite at 6400 m/s (Raiga-Clemenceau et al., 1988). The resulting burial anomaly for all wells, except one, with velocities above 5000 m/s indicates that these deeply buried high-velocity chalks are overpressured, which is the case in the central North Sea quadrants N 7, UK 23, and southernmost UK 22 where these wells are located.

The normal velocity-depth trend, V_N, for the Chalk Group gets the following form:

$$\begin{aligned} V_N &= 1600 + z && V < 2700 \text{ m/s} \\ V_N &= 500 + z \times 2 && 2700 \text{ m/s} < V < 4000 \text{ m/s} \\ V_N &= 937.5 + z \times 1.75 && 4000 \text{ m/s} < V < 4875 \text{ m/s} \\ V_N &= 2625 + z && 4875 \text{ m/s} < V < 5500 \text{ m/s} \end{aligned} \quad (8)$$

where z = depth below top of the sediments. The North Sea Chalk has mainly velocities corresponding to segments B and C, for which the fixpoints for the upper depth interval are defined by minimum velocities and maximum burial, and by maximum velocities and absence of overpressure for the deeper interval. The trace of segments B and C is well defined by velocity data from the North Sea Chalk, whereas the extrapolation along segment D

Table 2. Chalk Group Velocity Data from Selected Wells*

Well Name	Danish Quadrant No.	z_m (m)	V_i (m/s)	dV (m/s)	dZ_B (m)	Δz (m)
Denmark						
Adda 1	5504	2119	3558	−1175	588	197
Alma 1	5505	2202	4120	−658	376	445
Amalie 1	5604	3421	4899	−1131	1131	948
Arnum 1	5508	652	2957	1182	−591	509
Børglum 1**	5709	292	2704	1634	−817	354
C-1	5607	825	3150	1032	−516	554
Diamant 1	5603	3274	4655	−1989	1136	647
Elna 1	5604	2517	4587	−752	430	284
F-1	5706	951	3504	1135	−567	583
Farsø 1**	5609	731	3244	1481	−740	1395
Felicia 1**	5708	344	2992	1844	−922	597
Fjerritsl. 1**	5709	145	2780	2001	−1001	285
Fjerritsl. 2**	5709	157	2828	2024	−1012	287
Fred.h. 1**	5710	267	2856	1824	−912	127
Gassum 1**	5610	511	2996	1578	−789	972
Glamsbj. 1	5510	499	2689	604	−604	670
Haldag. 1**	5609	217	2455	644	−644	398
Hyllebj. 1**	5609	705	3243	1525	−762	1372
Ida 1	5606	1228	3818	877	−439	423
Inez 1	5606	1006	3808	1310	−655	417
J-1**	5708	103	2372	670	−670	134
Jelling 1	5509	591	2976	1348	−674	700
K-1	5707	746	3184	1248	−624	728
Karl 1	5604	3518	4837	−2190	1252	1125
Kvols 1	5609	990	3534	1261	−630	1488
L-1	5605	2110	4495	−131	75	301
Liva 1	5503	3297	4504	−2160	1234	883
M-1	5505	1866	3228	−994	497	289
Mejrup 1	5608	981	3332	949	−474	886
Mors 1	5608	815	3584	1624	−812	1357
Nøvling 1	5608	929	3384	1087	−543	785
Oddes. 1	5608	887	3333	1151	−576	955
Olaf 1	5603	3525	4516	−2505	1431	1228
Rødby 1	5411	244	2472	634	−634	430
Rødding 1	5608	861	3297	1219	−610	1200
Rønde 1	5610	1049	3600	1314	−657	1854
S-1	5606	1147	3078	299	−149	372
Skive 1	5609	827	3396	1392	−696	1245
Skive 2	5609	600	3321	1707	−853	920
Stenlille 1	5511	691	3321	1541	−770	1008
Stenlille 6	5511	699	3346	1559	−780	1062
Thisted 2**	5608	434	2736	1447	−724	803
Tønder 1	5408	657	2680	431	−431	480
Vemb 1	5608	1023	3389	896	−448	727
Voldum 1**	5610	632	3104	1499	−749	1220
Ørslev 1	5411	223	2299	483	−483	407
Års 1	5609	955	3491	1342	−671	1665
Holland						
A11-01		2585	4359	−1089	622	449
B13-02		1832	3434	−695	347	589
E16-01		1266	3571	574	−287	607
F02-01		1703	3540	−362	181	177
F03-06		1718	3169	−762	381	206
G17-01		1909	3993	−216	108	1146
K04-01		1679	4088	297	−169	1155
K08-09		2030	4401	42	−24	1505

Table 2. Continued.

Well Name	Danish Quadrant No.	z_m (m)	V_i (m/s)	dV (m/s)	dZ_B (m)	Δz (m)
L08-02		2363	4429	–514	294	1497
L16-04		1643	3840	288	–144	1651
M07-01		1715	3956	71	–35	726
N04-01		1405	3312	77	–38	861
P04-01		1482	3690	383	–192	1321
Q01-012		1343	4196	961	–549	919
Norway						
1/5-2		3344	4267	–2464	1408	992
2/1-1		3351	4500	–2278	1302	648
3/5-1†		2353	4444	–598	341	480
7/11-1†		3351	5349	–622	622	575
7/3-1†		1971	4170	–207	118	367
8/1-1†		1583	4027	325	–186	294
9/4-3†		1536	4177	578	–330	662
10/5-1		569	2950	1370	–685	711
11/10-1		1157	3981	1181	–590	410
15/6-3†		2866	4305	–1625	929	607
16/1-2†		2047	2914	–1678	839	51
16/3-2		1485	3302	–159	79	312
16/6-1		1413	3287	–19	10	429
17/4-1†		1171	3389	556	–278	283
18/10-1		907	2935	658	–329	568
25/8-1†		1753	4044	41	–23	91
United Kingdom						
12/29-1**†		92	2288	597	–597	143
13/14-1†		760	3585	1595	–798	570
13/28-2†		1118	4243	1368	–781	541
13/30-1†		1488	4498	975	–557	578
14/4-1†		933	3740	1379	–689	230
15/3-1†		1395	4246	869	–496	121
15/16-1†		2335	4061	–948	542	465
15/18B-4A†		2077	4254	–313	179	251
15/21-4		2077	4580	9	–5	151
15/28-2†		2783	4229	–1543	881	776
16/16B-1†		2222	4240	–585	334	53
16/29-2†		2713	5388	52	–52	229
19/4-1†		1145	4144	1227	–701	634
20/1-1†		1248	4080	975	–557	510
21/1-1†		2243	4024	–822	470	511
21/6-2†		2163	4810	93	–53	303
21/24-1†		1800	3288	–811	405	120
22/1-2A†		2775	4082	–1709	977	149
23/11-1†		2698	4587	–1068	610	250
23/26A-3RE†		3875	5053	–1429	1429	1056
23/27-6†		3325	5333	–613	613	488
27/3-1†		448	2906	1526	–763	369
28/5-1†		1763	3660	–364	182	97
29/2-1†		3146	4707	–1714	980	619
30/2-1†		3697	4864	–2487	1421	1036
31/21-1†		2959	4583	–1523	870	401
36/15-1†		910	3539	1245	–622	522
37/10-1†		1344	3330	151	–76	308
38/1-1†		1486	3621	153	–76	210
38/25-1†		1643	3680	–93	47	357
39/2-1†		2498	4133	–1170	669	279

Table 2. Continued.

Well Name	Danish Quadrant No.	z_m (m)	V_i (m/s)	dV (m/s)	dZ_B (m)	Δz (m)
42/13-1**†		351	3497	2340	−1170	675
43/12-2†		463	2618	564	−564	534
44/19-3†		935	2668	145	−145	611
44/7-1†		1075	3095	474	−237	503
47/3-1† ††		349	3158	2012	−1006	698
48/10-2†		977	3649	1257	−629	821
49/1-2†		2245	4716	−103	59	929
50/16-1†		1345	3382	319	−159	1133
52/5-3† ††		91	2394	704	−704	85
53/4-5†		732	2893	951	−476	444
54/1-2†		819	2826	696	−348	260
Cleethorpes 1**††		124	3768	1598	−1598	105

*First well in each quadrant (numerically or alphabetically); wells referenced in the text and in Japsen (1993b). See Appendix 1 for list of symbols.
**Quaternary deposits overlying Chalk Group.
†Data source Hillis (1995a); upper and middle Chalk.
††Data source Petroleum Information (Erico).

is based on limited data. Data from the North Sea along segment A are not identified in this study.

REDUCTION OF CHALK POROSITY WITH DEPTH

Exponential decay of Chalk porosity, ϕ_{SC}, with depth as suggested by Sclater and Christie (1980) provides a general description of the compaction process (equation 9 in Appendix 2). A comparison of ϕ_{SC} with V_N (equation 8) is made based on a tentative conversion of V_N from a velocity-depth trend to a porosity-depth trend by means of the velocity-porosity conversion for chalk given by equation 15 in Appendix 3. The normal compaction curve defined by V_N rather corresponds to a superposition of three different porosity-depth trends. In the upper kilometer, the porosity reduction estimated from V_N is slower than ϕ_{SC} (porosity is predicted to 42 and 35%, respectively, at a depth of 1000 m). Conversely, the porosity reduction estimated from V_N is faster than predicted by ϕ_{SC} in the interval from 1 to 2 km, and the two curves meet around a porosity of 15% at a depth of 2200 m. The porosity reduction predicted by the two curves is identical in the depth interval from 2200 to 2875 m. This pattern corresponds to the interpretation of the porosity reduction in carbonate deposits on the Ontong Java Plateau by Borre and Lind (in press). According to their interpretation, mechanical compaction is active from the surface down to a porosity around 20%, whereas cementation accelerates porosity reduction below about 1 km.

The steep increase of V_N below 1100 m matches the sharply increasing velocity measured on carbonate samples over the interval from about 1000 to 1300 m below the sea bed on the Ontong Java Plateau (Site 807) (Shipboard Scientific Party, 1991). This increase in velocity around a porosity of 40% is the combined effect of accelerated porosity reduction due to cementation and the stiffer grain contacts created by cementation of the particles (see Appendix 3). The onset of cementation below a depth of 1 km thus appears to take place for the North Sea Chalk as has previously been suggested (Davis, 1987; Taylor and Lapre, 1987); however, this depth is difficult to correlate between individual wells in the North Sea Basin because the Chalk in most wells is far from compaction equilibrium relative to the present depth. The correct depth scale for comparison of porosities and velocities is obtained only if present depths are corrected by the burial anomalies.

AREAS OF VELOCITY ANOMALY IN THE NORTH SEA BASIN

Chalk velocity anomalies calculated relative to V_N constitute geographically well-defined areas and reflect the burial history of the North Sea Basin during the Cenozoic (equations 1, 8; Table 2; Figure 8). The velocity-anomaly map in Figure 8 is contoured from kriged estimates based on a spherical model (nugget = 5000; sill = 75,000, range = 35 km; sill = 450,000, range = 400 km) and block kriging (4×4; grid increment = 10 km) (compare Hohn, 1988). The maps of Chalk burial anomalies are contoured

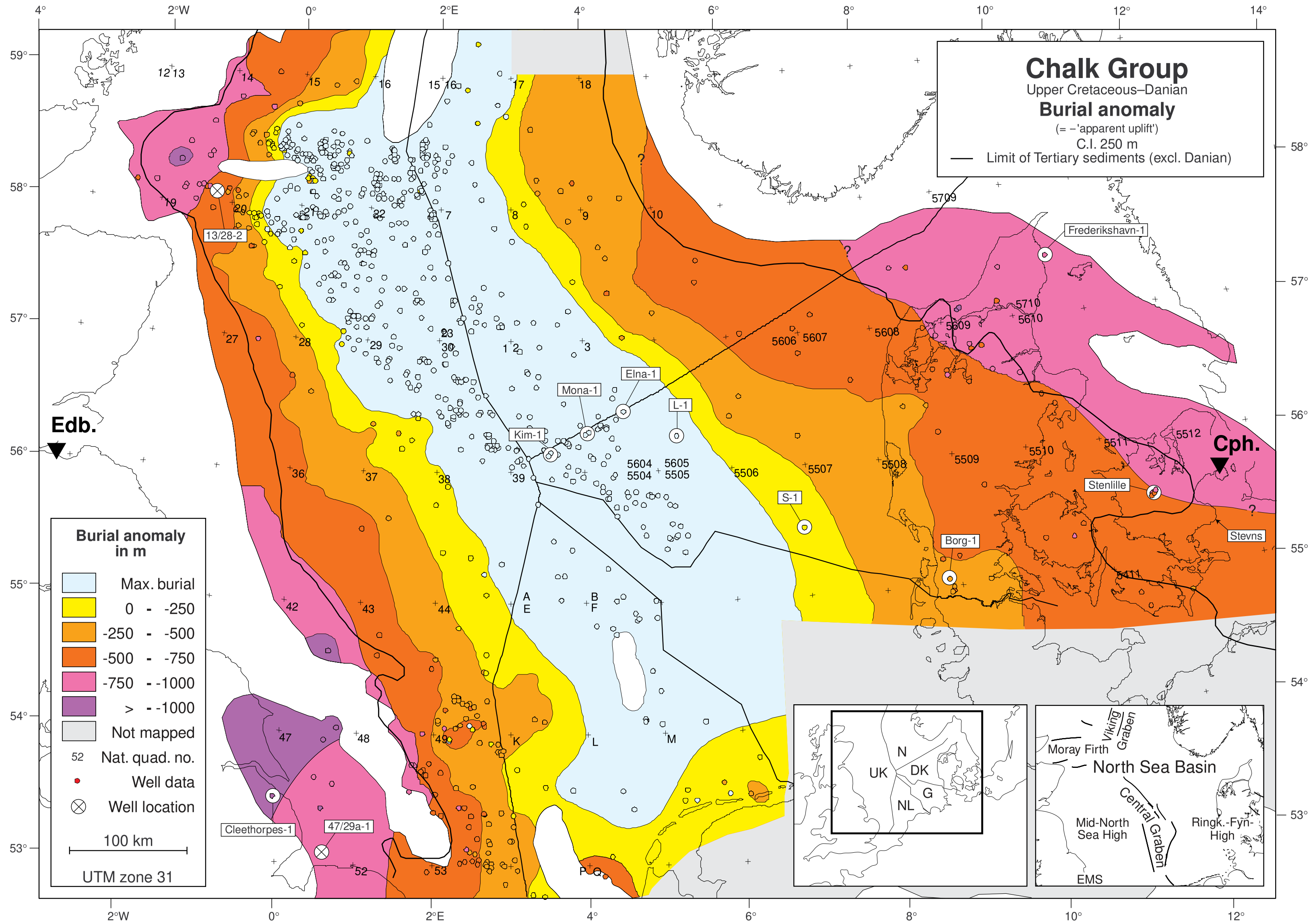

Figure 9—Chalk burial anomalies relative to the normal velocity-depth trend (equations 2, 8; Table 2). Overburden reduction increases away from the late Cenozoic depocenter in the central North Sea and reaches approximately 1 km along the present-day limit of the Chalk. The uniformity of this map with that of the pre-Quaternary (Figure 4) suggests that the Chalk burial anomaly is a measure of exhumation. The negative burial anomalies indicate a reduction in burial. Contouring from kriged estimates using the same kriging parameters as in Figure 8. EMS = East Midlands Shelf. On inset, UK = United Kingdom, N = Norway, DK = Denmark, G = Germany, and NL = Holland.

based on the same kriging parameters as the velocity anomaly map (equation 2; Table 2; Figures 8, 10).

Three main areas are delineated on the map of Chalk velocity anomalies (Figure 8).

(1) Positive velocity anomalies along the basin margin. The anomalies reflect Neogene erosion of the overburden; see also the corresponding map of negative burial anomalies (Figure 9) and the section of this paper on the Neogene exhumation of the North Sea Basin.

(2) Velocity anomalies near zero in an intermediate zone where the Chalk is normally compacted.

(3) Negative velocity anomalies in the central North Sea. The anomalies are a measure of the overpressure in the Chalk in the central and southern North Sea (equation 5), whereas to the north clastic content in the Chalk reduces velocity (see also the corresponding map of positive burial anomalies in Figure 10, and the section in this paper on overpressuring of the North Sea Chalk aquitard.)

These simple physical interpretations of the velocity anomalies, discussed in detail in the following section, provide evidence that the suggested normal velocity-depth trend reflects the physical properties for the Chalk Group.

NEOGENE EXHUMATION OF THE NORTH SEA BASIN

The present-day limit of the Chalk Group follows the trend of the British, Norwegian, and Swedish coasts (Figure 4) and outlines the North Sea Basin where Pliocene deposits are present in the basin center. The age of the pre-Quaternary rocks increases toward the coasts, and pre-Mesozoic rocks outcrop in Britain, Scandinavia, and central Europe. The symmetry in the pre-Quaternary subcrop pattern across the North Sea suggests a corresponding symmetry in the burial history across the area. The fundamental question is whether the pre-Quaternary hiatus represents a period of nondeposition or a period of deposition followed by erosion.

In recent years, regional Cenozoic exhumation of the North Sea Basin has been documented by sediment compaction studies. In the eastern North Sea Basin, exhumation was found to have happened during the Neogene/late Cenozoic (Jensen et al., 1992; Japsen, 1993a; Jensen and Schmidt, 1993; Michelsen and Nielsen, 1993; Hansen, 1996), whereas in the UK southern North Sea (Bulat and Stoker, 1987; Hillis, 1995a) and the Inner Moray Firth (Hillis et al., 1994; Thomson and Hillis, 1995) the timing beyond a Tertiary age was unclear because no direct information about the timing can be deduced from sediment compaction studies. The Tertiary age of the exhumation was based on the fact that several stratigraphic units, including the Chalk Group, had experienced similar magnitudes of exhumation (Bulat and Stoker, 1987; Hillis, 1995a). Bulat and Stoker (1987) found the exhumation of the southern North Sea to be of late Tertiary age, whereas Hillis (1995b) suggested that it could be associated with either regional Paleocene or Oligocene–Miocene unconformities. Hillis et al. (1994) found that the Chalk in the Inner Moray Firth had been at maximum burial before the deposition of the thick Paleocene succession encountered there today. Japsen (1997) suggested that Britain and the western North Sea suffered regional Neogene exhumation based on a compilation of exhumation studies from onshore and offshore Britain.

Recognition of the differential Cenozoic subsidence, sedimentation, and exhumation in the North Sea Basin is important for understanding its petroleum systems. The influence of exhumation of sedimentary basins on hydrocarbon prospectivity was discussed by Doré and Jensen (1996). They found that negative effects include spillage of hydrocarbons, the potential for seal failure, and cooling of source rocks, but suggested that these aspects have been overstated in the past, and that many of the world's petroleum provinces have been recently uplifted. An indirect, but important, positive effect of uplift and erosion was found to be redeposition of eroded material, thus contributing to the maturation of source rocks through increased burial; furthermore, mature source rocks at shallow levels, fracturing of tight reservoirs, and remigration of hydrocarbons to shallower reservoirs were found to be among the positive effects. Better paleogeographic constraints and understanding of burial history may be added as important aspects of recognizing exhumation of sedimentary basins.

Here it will be demonstrated that the map of Chalk burial anomalies relative to a normal velocity-depth trend is consistent with the map of the pre-Quaternary geology of the North Sea Basin, and the burial anomalies on a regional scale are measures of the erosion (equations 2, 8; Figures 4, 9). The exhumation was caused by uplift and erosion during the Neogene along both the western and eastern margins of the basin, symmetric relative to the basin axis, as is the age of the pre-Quaternary surface.

Magnitude of Exhumation Based on Chalk Burial Anomalies

Negative chalk burial anomalies are mapped in a broad zone along the present margin of Chalk deposits, whereas the Chalk is at maximum burial

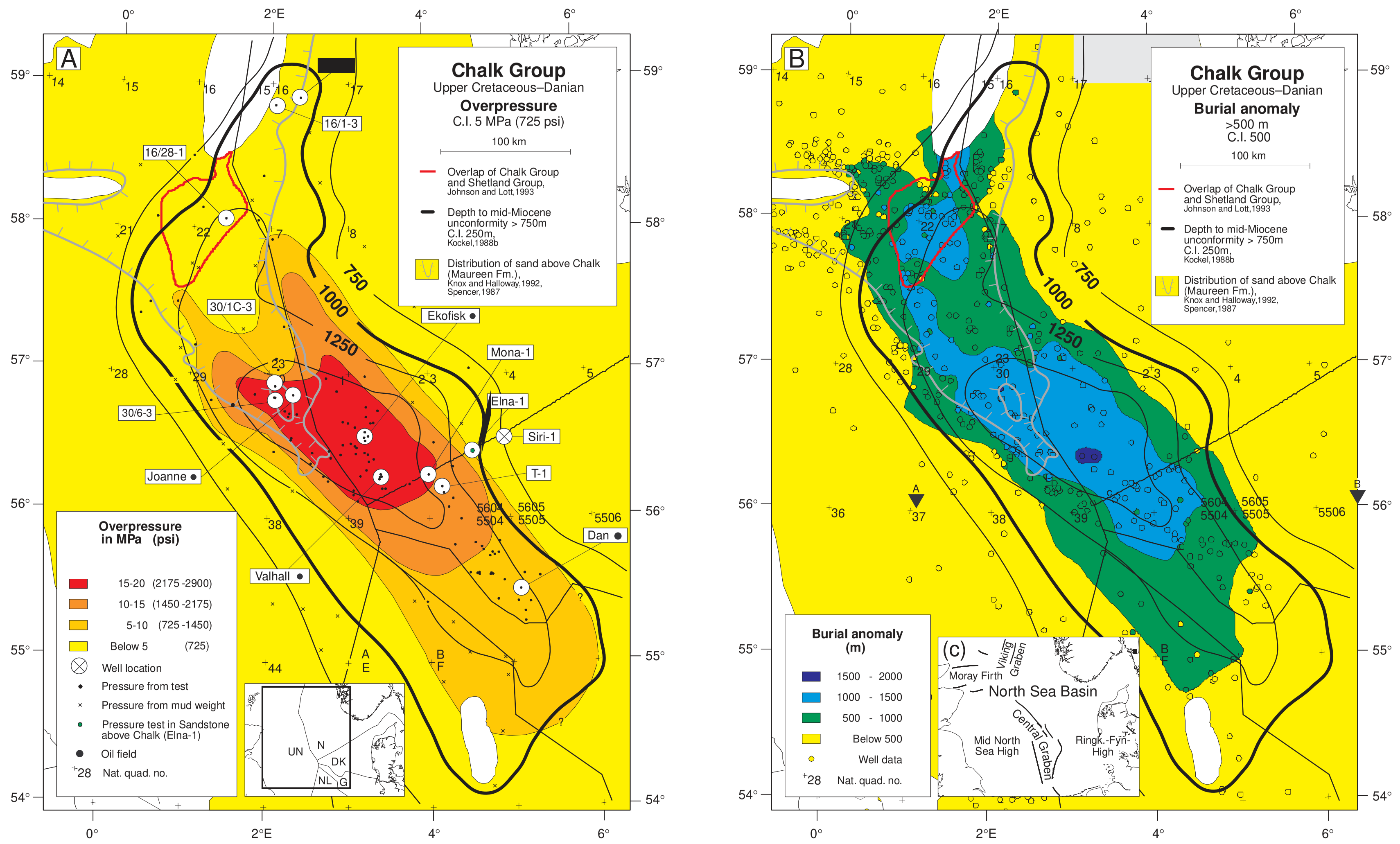

Figure 10—Corresponding areas of overpressured Chalk outlined from pressure measurements and from Chalk burial anomalies coincident with the late Cenozoic depocenter. (A) Chalk formation overpressure (Table 3). (B) Chalk burial anomalies relative to a normal velocity-depth trend (Table 2). (C) Late Cretaceous–Cenozoic structural elements. The overpressured zone corresponds to maximum thickness of the upper Post Chalk Group (Table 3), whereas Paleocene sands overlying the Chalk to the northwest cause bleed-off of overpressure. South of the Viking Graben, shaly Chalk causes positive velocity anomalies even where the Chalk is normally compacted. On (B), points A and B indicate the location of the depth profile in Figure 19. Inset abbreviations as in Figure 9.

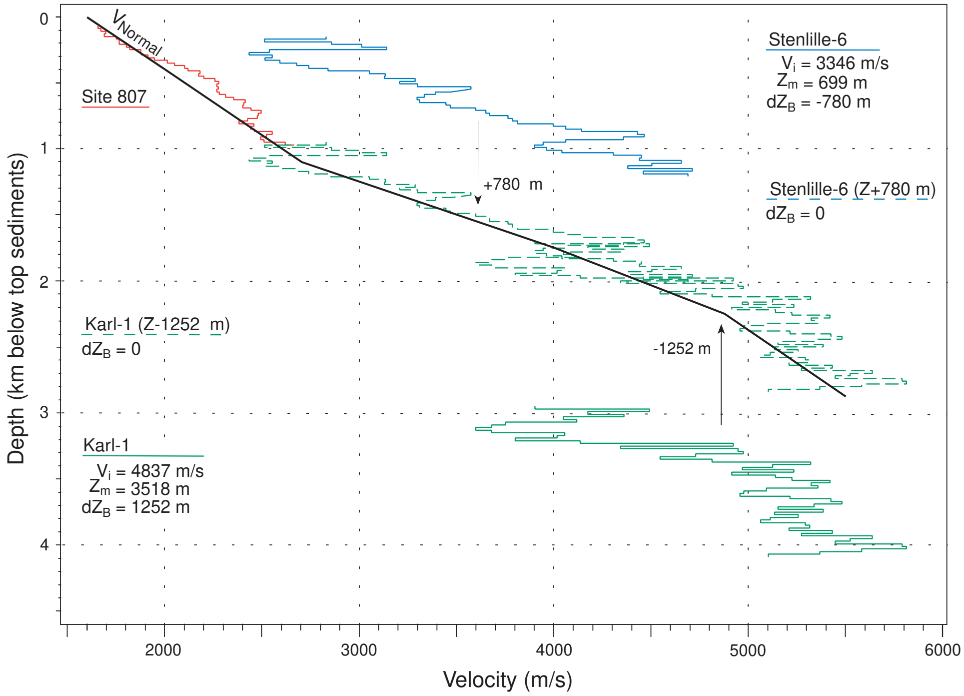

Figure 11—Comparison of V_N and sonic logs from (A) pelagic carbonate deposits of Eocene–Pleistocene age drilled in hole 807, ODP Leg 130 (Shipboard Scientific Party, 1991), and the Chalk Group in (B) the Danish Stenlille-6 and (C) the Karl-1 wells (locations on Figure 8) (equation 8). Only after shifting the logs toward V_N do the sonic logs line up.

in the central North Sea (Figure 9). This trend indicates that the burial depth of the Chalk Group in this zone has been reduced from a maximum burial attained during the Cenozoic.

The zone of exhumation extends along the British coast, as indicated by the continuous –500 m burial-anomaly contour. Erosion increases in a landward direction, and in the southwestern UK sector, a maximum of 1600 m is computed for the Cleethorpes 1 well, whereas the burial anomaly is zero 250 km to the east. To the north, overburden reduction reaches 1000 m in the Inner Moray Firth, and the transition zone between zero and the –500 m anomaly is narrow, only 30 km. Farther north, the –500 m burial-anomaly contour turns northeast in the direction of the Viking Graben. On the Norwegian side of the Viking Graben, well control is poor, but farther south the area where overburden reduction exceeds 500 m follows the general trend of the Norwegian and Swedish coasts, and covers most of onshore Denmark. In northern Denmark, data from several wells indicate exhumation in excess of 750 m. Along the Dutch coast, the Chalk appears to be close to normal compaction for its present depth, and only a minor reduction in burial is indicated to the south. Lack of data close to the truncation of the Chalk makes contouring of areas of maximum erosion difficult in the Norwegian and Danish sectors, and the in UK sector between 55° and 57°N. The course of the burial-anomaly contours east of the study area, in the Baltic Sea, awaits further investigation.

Comparison With Other Studies and Evidence of Exhumation

The map of the Chalk burial anomaly shows a striking resemblance to the map of the pre-Quaternary geology (Figures 4, 9). The deeper the erosion, the greater the span of the pre-Quaternary hiatus. The Chalk is now at maximum burial in the central North Sea below the Pliocene depocenter, whereas the estimated erosion reaches approximately 1 km along the limitation of the Chalk. The east-west symmetry of both maps suggests symmetry in the causes generating this pattern across the North Sea.

The validity of the estimated overburden reduction based on Chalk velocities is stressed by the similarity with estimates found by different methods in studies of the North Sea Basin, such as studies done on the eastern North Sea Basin (shale compaction, density, and vitrinite reflectance) (Jensen and Schmidt, 1992, 1993; Japsen, 1993a; Michelsen and Nielsen, 1993; Hansen, 1996)and the UK southern North Sea/East Midlands Shelf (fission-track analysis, vitrinite reflectance, chalk and shale compaction) (Bulat and Stoker, 1987; Green, 1989; Bray et al., 1992; Hillis, 1995a). Regional exhumation in the Inner Moray Firth also has been demonstrated, but with a smaller amplitude than the estimates presented here (Hillis et al., 1994; Thomson and Hillis, 1995). A comparison with studies with wells in common with this study is given in Table 4. Fission-track studies indicating kilometer-scale

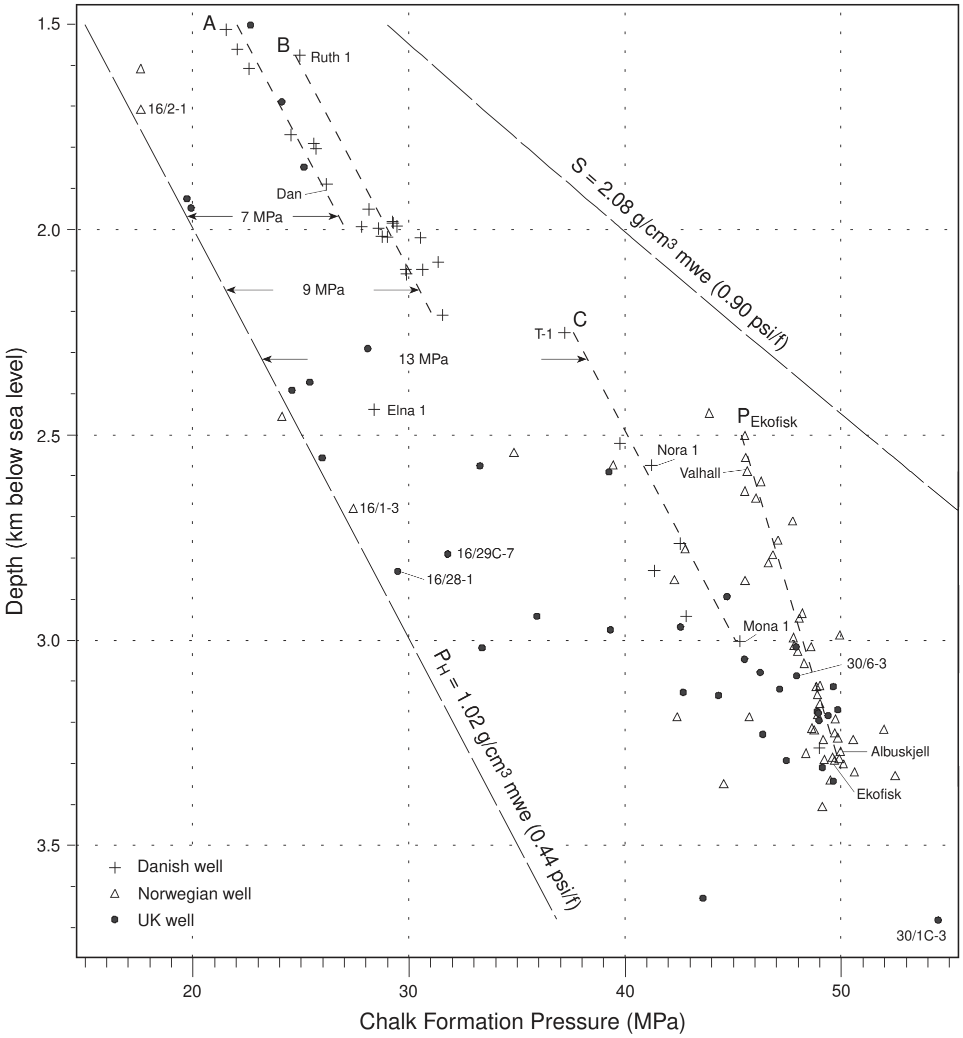

Figure 12—Chalk formation pressures vs. depth below sea level, central North Sea (Table 3). Dashed lines A, B, and C mark geographically coherent, apparent pressure compartments in the Danish Central Graben with overpressures of 7 ±1, 9 ±1, and 15 ±1 MPa, respectively. These apparent pressure compartments may be explained by the small, local variations of the overburden rather than by hydraulic communication. $P_{Ekofisk}$ shows the pressure-depth trend for Norwegian Chalk fields in the Greater Ekofisk area. Vertical pressure communication in the hydrocarbon phase may explain the apparent drop in overpressure with depth in the Ekofisk area. mwe = mud weight equivalent.

Tertiary erosion over wide areas of the onshore UK also are in line with this study (Green, 1986, 1989; Bray et al., 1992; Lewis et al., 1992).

Magnitude of Erosion in the Eastern North Sea Basin

The course of the line of zero burial anomaly found in this study is similar to that of Jensen and Schmidt (1993) (their hinge-line). At 56°N, the locations found in this paper and in Jensen and Schmidt are identical, just east of well DK L-1, whereas at 58°N this study suggests a position 30 km farther west into the basin. The same relation applies for a comparison with the zero line indicated by Hansen (1996), only at 58°N the shift is 60 km. The estimates of Hansen (1996) are on average 196 m smaller than those presented here, but still within the average standard deviation of 260 m determined in that study. In northernmost Denmark, Chalk burial anomalies appear to underestimate erosion due to relatively high siliciclastic content in the basal Chalk, which has avoided deep erosion in the area (quadrants DK 5709–10) (Sorgenfrei and Buch, 1964). A glacially induced reduction in velocity commonly observed in the upper 20 m of the Chalk below the Quaternary cover in Denmark may add to this underestimation (C. Andersen, 1995, personal communication).

The area in Denmark where overburden reduction may be estimated is enlarged to the south by the use of Chalk velocities relative to previous works based on deeper, but less extensive, strata (Japsen, 1993a; Jensen and Schmidt, 1993; Michelsen and Nielsen, 1993). A minimum of 300 m is estimated in southwesternmost Denmark (the Borg 1 well), whereas estimates from the eastern islands are above 500 m and reach a maximum of approximately 750 m in the Stenlille wells, only 100 m lower than the estimate of Japsen (1993a) (Figure 9).

Table 3. Chalk Group Pressure Data From Selected Wells*

Well or Field Name	Pressure Compartment	Quadrant No.	Δz_{up} (m)	Δz_{low} (m)	z^{**} (m)	P^{**} (MPa)	ΔP† (MPa)	Mud Wt. Equiv. (Mg/m^3)	dZ_B (m)	DC (%)
Denmark										
A-2	A	5505	1180	554	1790	25.6	7.7	1.46	–	–
Adda-1	B	5504	1143	877	2208	31.6	9.5	1.46	588	49
Bo-1[††]		5504	1274	708	2079	31.4	10.6	1.54	788	38
Dan/Kraka	A	5505	1155	613	1890	26.2	7.3	1.41	434	64
E-1	B	5504	1205	773	2018	29.0	8.8	1.47	–	–
E-2[†† §§]	B	5504	1205	712	1992	29.5	9.5	1.51	891	26
E-3[††]	B	5504	1222	725	1984	29.3	9.4	1.50	624	49
E-4[†† §§]	B	5504	1229	682	1981	29.3	9.4	1.51	838	32
Elly-2		5504	1429	1345	2941	42.8	13.4	1.49	973	32
Elna-1[§]		5604	1261	1537	2438	28.4	4.0	1.19	430	64
G-1[††]	B	5505	1098	831	1997	28.6	8.6	1.46	410	63
Gert-1		5603	1430	1618	3262	49.0	16.4	1.53	1432	0
H-1[†† §§]		5504	1247	706	2020	30.5	10.3	1.54	859	31
I-1[††]	C	5604	1408	1262	2765	42.6	14.9	1.57	1439	–2
John Fl.-1[‡‡]	A	5504	1250	230	1561	22.1	6.4	1.44	–55	104
Lulu-1		5604	1321	1335	2831	41.4	13.0	1.49	1496	9
M-8	A	5505	1155	605	1803	25.7	7.7	1.45	434	62
M. Rosa-1	B	5504	1365	446	1951	28.2	8.6	1.47	161	88
Mona-1	C	5604	1496	1427	3002	45.3	15.3	1.54	1271	15
N-1[§§]	B	5504	1341	690	2108	29.9	8.8	1.45	699	48
N-2	B	5504	1325	614	2017	28.8	8.6	1.45	–	–
N-3[§§]	B	5504	1316	657	2098	29.9	8.9	1.45	807	39
Nils-1	A	5505	1157	494	1770	24.5	6.8	1.41	–261	123
Nora-1	C	5504	1340	1171	2574	41.2	15.9	1.61	910	32
Otto-1	C	5604	1419	960	2521	39.8	14.6	1.61	914	36
Roar-2[††]	B	5504	1243	700	2098	30.6	9.6	1.49	762	39
Ruth-1	B	5504	1138	374	1576	23.8	8.0	1.54	–168	115
S.E. Igor-1	A	5505	1059	885	1993	27.8	7.9	1.42	454	57
T-1	C	5604	1328	801	2251	37.5	15.0	1.70	555	58
Tove-1	A	5505	1178	351	1608	22.6	6.5	1.43	149	87
Vagn-2	A	5505	1104	352	1513	21.6	6.4	1.45	32	97
Norway										
Albuskjell		1, 2	1706	1364	3270	50.0	17.3	1.56	1492	13
Edda[‡‡ §§]		2	1450	1613	3285	49.6	16.7	1.54	1401	3
Ekofisk[‡‡]		2	1624	1264	3288	49.9	17.0	1.55	–	–
Ekofisk W[‡‡]		2	1675	1390	3300	50.1	17.1	1.55	–	–
Eldfisk E		2	1502	1423	3015	48.6	18.5	1.64	1553	–3
Eldfisk N		2	1502	1298	3056	48.3	17.7	1.61	1553	–3
Eldfisk S		2	1502	1198	3027	48.0	17.7	1.62	1264	16
Hod E		2	1382	1268	2755	47.1	19.5	1.72	1139	18
Hod W[‡‡]		2	1440	1432	2653	46.1	19.5	1.77	1139	21
Tommeliten A		1	1525	1500	3180	48.9	17.1	1.57	1505	1
Tommeliten G		1	1525	1475	3290	49.2	16.3	1.53	–	–
Tor		2	1659	1213	3292	49.7	16.8	1.54	–	–
Valhall		2	1435	965	2588	45.7	19.8	1.80	1245	13
1/3-4			1480	–	2854	45.6	17.0	1.63	–	–
3/7 2[‡‡]			1339	1056	2573	39.5	13.7	1.56	–	–
6/3-2			1033	1261	2543	34.9	9.4	1.40	–	–
9/11-1			588	912	1608	17.6	1.5	1.12	–269	146
15/9-9[‡]			984	1330	2454	24.1	–0.4	1.00	436	56
16/2-1			876	717	1707	17.6	0.5	1.05	–95	111
United Kingdom										
15/28-1[‡]			756	–	2392	24.6	0.7	1.05	–	–
16/28-1[‡ ‡‡]			1067	1636	2832	29.5	1.2	1.06	944	11
16/29C-7[‡ ‡‡]			1149	–	2790	31.8	3.9	1.16	–	–

Table 3. Continued.

Well or Field Name	Pressure Compartment	Quadrant No.	Δz_{up} (m)	Δz_{low} (m)	z** (m)	P** (MPa)	ΔP† (MPa)	Mud Wt. Equiv. (Mg/m³)	dZ_B (m)	DC (%)
21/17-2			878	–	1925	19.7	0.5	1.05	–	–
21-20B-3‡‡			1150	–	2974	39.3	9.6	1.35	–	–
22/21-2‡			1201	1437	3018	33.4	3.2	1.13	1099	8
23/21-3A			1272	–	2941	35.9	6.5	1.25	–	–
29/7-1‡‡			1074	1397	2575	33.1	7.5	1.32	752	30
29/10-3			1299	–	3310	49.1	16.0	1.51	–	–
30/6-3			1465	1359	3086	48.0	17.1	1.58	1288	12
30/16-4‡‡			1163	1012	2290	28.1	5.2	1.25	–	–
31/26-1			1431	1024	2590	39.3	13.4	1.55	872	39

*See Appendix 1 for list of symbols. Norwegian and UK well pressure data courtesy Petroleum Information (Erico). Danish pressure data from in-house reports and original data; Dan/Kraka from Andersen (1995). Estimated aquifer pressures for Norwegian fields from Caillet et al. (1997). Field data: z_{up} and dZ_B from well in field; z_{low} over crest of field. All Norwegian fields belong to the Greater Ekofisk area. Under Pressure Compartments: A, B, and C are geographically coherent pressure compartments in the Danish Central Graben. A = 7 ±1 MPa, B = 9 ±1MPa, C = 15 ±1 MPa.

**Mean value of several measurements.

†Overpressure relative to a hydrostatic gradient of 1.02×10^3 kg/m³ (mud weight equivalent).

††Gas show in Chalk (Britze et al., 1995a).

‡Shaly Chalk, overlap of Chalk Group and Shetland Group.

‡‡Δz_{up} estimated from map.

§Test results from Paleocene sandstone 30 m above top Chalk.

§§Chalk Group not penetrated.

On top of Danian carbonates found today at Stevns Klint, eastern Denmark (Figure 9), a sedimentary column of about 750 m must have been deposited and subsequently eroded, according to the results presented here. This scenario agrees with the occurrence of incipient stylolites in the Maastrichtian Chalk at this locality. The formation of stylolites is believed to be depth dependent, and incipient stylolites occur in the Chalk from 470 to 830 m below sea bed on the stable Ontong Java Plateau (Lind 1988, 1993).

Magnitude of Erosion in the Western North Sea Basin

The estimates of overburden reduction based on Chalk Group velocities presented here are, on average, only 54 m smaller than estimates based on velocity of Turonian–Maastrichtian Chalk, UK southern North Sea (Hillis, 1995a) (38 wells in common, correlation coefficient 0.97, Table 4). The difference in the estimates of erosion is due to a slight shift between the normal velocity-depth trends for Chalk used in the two studies in the relevant depth interval (Appendix 2). The exclusion of the Cenomanian and Danian parts of the Chalk Group in Hillis's (1995a) investigation does not appear to affect the close similarity of the two studies. The estimated overburden reduction for well UK 47/29a-1 of 1280 m based on fission tracks and vitrinite data (Bray et al., 1992) is in good agreement with nearby wells covered by this study (well UK 47/18-1; dZ_B = –1055 m) (Figure 9). Erosion of inversion zones in the southern North Sea was estimated relative to supposedly stable nearby areas in a number of studies in the southern North Sea (Marie, 1975; Glennie and Boegner, 1981; Barnard and Cooper, 1983; Allsop and Kirby, 1985; Cope, 1986).

In the Inner Moray Firth, moderate erosion estimates (<700 m in quadrant UK 13) based on Chalk velocity data were presented by Hillis et al. (1994). Their estimates are too low because their reference wells are from an area affected by nearly 500 m of erosion (Appendix 2). Relatively high estimates (<1300 m, quadrant UK 12) based on sonic data from Upper Jurassic shale (Hillis et al., 1994) are more compatible with the results of this study.

In Dutch waters, no studies of regional Cenozoic exhumation are available. Here, the Chalk, in parts, is buried under a thick Quaternary cover (>500 m) (Caston, 1977), and exhumation is not easily recognized.

Timing of the Cenozoic Exhumation of the North Sea Basin

Timing and the existence of the regional Cenozoic exhumation of the North Sea Basin is difficult to assess because of its basinwide scale, and because reference locations are difficult to identify. By contrast, local zones of Late Cretaceous–early Tertiary inversion related to the Alpine orogeny may be recognized on seismic sections, and their

Table 4. Previous Exhumation Studies Compared with This Study

Study*	Method**	Stratigraphic Level	Area†	Wells Compared / Total	Difference Estimate†† (m)	Correlation‡	Late Cretaceous–Cenozoic Exhumation
Japsen (1993b)	ShC	Lower Jurassic	DK northeast onshore & offshore	19 / 32	–67 / –	0.85	Late Cretaceous–early Tertiary + Neogene
Jensen & Schmidt (1993)	ShC density (VR)	pre-Upper Cretaceous?	DK/N onshore & offshore	21 / 35	69 / –	0.89	Neogene
Michelsen & Nielsen (1993)	ShC	Lower Jurassic	DK northeast onshore & offshore	3 / 7	282 / –	–	Late Cretaceous–early Tertiary + Late Cenozoic
Hansen (1996)	ShC	Lower Jurassic –Tertiary	N south of 66°N	20 / 64	–196 / –	0.61	Late Cenozoic
Hillis et al. (1994)	ChC / ShC	Upper Cretaceous / Upper Jurassic	UK northeast offshore	8 / 26	–518 / –	0.95	Early Tertiary
Thomson & Hillis (1995)	VR	pre-Upper Cretaceous?	UK northeast offshore	1 / 10	–606 / 370	–	Early Tertiary
Green (1989)	AFTA	pre-Late Cretaceous	UK southeast offshore	1 / 27	35 / ~1500	–	Early + middle Tertiary
Bray et al. (1992)	AFTA / VR		UK southeast onshore & offshore	(1) / 2(+5)	225 / 1280	–	Early + middle Tertiary
Hillis (1995a)	ChC / ShC	Upper Cretaceous / Triassic	UK southeast approximately offshore	38 / 149	54 / –	0.97	Tertiary

*Japsen (1993a): 28 wells with dZ_B from both studies excluding one well with dZ_B (study) >0, four wells drilled over salt diapirs (different burial history for the Jurassic and the Late Cretaceous), four wells with overestimated dZ_B (study) [DK Børglum-1, J-1, Fjerritslev-1, Fjerritslev; Petersen et al. (in press)]. Jensen and Schmidt (1993): 24 wells with dZ_B from both studies excluding DK Børglum-1, Haldager-1, J-1 (inversion zone). Michelsen and Nielsen (1993): Excluding DK J-1 (inversion zone). Exhumation overestimated because velocity of overpressured Jurassic shales in the Central Graben were used as reference (cf. Japsen , 1993a). Hillis et al. (1994): Comparison with estimates based on Chalk data (mean of Hod and Tor formations). Thomson and Hillis (1995): Exhumation estimates from velocity data are from Hillis et al. (1994). Comparison for UK 12/30-1. Green (1989): Wells and outcrop data. Comparison for UK Cleethorpes 1. Bray et al. (1992): AFTA data for 5 wells from Green (1989). Well UK 47/29-1 compared with UK 47/18-1. UK Cleethorpes 1 also included, dZ_B (study) = 770 m (VR only). Hillis (1995a): Comparison with estimates based on Chalk data.

**AFTA = Apatite fission track analysis, ChC = Chalk compaction, ShC = Shale compaction, VR = Vitrinite reflectance.

†DK = Denmark, N = Norway, UK = United Kingdom.

††Difference = $-dZ_B$(study) + dZ_B(Chalk), well average/estimate of dZ_B(study) if 1 well.

‡Correlation between dZ_B(study) and dZ_B(Chalk) if more than 3 wells.

timing may be determined. The regional erosion of the Chalk may have taken place at any time during the Cenozoic, because the timing of exhumation cannot be inferred directly from velocity data; however, in areas where the Chalk Group is preserved today, it is more likely that relatively stable conditions prevailed immediately after deposition of the Chalk, rather than that extensive Paleocene tectonic activity and exhumation took place. High burial rates result if a kilometer-thick missing section is interpreted to have been deposited over the few million years between deposition of the preserved Chalk and possible Paleocene erosion, as suggested by some workers (Figure 13) (Green, 1989; Green et al., 1993; Hillis et al., 1994). If maximum burial of the preserved Chalk occurred during the Neogene, a much longer time span is available for the deposition of the removed overburden, and moderate Cenozoic burial rates would be the result (Japsen, 1997).

Timing of Exhumation of the Eastern North Sea Basin

In the eastern North Sea Basin, the regional Cenozoic exhumation was interpreted as being Neogene in age by Jensen and Schmidt (1992, 1993) and Japsen (1993a), whereas Michelsen and Nielsen (1993) restricted their estimate to the late Cenozoic. The increasing erosion observed toward the Norwegian and Swedish coasts matches an increase in the age of the Quaternary subcrop in the area, and only the pre-Quaternary unconformity has an areal extent similar to the Cenozoic exhumation (Japsen, 1993a). Tectonism during the late Oligocene and Miocene was suggested by Spjeldnæs (1975) to be a major factor in the shift from open-marine to terrigenous facies in the Tertiary of Denmark.

Timing of Exhumation of the Western North Sea Basin

Tertiary exhumation of Britain and the western North Sea was suggested by Japsen (1997) to have taken place in two episodes, each with an amplitude of about 1 km. The first episode was a Paleogene phase that principally affected the present onshore Britain (west of the present extent of the Chalk Group), and the second episode was a Neogene phase that affected both onshore areas and the western North Sea. Consequently, maximum burial of Mesozoic and older rocks in the present onshore areas generally occurred in the Paleocene (~60 Ma), as suggested by interpretation of fission tracks (e.g., Green, 1989). In the western North Sea, however, maximum burial for these rocks was interpreted by Japsen (1997) generally to have occurred in the Neogene. This suggestion is consistent with published estimates of overburden reduction based on studies of sediment compaction (mainly offshore) (Bulat and Stoker, 1987; Hillis et al., 1994; Hillis, 1995a; Thomson and Hillis, 1995) and of fission tracks (onshore) (Green, 1986, 1989; Bray et al., 1992; Lewis et al., 1992; Green et al., 1993), as well as with the concept of two periods of Tertiary exhumation (Lewis et al., 1992; Green et al., 1993).

In the southern North Sea, regional exhumation was found to be of late Tertiary age by Bulat and Stoker (1987), and upper Paleocene argillaceous deposits on the east Midlands Shelf were suggested to represent remnants of a more extensive Paleogene cover (Stewart and Bailey, 1996). The thick, shallow-marine sandstones of the middle–late Miocene Utsira Formation may result from Neogene exhumation of northern Britain and the surrounding shelf. This formation is present in the Viking Graben area between 58° and 62°N and is interpreted to be sourced from the west (Isaksen and Tonstad, 1989).

In the Dutch sector, base Miocene, middle Miocene, and base Quaternary unconformities are prominent (van Wijhe, 1987; Zagwijn, 1989). The Chalk may have been at maximum burial depth at the time represented by any of the unconformities that separate the thin Neogene units. South of the study area, the Rhenish Massif has been subject to uplift since the end of the Oligocene, and at an accelerated rate since the end of the Miocene (Meyer, 1983). These observations agree with a Neogene timing of Chalk maximum burial in the southern Dutch sector of the North Sea.

Onset and Cessation of Neogene Exhumation of the North Sea Basin

The dating of maximum Chalk burial to the Neogene indicates a crude time interval (25–2 Ma) (Haq et al., 1987) during which the exhumation of the North Sea Basin took place; however, where parts of the Neogene succession are preserved, the timing of exhumation can be specified by identifying hiatuses in the stratigraphic record during which deposition followed by exhumation may have taken place. Where most of the Tertiary sediments are removed, the timing of erosion can be dated only indirectly by inference from less exhumed areas.

Within the North Sea Basin, the middle Miocene unconformity has been suggested to represent the onset of pronounced uplift by several workers (Bulat and Stoker, 1987; Jensen and Schmidt, 1993; Jordt et al., 1995; Riis, 1996; Stewart and Bailey, 1996). The middle Miocene unconformity (14 Ma) (Jordt et al., 1995) is a basinwide regional downlap

Figure 13—Burial diagrams for the Chalk Group with Paleogene or Neogene exhumation for well UK 47/29a-1 (Figure 9). Note the differences in the derived burial rates. (A) Maximum burial at 60 Ma (cf. Green, 1989, his figure 9; Green et al., 1993, their figure 4). (B) Maximum burial at 15 Ma (cf. Hillis, 1995b, his figure 5). Well data and exhumation estimate from Bray et al. (1992). After Japsen (1997).

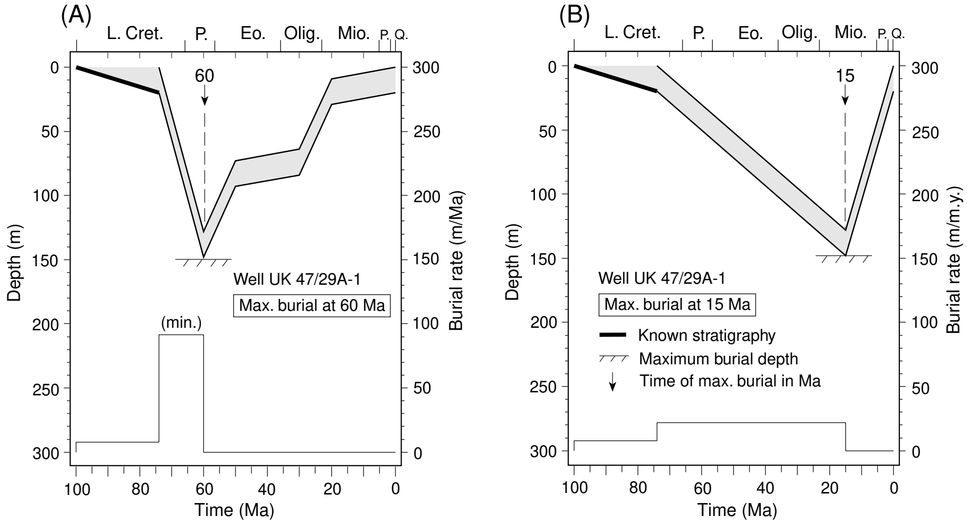

surface (Jordt et al., 1995) that is present throughout the North Sea, apart from a narrow zone of continuous late Cenozoic sedimentation in the central North Sea (see following sections) (Deegan and Scull, 1977; Michelsen, 1982; van Wijhe, 1987; Isaksen and Tonstad, 1989). Thick deposits overlie the unconformity in the central North Sea, where accelerated Neogene sedimentation was found to be evidence of Neogene uplift of the basin margin (Nielsen et al., 1986; Jensen and Schmidt, 1992). In the Danish Central Graben, the increased input of terrigenous weathering products is indicated by the abrupt increase in grain size at the transition from the Paleogene to the Neogene, and by the increasing amount of kaolinite (Nielsen, 1979). Jordt et al. (1995) found that significant basinal tectonic subsidence was initiated in the middle Miocene in the Norwegian North Sea coeval with the uplift of southern Norway. They concluded that the present geometry of the Cenozoic sequences is the result of tectonic uplift through the Oligocene–Pliocene, and further uplift related to late Pliocene–Pleistocene glacial erosion and isostatic adjustments.

Pleistocene sediments overlie older Cenozoic sediments unconformably throughout the North Sea Basin (Figure 4) (Cameron et al., 1992; Laursen, 1992; Gatliff et al., 1994; Jordt et al., 1995; Riis, 1996). Thus, the upper Pliocene is missing as far west as 4°E in the Danish North Sea (the Mona-1 well, Figure 9) (Laursen, 1992). Late Cenozoic sedimentation was continuous only in the narrow zone of maximum Quaternary subsidence in the central North Sea (Figure 14C) (Gatliff et al., 1994); e.g., in Danish well Kim-1, where the earliest Pleistocene is represented by marine sediments (Figures 9, 16) (Konradi, 1995). The cessation of the Neogene exhumation of the North Sea Basin thus appears to be marked by the regional unconformity at the Pliocene–Pleistocene transition (~2.4 Ma) (Zagwijn, 1989; Gatliff et al., 1994). Quaternary erosion may be important where the Chalk is found below a thin cover of primarily upper Quaternary sediments (e.g., onshore Denmark), in contrast to where both the upper and lower part of the Quaternary sediments are present, as in most of the Norwegian sector (Jordt et al., 1995).

Missing Section Removed During Exhumation

In the North Sea Basin, the post-exhumational burial, B_E, relative to the Neogene exhumation is here approximated by the thickness of the Quaternary deposits, based on the assumption that the exhumation ceased by the end of the Neogene (equation 14 in Appendix 3; Figure 14B). The Quaternary thickness, however, is not well known in parts of the area due to uncertainty about the position of the Pliocene–Pleistocene boundary (Gatliff et al., 1994). The map of the computed estimate of the missing section (Figure 14C) shows greater values toward the basin center than the burial-anomaly map because the Quaternary thickness increases toward the basin center, whereas the Chalk burial anomalies increase toward the basin margins. At the basin margin, where the Quaternary cover is thin, $\Delta z_{miss} = -dZ_B$, and the removed sediments are likely to have been of mainly Paleogene age (Figure 13) (Japsen, 1997).

Along the line of zero burial anomaly, a succession of several hundred meters appears to have been removed (Figure 14C); however, the computed missing section exceeding 750 m along this zero line in the southwestern North Sea where

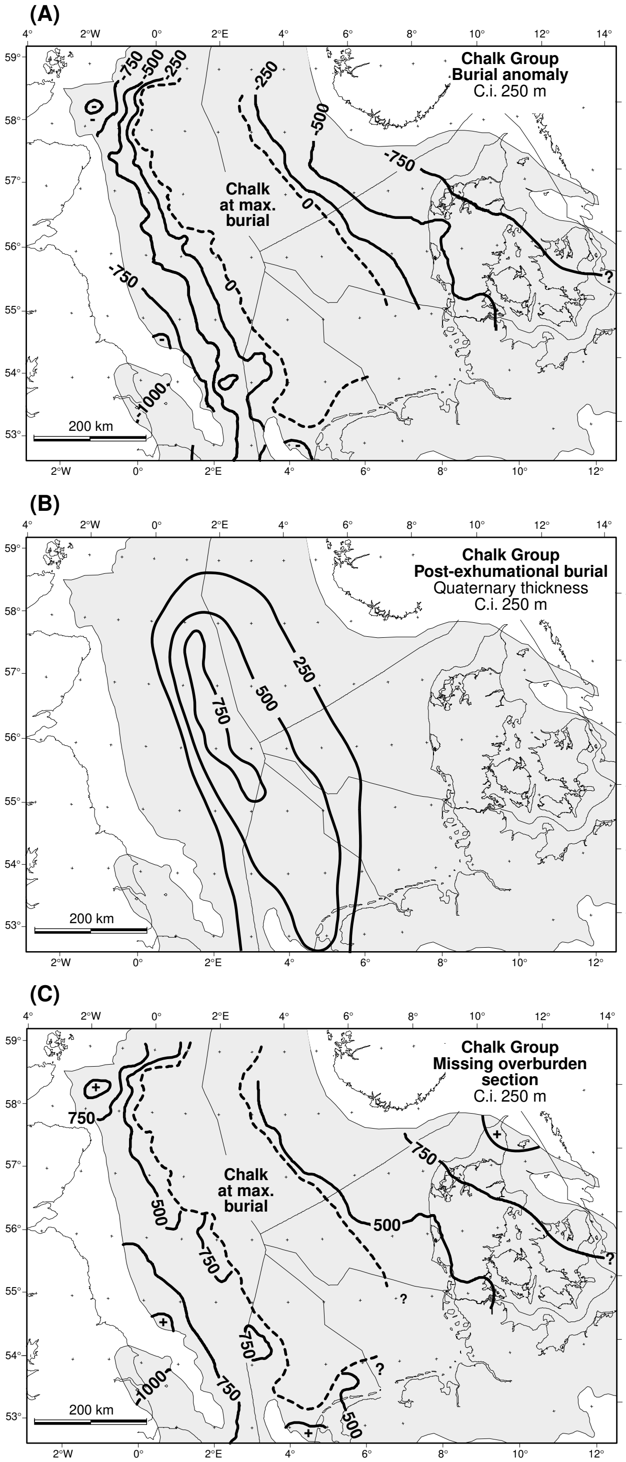

Figure 14—Estimate of missing overburden section, Δz_{miss}, relative to the Chalk Group. (A) dZ_B, which is Chalk burial anomaly (Figure 9). (B) B_E, which is post-exhumational burial = Quaternary thickness (Caston, 1977; Andrews et al., 1990; Cameron et al., 1992; Johnson et al., 1993; Gatliff et al., 1994). Exhumation is assumed to be Neogene. (C) Δz_{miss}, which is missing overburden section = $B_E - dZ_B$ (equation 3).

the Quaternary is thick may well be an exaggeration due to a too easterly location of the zero line. The Danish L-1 well is close to the zero line, and the Chalk is at maximum burial: dZ_B = +75 m (Figure 9). In this well a 37-m-thick lower Pliocene unit is overlain by lower Pleistocene sediments at the base of a 322-m-thick Quaternary succession (Laursen, 1992). If we put $dZ_B \approx 0$, the missing section becomes the thickness of the Quaternary. About 300 m of Pliocene–lowermost Pleistocene sediments are thus likely to have been eroded at the Pliocene–Pleistocene transition at this location.

Toward the basin center, the thickness of the removed section is gradually reduced, and must be zero below the Quaternary depocenter, where sedimentation was continuous throughout the late Cenozoic (Figure 15) (Gatliff et al., 1994). The central parts of the basin were thus affected by Neogene exhumation much later than the margins in accordance with the notion of Stuevold and Eldholm (1996), who suggested that increasingly greater shelf areas would become affected by tilting and erosion as uplift is progressing.

In the Inner Moray Firth, a Neogene timing of exhumation means that no or only limited post-exhumational burial took place, because the Quaternary depocenter lies east of the eroded area (Figure 14B) and, consequently, $\Delta z_{miss} \approx -dZ_B$ (>1000 m in quadrant UK 13). Hillis et al. (1994), however, assumed early Paleocene maximum burial of the Chalk in that area, and that the post-exhumational burial equaled the thickness of the entire Cenozoic sequence (500–1000 m in quadrant UK 13). The model of Hillis et al. (1994) thus resulted in the unlikely prediction of removal of about 1 km of Danian deposits before deposition of the Paleocene sandstones encountered today. At the estimated line of zero burial anomaly (well UK 13/30-2), the missing section was found to exceed 1 km, and the possibility of erosion on this order east of the zero line, across the Viking Graben, was mentioned but later considered unlikely (Hillis et al., 1994; Hillis, 1995b). According to this study, the missing section is less than 500 m near the zero line on both the eastern and western sides of the Viking Graben (Figure 14C), and probably zero below the Pliocene depocenter in the Viking Graben (Figure 15).

Near the Dutch coast, the estimated missing section reaches 750 m due to the substantial Quaternary thickness even where the burial anomaly is moderate. This finding seems to suggest that at least the southern part of the Dutch territory was affected by the Neogene exhumation, as indicated by truncation of the Chalk along 53°N, also on German territory.

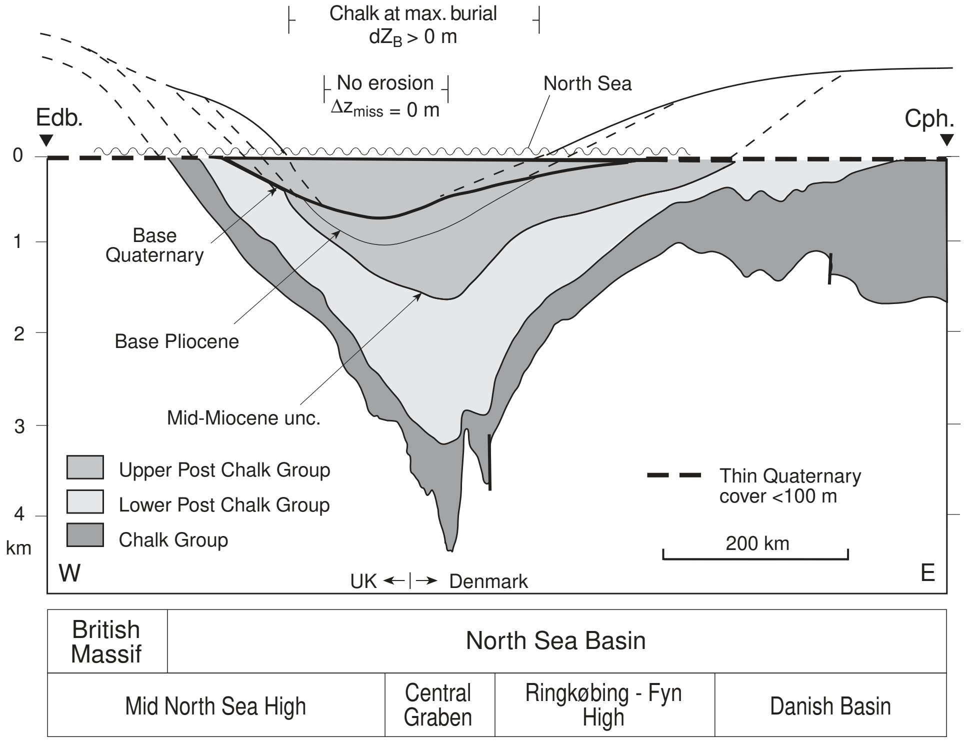

Figure 15—Estimate of the missing section eroded during the Neogene indicated above the base Quaternary unconformity. The height of the exhumed wedge above the sea bed is the burial anomaly, dZ_B, the part below the sea bed is the post-exhumational burial, B_E. Mesozoic and Late Cretaceous–Cenozoic structural elements are indicated. Profile from Edinburgh (Edb.) to Copenhagen (Cph.) is shown on Figure 9.

Observations of Neogene Uplift and Tectonics Around the North Atlantic

The main vertical movements affecting the North Sea Basin since the middle Tertiary are symmetrical about the basin axis (Figure 16). Rapid late Cenozoic burial of up to 1.5 km took place in the central part of the basin at an accelerating rate (Nielsen et al., 1986), whereas Neogene overburden reduction reached about 1 km along the present-day limit of the Chalk. The accelerating subsidence rate in the late Cenozoic has long been known (e.g., Sclater and Christie, 1980; Nielsen et al., 1986), whereas the effect of Neogene exhumation of the eastern North Sea Basin has gained general recognition within recent years (e.g., Jensen et al., 1992), but the timing of exhumation of the western North Sea Basin has been disputed (Japsen, 1997). The observation that the base of the Quaternary deposits is a major angular unconformity cutting across Pliocene–Paleozoic strata toward the British, Danish, and Norwegian coasts strongly indicates that uplift and erosion caused the Neogene exhumation of the North Sea Basin (Figure 3) (Cameron et al., 1992; Jensen and Schmidt, 1993; Gatliff et al., 1994).

These observations are inconsistent with an interpretation of the North Sea Basin following a McKenzie model in which sedimentary basins were formed by stretching and thermal subsidence (McKenzie, 1978). Sclater and Christie (1980) found, on the basis of a McKenzie model, that the post-middle Cretaceous sedimentation in the North Sea Basin was uniform and created a saucer-shape basin; however, Sclater and Christie (1980) noted the high, late Cenozoic rate of sediment accumulation in the central North Sea. They suggested the high rate to be caused by shallowing water depth and high porosity of surface shales, whereas Vejbæk (1992) suggested phase transitions in the upper mantle played a role for the rapid subsidence. Such mechanisms alone, however, do not explain the coincidence of uplift and rapid subsidence in the North Sea Basin during the late Cenozoic. Thermal rejuvenation and a renewed rifting phase were suggested by Thorne and Watts (1989) as possible causes for the high subsidence rates, whereas Kooi et al. (1991) found the occurrence to be consistent with the present intraplate stress field. Rohrman et al. (1995) observed a Neogene domal uplift of southern Norway, and found it to be coincident with Oligocene and Pliocene plate reorganizations in the North Atlantic. Van Wees and Cloetingh (1996) found that accelerated subsidence as observed for the Quaternary in the North Sea Basin could be predicted from a three-dimensional model, assuming an increase of compressive intraplate forces in agreement with observed stresses. Stuevold and Eldholm (1996) considered the Fennoscandian

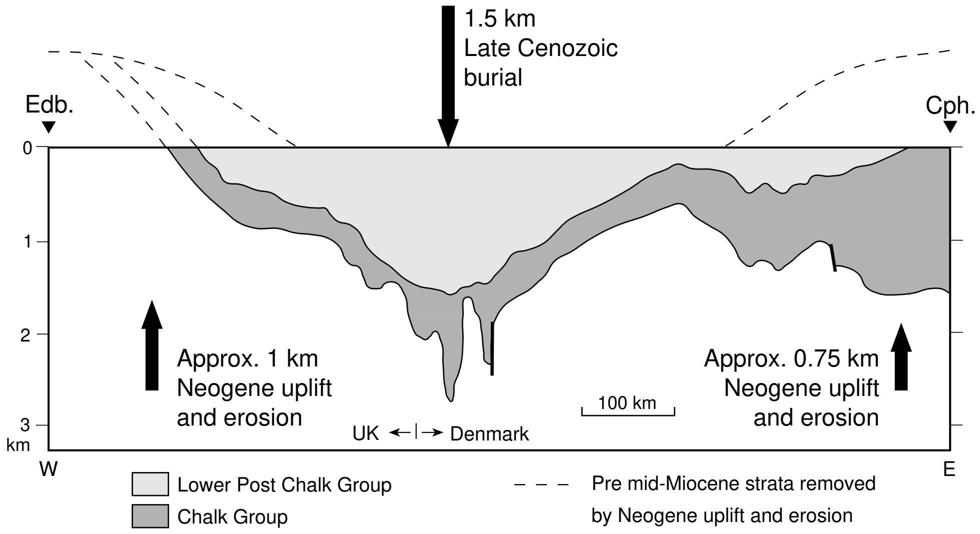

Figure 16—Vertical movements affecting the North Sea Basin during the Neogene/late Cenozoic. Neogene uplift and erosion along the margins of the basin leading to reduction of the Chalk overburden, and rapid late Cenozoic burial in the basin center. Profile is flattened at the mid-Miocene unconformity; profile from Edinburgh (Edb.) to Copenhagen (Cph.) is shown on Figure 9.

continental uplift to represent a flexural intraplate deformation that was separated in time and space from the uplift associated with the early Tertiary crustal breakup.

An increasing amount of documentation has emerged that suggests that Neogene exhumation and compressional tectonics have affected areas around the entire North Atlantic, and rapid late Cenozoic subsidence and sedimentation have been observed throughout the region (compare Boldreel and Japsen, 1998). Major regional Neogene exhumation is documented offshore west of Scandinavia from the Barents Sea to Denmark (e.g., Jensen et al., 1992; Japsen, 1993a; Rohrman et al., 1995; Doré and Jensen, 1996; Riis, 1996; Stuevold and Eldholm, 1996), and an accelerated late Cenozoic sedimentation is well known in a zone west of the same area (e.g., Nielsen et al., 1986; Kooi et al., 1991; Doré and Jensen, 1996). Neogene uplift and erosion onshore Scandinavia has been deduced from studies of landforms and fission tracks (e.g., Rohrman et al., 1995; Lidmar-Bergström, 1996; Riis, 1996). Regional Neogene exhumation of Britain and the western North Sea was suggested by Japsen (1997), and is documented for the western North Sea by this study. The Faeroe-Rockall area suffered Miocene compression, suggested to be associated with sea-floor spreading in the North Atlantic (Boldreel and Andersen, 1993). Jameson Land in East Greenland experienced Cenozoic uplift and erosion at a rate that accelerated during late Cenozoic times (Christiansen et al., 1992; Mathiesen et al., 1995). West of Greenland, Neogene uplift and erosion is recognized in parts of the area (Chalmers, 1998), while thick late Cenozoic deposits have accumulated in other parts of that area (Cloetingh et al., 1990; Whittaker et al., 1997). Around the North Atlantic, rapid late Neogene subsidence and sedimentation, as well as relative uplift along basin edges, were observed by Cloetingh et al. (1990), and studies of North Atlantic passive margin uplift were reviewed by Eyles (1996), including studies documenting late Cenozoic exhumation of eastern North America.

Explanations for these observations have commonly been local, involving mechanisms not applicable to the entire area; however, vertical movements appear to have affected many, if not all, continental margins around the North Atlantic. A model explaining these large-scale, late Cenozoic phenomena must separate the effects of Paleogene synrift plate-boundary-related uplift from the effects of Neogene intraplate uplift (Rohrman et al., 1995; Stuevold and Eldholm, 1996; Japsen, 1997). Such a model must be constrained by global observations of these intraplate events rather than by data from a single region, and by the fact that their effects reach beyond passive margins, as is demonstrated here in the case of the North Sea.

Conclusions Regarding Neogene Exhumation

The Chalk Group is overcompacted due to a previous greater burial depth along the western and eastern margins of the North Sea Basin. The burial anomalies estimated from Chalk velocities are comparable to estimates of overburden reduction from other studies, but through the large areal coverage of this study I can demonstrate the link between the areas covered by these previous studies using a uniform data set (Figure 9). The exact magnitude and timing of the overburden reduction and the location of the line of zero burial anomaly may be disputed, but the regional scale of the erosion, and the fact that both the western and the eastern margins of the basin were affected, are documented in this study.

The uniformity of the patterns of Chalk burial anomalies and the pre-Quaternary subcrop also suggests that the anomalies are measures of erosion and, moreover, that the erosion occurred during the Neogene (Figure 4). Only Neogene maximum burial of the Chalk leaves time for the deposition, at moderate rates, of the kilometer-thick deposits that are now missing on top of the Chalk (Figure 13). I suggest that the onset of uplift and erosion of the margins of North Sea Basin is reflected by the mid-Miocene unconformity (14 Ma), whereas termination of the erosion of the shelf is indicated by the base Pleistocene unconformity encountered throughout the basin (2.4 Ma) (Zagwijn, 1989) [mid-Pliocene according to Haq et al. (1987)]. Quaternary erosion may have played a role where the Chalk is covered by a thin layer of Quaternary sediments.

Along the present-day limit of the Chalk, the missing kilometer-thick section is likely to have been of mainly Paleogene age, whereas several hundred meters of mainly Pliocene sediments are missing along the line of zero burial anomaly (Figure 14). Here, the Chalk is at maximum burial today due to Quaternary reburial. The southern part of the mapped Dutch sector appears to have been affected by Neogene exhumation, but this is masked by substantial Pliocene–Quaternary reburial.

Large-scale late Cenozoic vertical movements affected the North Atlantic region, including Scandinavia and its seaward margin from the Barents Sea to Denmark, the North Sea, Britain, the Faeroe Islands, Greenland, and eastern North America. The Neogene exhumation of the margins of the North Sea Basin documented here, and the accelerated sedimentation rates in the basin center during the late Cenozoic, differ from the predicted saucer-shape Cenozoic basin of a McKenzie (1978) model (Figure 16). A model explaining the late Cenozoic vertical movements must be confined by knowledge of their distribution in time and space.

OVERPRESSURING OF THE NORTH SEA CHALK AQUITARD

Chalk reservoir properties depend strongly on pressure conditions in the central North Sea (Scholle, 1977). Where the Chalk is characterized by overpressure, it contains important hydrocarbon accumulations, such as the Ekofisk and Dan fields in the Norwegian and Danish sectors (Figure 10). Here, the Chalk has been considered as a regional aquifer (Megson, 1992, 1998). Where Chalk formation pressure is close to hydrostatic, hydrocarbon accumulations are marginal or absent, as in the UK sector (Sørensen et al., 1986; D'Heur, 1993). In that sector, the Chalk has been considered as a regional aquitard (Cayley, 1987; Darby et al., 1996), just as the lateral flow in the Greater Ekofisk area has been considered insignificant (Caillet, 1998). The normally pressured Chalk in the UK sector is drained by overlying Paleocene sandstones (e.g., Darby et al., 1996), whereas the overpressure in the Chalk in the Danish sector has been suggested to be governed by regional hydrodynamic flow in the Chalk (Megson, 1992). Whether lateral or vertical fluid migration in the Chalk is dominant is a fundamental question for understanding the petroleum system in the North Sea Basin.

The overpressure in the North Sea Chalk is interesting in a wider perspective because the number of possible causes for the overpressuring is limited. In a review of mechanisms that generate overpressure, Osborne and Swarbrick (1997) grouped these causes into three main categories: (1) ineffective volume reduction due to imposed stress leading to disequilibrium compaction, (2) volume expansion of pore fluid or rock matrix, and (3) hydraulic head and hydrocarbon buoyancy. In addition, transference of overpressure generated elsewhere must be considered. According to these workers, the principal mechanisms are disequilibrium compaction and volume expansion during gas generation. In the case of the North Sea Chalk, volume expansion mechanisms can be ruled out. Within the Chalk there is no source potential and only small amounts of shale that could release water during transformation of clay minerals (Cayley, 1987; Kennedy, 1987); furthermore, aquathermal pressuring as suggested by Hunt (1990) and Leonard (1993) is not feasible in the case of the relatively permeable Chalk because this mechanism requires a seal with permeability of close to zero (Hall, 1994; Osborne and Swarbrick, 1997). Disequilibrium compaction previously has been suggested as the main cause of the overpressure in the Chalk and the overlying shales based on qualitative arguments (Carstens, 1978; D'Heur, 1993; Hall, 1993; Japsen, 1994).

In the pre-Chalk section, high pressures (up to 40 MPa at 4500 m depth) (Darby et al., 1996) are encountered below a seal formed by shales and marls (Chiarelli and Duffaud, 1980; Carstens and Dypvik, 1981; Buhrig, 1989; Gaarenstroom et al., 1993; Darby et al., 1996). The main source rocks in the area are found in these synrift sediments of the mainly Late Jurassic Central and Viking grabens (Gatliff et al., 1994). In this interval, volume expansion processes such as gas generation may play a role in generating overpressure (Buhrig, 1989), as well as the process of disequilibrium compaction

(Chiarelli and Duffaud, 1980; Carstens and Dypvik, 1981; Buhrig, 1989).

Overpressured shales are observed below the mid-Miocene unconformity in the central North Sea (Michelsen, 1982; Cartwright, 1994; Japsen, 1994), and this level commonly is referred to as top overpressure. The unconformity marks the onset of pronounced uplift of the margins of the North Sea Basin (e.g., Jensen and Schmidt, 1993; Jordt et al., 1995), and the onset of overpressure in the Chalk probably coincided with the increase in sedimentation rates from the middle Miocene onward (Nielsen, 1979; Nielsen et al., 1986), an idea supported by basin modeling (Caillet et al., 1997).

The Chalk overburden (the Post Chalk Group) (Nielsen and Japsen, 1991) may be divided into an upper and a lower part at the mid-Miocene unconformity (Japsen, 1994) (Figures 1, 3). This simple subdivision is applied to help analyze the relation between the overpressure in the Chalk and its degree of undercompaction as expressed by Chalk burial anomalies relative to a normal velocity-depth trend (equations 2, 8). I argue in the next section that the load of the upper Post Chalk Group acts as the stamp that generates the main part of the overpressure, whereas the thickness and sealing quality of the lower Post Chalk Group determine overpressure retention in the Chalk.

Areal Extent of the Overpressured Chalk

The zone of overpressured Chalk in the central North Sea (ΔP > 5 MPa) strikes north–northwest and affects British, Danish, Dutch, German, and Norwegian territory covering an area of about 425 × 125 km^2 (Figure 10A). The overpressure reaches 20 MPa near the center of the zone in the Hod and Valhall fields. The northern limitation of the zone is in the Jæren area (58°N, quadrants N 6, N 15, UK 16). The continuity of the zone between the Ekofisk and the Jæren areas, however, is not well established due to limited data. The southern limitation probably reaches south of 55°N, into the Dutch quadrant F. The northwest-striking limitations of the zone are established on a regional scale partly using mud weight data.

Paleocene sandstones overlie the Chalk in the northwestern part of the North Sea (Figure 10) (Knox and Holloway, 1992). These sandstones originate from uplifted areas north and northwest of the area (Gatliff et al., 1994), and reach into the area of the late Cenozoic depocenter. The shape of this sandstone wedge matches the crescent-shape northwestern limitation of the overpressured zone with hydrostatic pressure in most of quadrant UK 22, whereas high pressures are encountered below the rim of the sandstone wedge. This match suggests that the Paleocene sandstones drain the Chalk to the northwest, as has previously been suggested (Cayley, 1987; Andersen, 1995; Darby et al., 1996; Osborne and Swarbrick, 1997). The drainage capacity of the sandstones depends on their contact with the Chalk, their hydraulic transmissivity, and the frequency of shaly units. These factors suggest a deterioration of the drainage efficiency of Paleocene sandstones in the distal parts of the wedge.

The region of overpressured Chalk is confined to the area where depth to the mid-Miocene unconformity is greater than 1000 m and the overpressure is proportional to this depth (for example, the 15 MPa contour matches the 1500 m depth contour) (Figure 10A). This agreement suggests a relationship between Chalk overpressure and the load of the upper part and the overburden. The areal extent of the overpressured Chalk also matches the area outlined by positive Chalk burial anomalies in the central and southern North Sea (Figures 5, 10B; equation 5), suggesting a relationship between the Chalk overpressure and undercompaction reflected in the relatively low velocities. A close correspondence is seen between the course of the 10 MPa overpressure contour and the 1000 m burial-anomaly contour, whereas the 5 MPa overpressure contour reaches farther south than the 500 m burial-anomaly contour.

Apart from undercompaction, other factors influence Chalk velocity and hence its burial anomaly (Figures 17, 18). One factor is a high shale content (e.g., well UK 16/28-1). A second factor influencing Chalk velocity is gas charge (e.g., the shaly Chalk south of the Viking Graben). Gas charge in the Chalk lowers the Chalk velocity and causes a relatively high burial anomaly. A third factor is overburden thickness that also reduces the burial anomaly (either over salt diapirs or due to regional erosion as in well N 16/2-1). South of the Viking Graben, the chalky limestone facies of the Chalk Group overlap with the mudstone facies of the Upper Cretaceous Shetland Group (Johnson and Lott, 1993). The northern limitation of the overpressured zone thus becomes difficult to map from Chalk velocities.

Sources of Overpressure in the North Sea Chalk

Disequilibrium Compaction

The Chalk formation overpressure, ΔP, is proportional to the thickness of the late Cenozoic deposits, Δz_{up}, for Δz_{up} > 1000 m (Figure 17A). We get $\sigma_{up} \approx \Delta z_{up}/100$ = 15 MPa in accordance with the contours on Figure 10 by substituting Δz_{up} = 1500 m into equation 4. The Chalk below the late

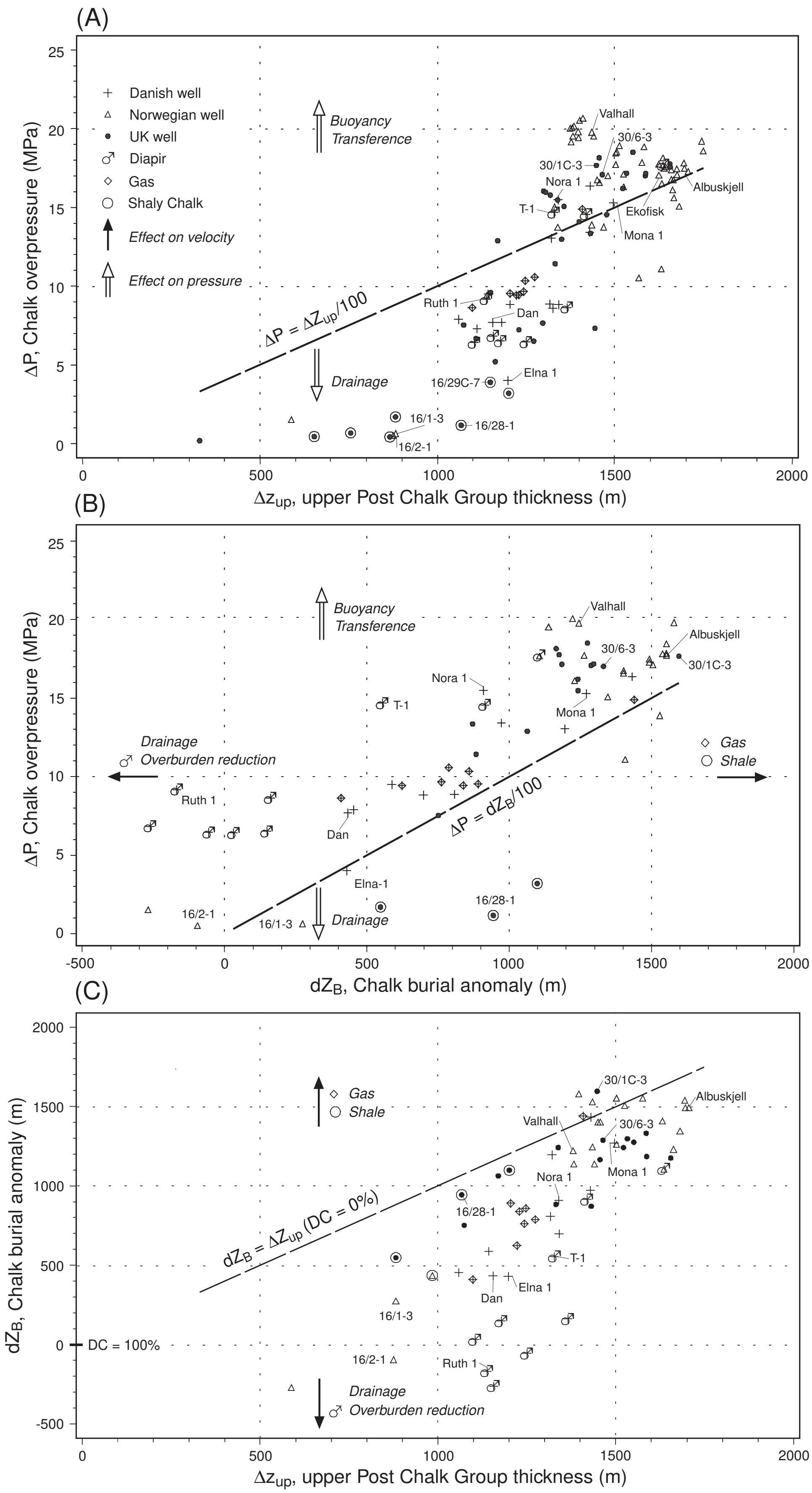

Figure 17—Crossplots of Chalk formation overpressure, ΔP, thickness of the upper Post Chalk Group, Δz_{up}, and Chalk burial anomaly relative to a normal velocity-depth trend, dZ_B (equations 14, 8; Tables 2, 3). (A) ΔP vs. Δz_{up}. The overpressure is proportional to Δz_{up}, and in the order of the effective load of the upper Post Chalk Group, σ_{up} ($\sigma_{up} = \Delta z_{up}/100$) (equation 4). (B) ΔP vs. dZ_B. The compactional part of the overpressure, ΔP_{comp}, is less than ΔP indicating that sources other than disequilibrium compaction contribute to the overpressure ($\Delta P_{comp} = dZ_B/100$) (equation 5). (C) dZ_B vs. Δz_{up}. In general $dZ_B < \Delta z_{up}$, indicating a net drainage of the Chalk (DC = 0%) (equation 6).

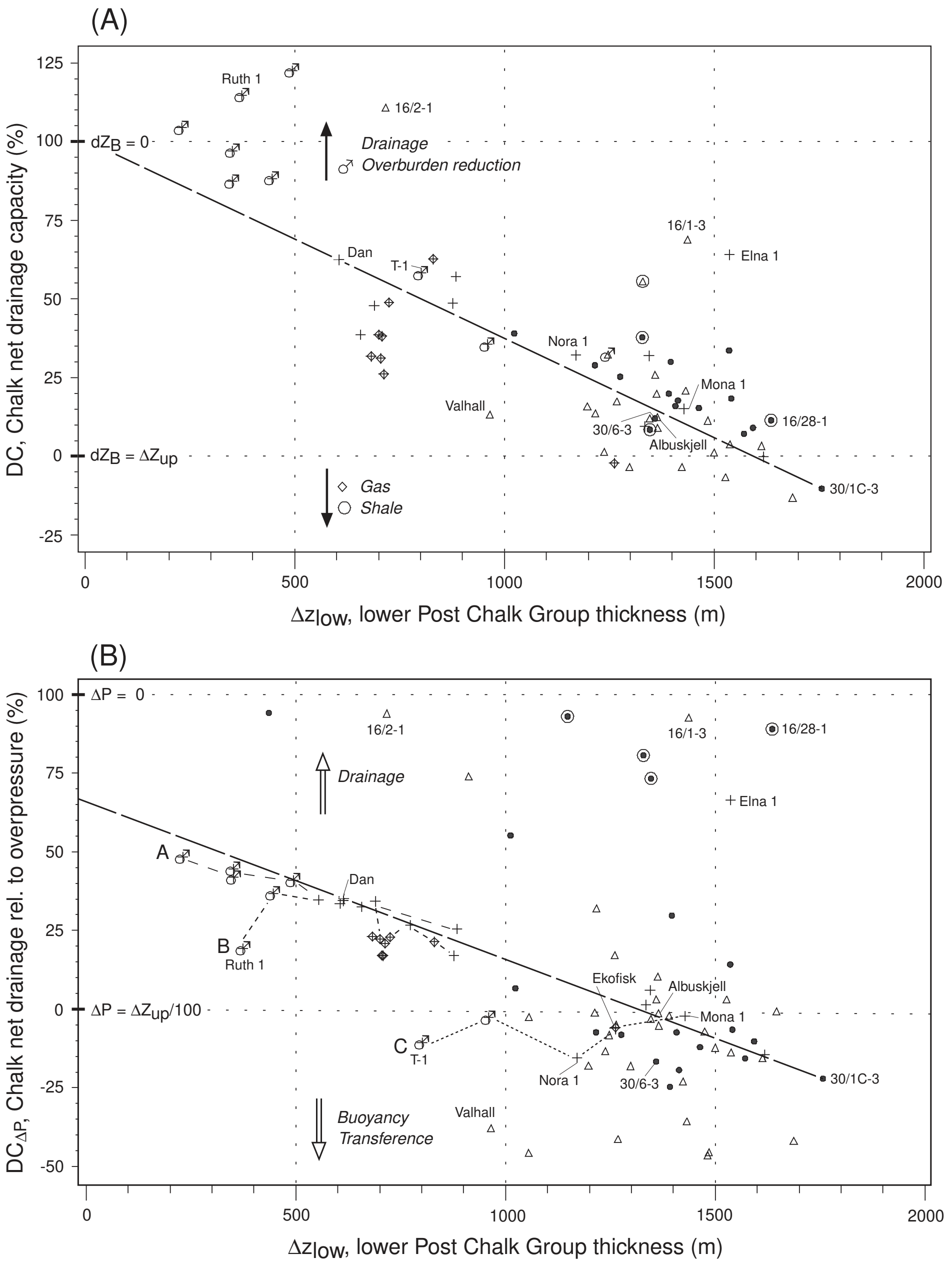

Figure 18—Crossplot of Chalk drainage capacity vs. thickness of the lower Post Chalk Group, Δz_{low} (Table 3). (A) Net drainage capacity, DC (equation 6) vs. Δz_{low}. (B) Net drainage capacity relative to overpressure, $DC_{\Delta P}$ (equation 7) vs. Δz_{low}. Both plots show that thick lower Tertiary shales prevent drainage of the Chalk. Extrapolation of the trend lines yields DC = 100% and $DC_{\Delta P}$ = 70% for zero seal thickness. The unlikely prediction of a drainage capacity, $DC_{\Delta P}$, that is smaller than 100% for zero seal thickness indicates that the Chalk overpressure has been increased by noncompactional sources, whereas DC (and the burial anomaly) reflects the irreversible compaction of the Chalk. The straight trend lines connect the data points for the Dan field and for the well with maximum Chalk formation pressure, well UK 30/1C-3. The bent lines in (B) connect data from the apparent pressure compartments A, B, and C (Figure 12). Legend on Figure 17.

Cenozoic depocenter thus is well sealed because the pore fluids carry the full effective load of the upper overburden; however, no significant overpressure is found in the Chalk where it is overlain by sandstone (e.g., wells DK Elna 1, UK 16/28-1) (Figure 19). Rapid, late loading probably generates the major part of the overpressure in the Chalk where the lower Tertiary sediments are sealing; however, a range of overpressures is recorded for given values of Δz_{up}; e.g., at about 1200 m, the range is from 4 to 13 MPa. Sources other than late burial must contribute to the overpressure, and overpressure must be preserved to different degrees.

The Chalk overpressure is on the order of the compactional part of the overpressure, ΔP_{comp}, as predicted by the burial anomaly, dZ_B (Figure 17B). We get ΔP_{comp} = 10 MPa in accordance with the contours on Figure 10 by substituting dZ_B = 1000 m into equation 5. The line $\Delta P = dZ_B/100 = \Delta P_{comp}$ in Figure 17B) marks a lower limit of the overpressure, and this indicates that factors other than disequilibrium compaction contribute to the overpressure. The mean of $\Delta P_{comp}/\Delta P$ is 80% for $\Delta\rho_{up} = 1.03 \times 10^3$ kg/m³ for 52 data points obtained away from diapirs and where $\Delta P \geq 4$ MPa.

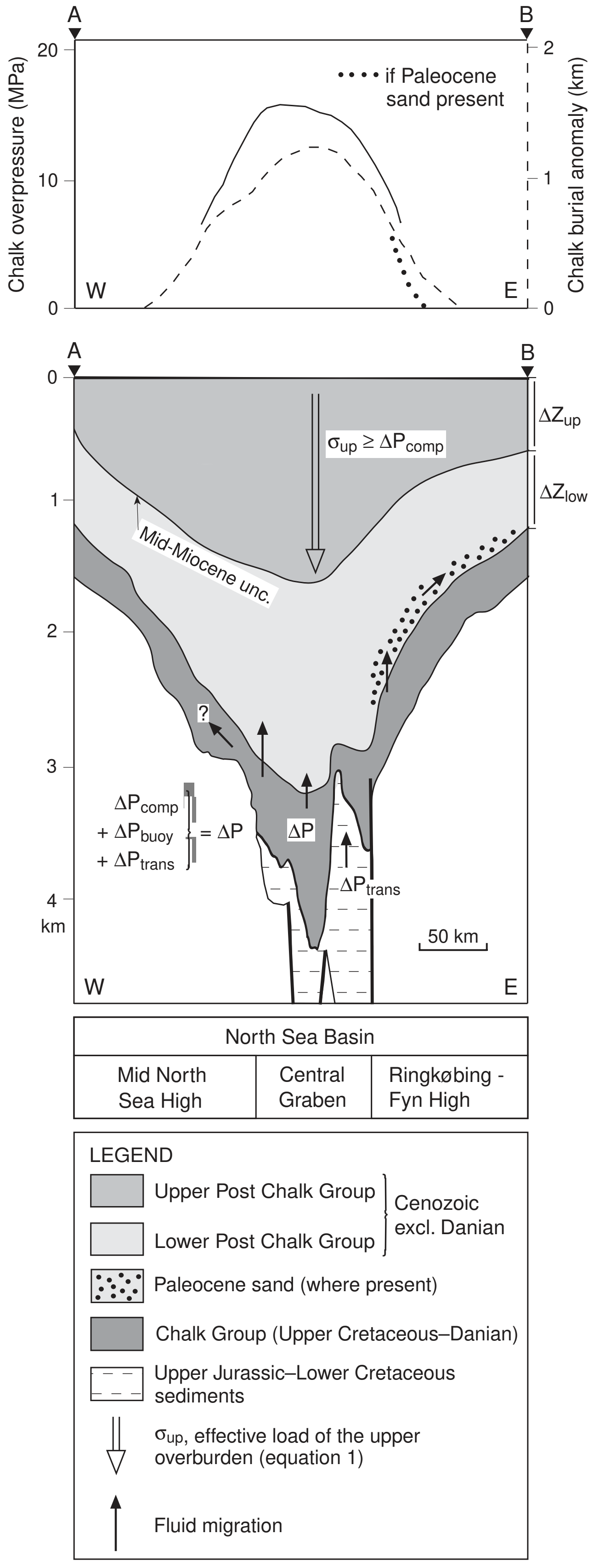

Figure 19—Sketch illustrating factors affecting Chalk overpressure, ΔP, and possible vertical or lateral fluid flow in the North Sea Basin. Chalk overpressure and burial anomaly occur along the profile indicated on top of sketch. Overpressure due to undercompaction, ΔP_{comp} (equation 5); overpressure due to transference, ΔP_{trans}; and overpressure due to buoyancy, ΔP_{buoy}. Location of profile along 56°N from A to B on Figure 10B.

Transference

From the preceding discussion it follows that the present overpressure in the Chalk is greater than predicted from its degree of undercompaction as estimated from velocity data (Figure 17B). The overpressure thus must have increased since maximum effective stress was exerted on the Chalk as it attained its present degree of compaction (see Hall, 1993). This implication is in accordance with the presence of tension fractures in the Chalk of the Norwegian Albuskjell field (Watts, 1983). The explanation for such unloading may be related to the twofold acceleration of the overpressure-generating processes by the increasing burial rates throughout the Cenozoic (Nielsen et al., 1986). First, the loading itself leads to increasing overpressure with time throughout the overpressured sedimentary column. Second, the burial causes increasing hydrocarbon generation in the mainly Upper Jurassic source rocks (Caillet et al., 1997; T. Bidstrup, 1997, personal communication), hence increasing overpressure due to volume expansion (Figure 19).

Loading, however, may increase pore pressure but not reduce the effective stress. If we consider a rock volume at a time for which $S = \sigma + P$ applies, after which the load is increased by δS, we get $S + \delta S = \sigma + P + \delta S$. Consequently, both σ and P are either unchanged or increasing; that is, the effective stress is increased by the part of the added load that is not carried by the pore fluids. Compaction fluids thus may only lower the effective stress by lateral fluid flow, but this is likely only over smaller distances (as is shown in following sections). The effective stress acting on the Chalk, however, may be reduced by transference (redistribution of overpressure) from the pre-Chalk section where volume-expansion processes, such as gas generation, are active (Figure 19). The principal direction in which these sediments can dewater is vertical, possibly along pressure-induced fractures in the Chalk over axial horsts, as evidenced by heat flow anomalies in the UK Central Graben (Darby et al., 1996).

Decreasing effective stress with time was erroneously suggested for a one-dimensional compaction model of the Chalk in the Norwegian Albuskjell field by Watts (1983), who estimated pressure from the rate of burial; however, he did not consider the possibility of late transference of overpressure from the pre-Chalk section as the cause of stress reduction.

Buoyancy

Formation pressure falls along a pressure-depth gradient of only 0.6×10^3 kg/m^3 mwe (mud weight equivalent) in the Chalk fields of the Greater Ekofisk area (Figure 12), leading to a drop in overpressure with depth from 20 to 17 MPa from the Valhall field to the Ekofisk field, where the latter's reservoir is buried about 700 m deeper. In addition, the individual hydrocarbon pressure gradients in the Norwegian Chalk fields line up along the Greater Ekofisk trend (Caillet et al., 1997). Vertical pressure communication in the hydrocarbon phase may explain these observations by differences in the height of a hydrocarbon column (density about 0.6 g/cm^3) on top of a regional pressure level. Such a column would generate an additional overpressure due to the buoyancy of the hydrocarbons of about 3 MPa [$= (1 - 0.6) \times 10^3$ kg/m$^3 \times 700$ m $\times 9.81$ m/s^2], which corresponds to the observed difference between the Valhall and Ekofisk fields. This difference is consistent with the observations made by Caillet et al. (1997) that oil-water contacts in the Chalk reservoirs are difficult to estimate, and that no free-water level may be defined in the Valhall field.

A potential for lateral flow from shallow to deeper Chalk reservoirs in the Greater Ekofisk area was suggested by Caillet et al. (1997) from the apparently higher overpressure for the more shallow fields resulting from comparison with hydrostatic pressure; however, this flow potential does not exist if the hydrocarbon phase is dominant throughout the area because there are no major differences in overpressure between the fields relative to the hydrocarbon gradient (Japsen, 1998).

The overpressure in the Valhall field clearly is in excess of the effective load of the upper Post Chalk Group (Figure 17A), as well as in excess of the pressure prediction based on Chalk velocities (Figure 17B). Sources other than disequilibrium compaction thus must contribute to the pressure, and this additional pressure was induced after the time when the Chalk attained its present degree of compaction. The hydrocarbons of the Greater Ekofisk area probably were emplaced into the Chalk at a late stage in the Cenozoic.

The area of the Greater Ekofisk accumulation may be outlined by identifying data along the trend $P = 31 + 5.7 \times 10^{-3} \times z$ [in MPa], $2500 < z < 3350$ m below sea level (Figure 12). The trend is drawn between the points of highest and lowest Chalk formation pressure in Caillet et al.'s (1997) figure illustrating hydrocarbon pressure gradients. The area strikes about 100 km from the Joanne field in the northwest to the Valhall and Hod fields in the southeast, with a width up to 50 km (Figure 10).

A hydrocarbon column of the order of 700 m is found in the Middle Jurassic sandstones of the Heather field, UK northern North Sea (Penny, 1991). Here, a free-water level is not observed, and the pressure gradient in the reservoir corresponds to a mud weight of about 0.7 g/cm^3. Perhaps the height of the hydrocarbon accumulation in the Greater Ekofisk area is less remarkable than its lateral extent of about 3000 km^2, as opposed to the 40 km^2 of the Heather field.

Migration Direction for Chalk Compaction Fluids

The compaction fluids expelled from the Chalk during late Cenozoic loading may have migrated laterally over long distances through the Chalk itself or vertically through the Tertiary deposits (Figure 19). According to the hydrodynamic model for the Danish Central Graben, hydrocarbons and brine moved updip in the Chalk aquifer along the regional pressure gradient from the Ekofisk to the Dan field in the southeast over distances of about 100 km (Figure 10) (Damtoft et al., 1992; Megson, 1992, 1998). This model provides a mechanism for moving hydrocarbons from the known mature source rocks near the Norwegian–Danish border to the Danish Chalk fields in the Dan area where good source potential is difficult to identify (Damtoft et al., 1992). No direct evidence has been given for regional fluid flow in the Chalk other than the southeastward dip of the free-water level in three Danish Chalk fields assumed to reflect water flow in the Chalk aquifer (Megson, 1992, 1998). Caillet (1998), however, suggested that dipping oil-water contacts in Chalk fields also could be caused by either reservoir heterogeneities and variations in capillary pressures, or by structural tilting and low oil permeability near the oil-water contact. As pointed out by Darby et al. (1996), a given pressure gradient presents only a potential for fluid flow. Whether fluid flow does occur depends on permeability and time.

The burial anomaly, dZ_B, generally is smaller than the thickness of the upper Post Chalk Group, Δz_{up}, and consequently a part of the late Cenozoic loading has led to compaction of the Chalk, and to a reduced burial anomaly (equation 5; Figure 17C). Thus, a net drainage has taken place to account for the partial compaction. The Chalk is found to dewater slowly below the Cenozoic depocenter, whereas this process is more rapid farther from the depocenter, as expressed by the drainage capacity, DC, a measure of the ratio between dZ_B and Δz_{up} (equation 6). The drainage capacity increases from only 0–10% around the Ekofisk field to about 60%

for the Dan field (Table 3). This difference in drainage capacity may be explained by the decrease in seal thickness from approximately 1500 to 600 m when moving from the Ekofisk to the Dan field. We get $dZ_B = \Delta z_{up} \times \Delta z_{low}/1600$ by combining the linear trend between DC and Δz_{low}, the thickness of the sealing lower Post Chalk Group, and the definition of the drainage capacity (equation 6; Figure 18A). The Chalk burial anomaly is thus proportional to the product of the thickness of the upper part of the overburden (which induces the overpressure due to undercompaction), and the thickness of the lower part (which determines the degree of overpressure retention).

Vertical flow through the lower Tertiary shales must be the dominant migration route to explain the dependency of drainage on seal thickness and, consequently, lateral flow in the Chalk must be negligible on a regional scale. This scenario is in agreement with the conclusions for the UK sector by Cayley (1987), who argued that the Chalk would lose fracture permeability away from anticlines, by Darby et al. (1996), who considered the Chalk as a regional aquitard, and by Caillet (1998), who found the pressure system in the Greater Ekofisk area to be controlled by seal efficiency and the continuing compaction due to burial. The lack of regional hydraulic communication within the Chalk also may be caused by discontinuity of permeable beds related to the diversity and the complex depositional history of the Chalk (e.g., Kennedy, 1987). Vertical migration through the Tertiary overburden is evidenced by gas clouds observed on seismic data above pronounced structures (Cayley, 1987; Megson, 1992; Andersen, 1995; Caillet et al., 1997). Cartwright (1994) found evidence for episodic, basinwide fluid expulsion from overpressured Tertiary shales in the North Sea Basin by analyzing small, closely spaced extensional faults from seismic sections.

Presence of thick and continuous Paleocene sand sheets overlying the Chalk determines if the Chalk is normally pressured (Cayley, 1987; Andersen, 1995; Darby et al., 1996; Osborne and Swarbrick, 1997). This condition also supports the conclusion that the Chalk drains vertically. Indeed, the hydraulic transmissivity of the Chalk must be small to maintain the observed high lateral differences in overpressure. This difference is about 10 MPa over the 40 km between the Danish wells Mona-1 and Elna-1, and data from intervening wells show that the difference is built up continuously, unaffected by the fault boundary of the Mesozoic Central Graben (Figures 10, 19). The fault boundaries do not act as primary pressure seals (Scholle, 1977) in a pressure system determined by vertical sealing and migration. The 1995 Siri discovery in lower Tertiary sandstones 25 km from the Central Graben proved long-distance eastward migration of hydrocarbons from Jurassic source rocks located within the graben, similar to the well-known westward hydrocarbon migration (Figure 10) (Cayley, 1987; Danish Energy Agency, 1996).

Are Chalk Pressure Compartments Only of Field Size?

A pressure compartment is defined by a constant level of overpressure according to Bradley and Powley (1994), and is seen by them as a body of rock containing overpressured fluids that are internally in free hydraulic communication. A hydrostatic gradient for a formation within an area is certainly a characteristic of hydrostatic communication, but is an ambiguous indicator of such communication. In the central North Sea, the main factors determining the Chalk overpressure are the load of the upper overburden and the thickness and sealing quality of the lower overburden. These factors change over long distances, and may indirectly lead to uniform overpressure in the Chalk within an area.

In the Danish Central Graben Chalk, three geographically coherent pressure compartments may be defined by having overpressures of 7 ±1, 9 ±1, and 15 ±1 MPa (compartments A, B, and C, Figure 12; Table 3). The compartments with higher pressures are closer to the Cenozoic depocenter, and within each compartment the pressure is gradually changing toward the next compartment; these compartments are about 40 km across, whereas the Chalk fields are 2–6 km wide. In compartment A, all wells fall on the main trend of drainage vs. seal thickness, as do the wells in compartment B, apart from the Ruth-1 well (Figure 18B). The constant overpressure within the compartments may be explained by the variations of the overburden. In compartment C, only one of five wells defining the compartment falls on the trend. The four remaining wells in compartment C (e.g., Nora-1, T-1) and the Ruth-1 wells all have relatively low drainage values (equation 7), suggesting that other than the regional mechanisms add to the overpressure. The Ruth-1 and T-1 wells are located over pronounced diapirs; therefore, hydrocarbon buoyancy or hydraulic connection to the nearby, more deeply buried Chalk may have elevated the pressure in these wells.

Conclusions Regarding Chalk Overpressure

The use of Chalk velocities to outline and estimate overpressure, presented here for the first time, show that Chalk compaction is stress induced to great depths. The causal relationship between overpressure and undercompaction of the North

Sea Chalk and the rapid, late Cenozoic burial of the Chalk are illustrated by the areal overlap of these occurrences (Figure 10).

Three sources contribute to the overpressure in the North Sea Chalk: (1) disequilibrium compaction, (2) transference of overpressure generated by volume-expansion processes in the pre-Chalk section or by short-range hydraulic communication with deeper buried Chalk, and (3) hydrocarbon buoyancy. Disequilibrium compaction contributes about 80% of the Chalk overpressure in the central North Sea (Figure 17B), and the overpressure is on the order of the effective load of the upper Post Chalk Group (the post-mid-Miocene sediments) (Figure 17A). The effective stress exerted on the Chalk has decreased after its present state of compaction was attained, as evidenced by tension fractures in the Chalk. This unloading may be explained by late transference of brine sourced by processes such as gas generation in the pre-Chalk section and by buoyancy of late-emplaced hydrocarbons. Vertical pressure communication in the hydrocarbon phase may explain the drop in overpressure with depth in the Greater Ekofisk area.

The degree to which overpressure generated by the effective load of the upper Post Chalk Group is retained in the Chalk depends on the thickness and the sealing capacity of the lower Post Chalk Group (Figure 18). This dependency suggests that lateral flow in the Chalk is negligible on a regional scale; furthermore, the almost constant overpressure in the Chalk within areas about 40 km across may be explained by the small, local variations of the overburden rather than by hydraulic communication (Figure 12). Consequently, the definition of pressure compartments by Bradley and Powley (1994) appears to be misleading when it is applied to the North Sea Chalk. The Chalk is consequently found to constitute a regional aquitard within the central North Sea, it has been suggested for the UK sector (Cayley, 1987; Darby et al., 1996), and the hydrodynamic model of long-distance migration within the Chalk in the Danish Central Graben is consequently rejected (Damtoft et al., 1992; Megson, 1992). The paradox of the Chalk acting as a local aquifer and a regional aquitard may be explained by deterioration of permeability away from structures and by discontinuity of permeable beds. The pressure gradients away from the late Cenozoic depocenter are important for the secondary migration of hydrocarbons in the area, but long-distance migration is possible only where carrier beds such as the Tertiary sandstones are present.

The level of overpressure in the petroleum system of the central North Sea is a result of dynamic processes, as was pointed out by Darby et al. (1996). I have demonstrated how Chalk overpressure evolves over time as the sedimentary load is increased, as compaction fluids are expelled vertically, and as fluids are added from the pre-Chalk synrift sediments (Figure 19).

CONSEQUENCES FOR DEPTH CONVERSION

Semiregional velocity-depth trends have been determined for the Chalk in the Danish Basin and the Danish Central Graben (Figures 2C, 7B) (Japsen, 1994). The trends are offset, and both are characterized by smaller velocity-depth gradients than the normal trend, V_N (equation 8) (1.1 and 0.7, respectively, as opposed to mainly 2 m/s/m). The shallow data ($z < 1500$ m) are from the eastern North Sea Basin that was affected by up to 1000 m of Neogene erosion (Japsen, 1993a) (Figure 9). The shallowest data represent wells from the basin margin where the erosion is deepest. The deep data ($z > 1500$ m) are from the central North Sea where overpressure leads to low velocities relative to depth (Figure 10). The deepest data represent wells from the basin center where overpressure is maximum. Consequently, the two semiregional trends deviate the most from the normal trend near the surface and at great depths.

The apparent depth range related to the observed velocity range becomes enlarged in both cases. The apparent velocity gradients (velocity range divided by depth range) for the resulting semiregional trends thus become smaller than those of the normal velocity-depth trend; however, across smaller areas where the burial anomaly (due to regional erosion or to overpressure) is nearly constant, differences in burial match the difference in effective stress exerted on the rock. Local velocity variations thus are determined by the normal velocity gradient and not by the semiregional gradient. The normal velocity gradient should be used in depth conversion as it is in velocity-anomaly depth conversion (Japsen, 1993a). In this method, a map of velocity anomalies for a given layer is used to tie a linear velocity-depth model to well data by adding the velocity anomaly to the expression $V = V_0 + k \times z$. Substitution of dV by $-dZ_B \times k$ (equation 2), yields $V = V_0 + k \times z + dV = V_0 + k(z - dZ_B) = V_0 + k \times z_N$ (Figure 5). Velocity variations are thus calculated at z_N, the normalized depth of the layer (the depth predicted by the normal velocity-depth trend for the measured velocity), which means that the local effect of either regional erosion or overpressure is taken into account.

DISCUSSION

The North Sea Chalk is fairly homogeneous on a regional scale (e.g., Kennedy, 1987; Ziegler, 1990), but differences in clay and flint content and local occurrences of facies such as bryozoan mounds, as well as resedimentation, have caused differences in the primary rock material (e.g., D'Heur, 1986; Kennedy, 1987; Taylor and Lapre, 1987; Maliva and Dickson, 1992; Surlyk, 1997). Salt diapirism and influx of hydrocarbons are secondary agents of strong, but localized, alterations of the physical properties of the Chalk. Finally, as I have shown, variations of the burial history of the Chalk across the North Sea Basin have induced major, regional deviations from normal compaction (cf. Scholle, 1977; Bulat and Stoker, 1987; Maliva and Dickson, 1992; Hillis, 1995a). A wide variation is consequently revealed when Chalk interval velocities from 845 North Sea wells are plotted against depth (Figure 7A). The influence of minor amounts of clay on the acoustic properties of chalk is not well established, but the velocity of shale in the North Sea Basin (Hansen, 1996) is below that of pure chalk. The difference is about 2000 m/s at a depth of 2500 m in accordance with the velocity anomalies observed for the shaly Upper Cretaceous interval south of the Viking Graben (Figure 8, equation 8). The Chalk Group is treated as one unit in this study because a subdivision was not possible due to the lack of relevant data, but a subdivision would set the focus on differences within the Chalk, and calculation of interval velocity over thinner units would result in a wider scatter.

The maps of velocity and burial anomalies for the Chalk represent a twofold averaging to suppress deviations from the mean conditions (Figures 8, 9, 10B), first by calculating the mean velocity of the Chalk section in each well (typically over hundreds of meters), and second by smooth contouring. Many wells drilled with Chalk objectives are drilled on structural highs on the top Chalk surface and are not structurally representative. Relative to the basinwide relief of the Chalk of more than 3000 m, that of nondiapiric structures is small; for example, less than 200 m for the Dan field (Britze et al., 1995b). Data from wells drilled on or near salt diapirs are omitted from the mapping to emphasize the regional trends; however, other outliers may not fit the contouring based on the kriging parameters. The standard deviation of Chalk burial anomalies may well be on the order of the 260 m found for shale by Hansen (1996).

Anselmetti and Eberli (1997) found little correlation between velocity and depth for pure carbonate rocks based on an observed velocity inversion in two drill holes of about 500 m penetrating carbonate reefs on the Great Bahama Bank; however, because chalk is dominated by stable, low-magnesium calcite, a wide depth interval of the burial diagenesis is controlled by compaction (Scholle, 1977; Borre and Lind, in press). In contrast, the Great Bahama Bank sediments are dominated by metastable aragonite and dolomite (Anselmetti and Eberli, 1997) prone to early cementation, and a compaction-controlled burial diagenesis will not take place.

The three sonic logs in Figure 11 illustrate how measured chalk velocities vary relative to the suggested normal trend. One log is from pelagic carbonate deposits from the stable Ontong Java Platform, and two logs are from the Chalk Group at the eastern margin and the central part of the North Sea Basin. The sonic logs from the Chalk Group are also shown shifted downward and upward, respectively, to a position of zero burial anomaly, resulting in an agreement between the logs.

CONCLUSIONS

The normal velocity-depth trend for the Chalk Group is formulated as four linear segments to describe how the velocity of Chalk in general increases slowly from about 1600 m/s at the sea bed to 2700 m/s at a depth of 1100 m, and then steeply to about 4900 m/s at a depth of 2250 m, and then more slowly to higher velocities beyond that depth. Simple mathematical expressions fail to match the depth-dependent increase of Chalk velocity as porosity approaches zero. Regional erosion and overpressure lead to an apparent reduction of the velocity-depth gradient. The gradient of the normal trend, however, is a measure of the stress-dependency of velocity and should be used in depth conversion.

The depth dependency of Chalk compaction previously has been approximated by single mathematical functions, and these were based on more restricted databases than this study (Appendix 2) (Sclater and Christie, 1980; Bulat and Stoker, 1987; Hillis, 1995a). The upper part of Hillis's (1995a) linear transit time-depth curve differs, however, only slightly from the suggested trend. Sclater and Christie's (1980) exponential porosity-depth curve provides a general description of the porosity reduction, but fails to account for depth variations in the compaction process. Porosities higher than 40% appear to be preserved to a depth of 1 km during normal compaction. Below this depth, the steep increase in Chalk velocity is interpreted to correspond to the onset of calcite cementation (Borre and Lind, in press).

Chalk interval velocities are readily available from most of the North Sea Basin. A basinwide map of the Chalk velocity anomalies relative to the suggested trend reveals a coherent pattern of the positive and negative anomalies that reflect the burial history of the Chalk during the Cenozoic, except south of the Viking Graben where a high clastic content reduces Chalk velocities. The velocity anomalies and the corresponding burial anomalies of ±1 km across the North Sea relate to two physical processes affecting the velocity-depth relation for the Chalk: (1) removal of up to 1 km of overburden along the western and eastern margins of the basin due to Neogene uplift and erosion and (2) overpressure within the Chalk exceeding 10 MPa that was induced by rapid, late Cenozoic burial where the lower Tertiary is sealing.

The agreement that I have demonstrated between the Chalk burial anomalies and these physical processes provides evidence that the suggested normal velocity-depth trend reflects normal compaction with depth for the Chalk Group. This emphasizes the information value of the vast well data set of interval velocities if the data set is combined with a constrained normal velocity-depth trend.

APPENDIX 1: LIST OF SYMBOLS

B_E	Post-exhumational burial (m)
DC	Net drainage capacity (equation 6) (%)
$DC_{\Delta P}$	Net drainage capacity relative to overpressure (equation 7) (%)
g	Gravitational acceleration 9.807 (m/s²)
itt	Interval transit time (s/m)
itt_f	Interval transit time of pore fluid (s/m)
itt_m	Interval transit time of matrix (s/m)
k	Velocity-depth gradient (m/s/m)
P	Formation pressure (Pa)
P_H	Hydrostatic pressure (Pa)
ΔP	Formation overpressure = $P - P_H$ (Pa)
ΔP_{buoy}	Overpressure generated by buoyancy (Pa)
ΔP_{comp}	Overpressure generated by compaction disequilibrium (equation 5) (Pa)
ΔP_{trans}	Overpressure generated by transference (redistribution of overpressure) (Pa)
S	Stress exerted by the load of the overburden per unit area (Pa)
ΔT	Two-way traveltime thickness of a layer (s)
V	Instantaneous velocity (m/s)
V_i	Interval velocity (m/s)
V_0	Velocity at the surface (m/s)
V_f	Velocity of pore fluid (m/s)
V_m	Velocity of matrix (m/s)
V_N	Normal velocity-depth trend (for the Chalk)
dV	Velocity anomaly relative to a normal velocity depth trend (equation 1) (m/s)
z	Depth (velocity data is below sea bed; pressure data is below sea level) (m)
z_m	Midpoint depth of a layer (below sea bed) (m)
z_t	Depth to top of a layer (below sea bed) (m)
z_b	Depth to base of a layer (below sea bed) (m)
z_{miss}	Missing overburden section removed by erosion (equation 3) (m)
z_N	Normalized depth corresponding to normal compaction based on V_N
dZ_B	Burial anomaly relative to a normal velocity depth trend (equation 5) (m)
Δz	Thickness of a layer (m)
Δz_{up}	Thickness of the upper Post Chalk Group (Figure 1) (m)
Δz_{low}	Thickness of the lower Post Chalk Group (Figure 1) (m)
ϕ	Porosity (%)
ρ_b	Mean bulk density (wet) of the overburden (kg/m³)
ρ_f	Mean density of pore fluid in the overburden (kg/m³)
$\Delta\rho_{up}$	Mean density contrast of the upper overburden ($=[\rho_b - \rho_f]_{up}$) (kg/m³)
σ	Effective stress = $S - P$ (Pa)
σ_{up}	Effective load of the upper overburden (equation 4) (Pa)

Conversion of Units

1 MPa = 145 psi

1 × 10³ kg/m³ mwe (mud weight equivalent) = 1 g/cm³ mwe = 9.807 MPa/km = 0.4335 psi/ft

APPENDIX 2: COMPARISON OF COMPACTION TRENDS FOR CHALK

Scholle (1977, p. 991) demonstrated that burial depth is the "only major factor which consistently correlates with regional porosity loss in chalks." He presented a plot of the most typical porosity-depth relations for chalks from 70% at sea bed to about 10% at 2200 m below the sea bed based on data from the Deep-Sea Drilling Project, the Scotian Shelf, and the well NL L16-1. Sclater and Christie (1980) extended the shallow part of Scholle's trend to pass through the lowest porosities in two normally pressured wells (UK 15/16-1, UK 15/28-2), and suggested an exponential normal porosity-depth trend, ϕ_{SC}:

$$\phi_{sc} = 0.7 \times e^{-0.71 \times 10^{-3} \times z} \quad (9)$$

The porosities at depth ($z \approx 3000$ m) were taken as the minimum porosity calculated from sonic logs using the velocity-porosity relations for limestone of Schlumberger (1974). V_N, however, does not pass through the data point for well UK 15/28-2 (equation 8, Figure 20A; Table 2) because the data point on Figure 20A indicates mean velocity, whereas ϕ_{SC} is defined from maximum velocity (Figure 8).

Bulat and Stoker (1987) estimated removed overburden based on interval velocities for several stratigraphic units in the UK southern North Sea by identifying data representing normal compaction as having the lowest velocity at a given depth. A linear velocity-depth trend was found to be a valid approximation for the depths considered, and V_{BS} for the Upper Cretaceous (approximately the Chalk Group) was estimated by Bulat and Stoker (1987, their figure 4b) as

$$V_{BS} = 2145 + 0.75 \times z \quad (10)$$

($z_m < 2000$ m for most wells). V_{BS} and V_N cross for $V = 3090$ m/s, and erosion becomes underestimated for smaller velocities due to the lack of data representing normal compaction because the Chalk is now above maximum burial in most parts of the basin where $z_m < 1500$ m (Figure 20A).

Hillis (1995a) proposed a normal trend, V_H, for the upper and middle Chalk in the UK southern North Sea based on the principles of Bulat and Stoker (1987), and furthermore assumed the velocity of Chalk at zero depth to be comparable to the velocity of saline water. Hillis (1995a) thus arrived at higher estimates of erosion than Bulat and Stoker (1987). The Cenomanian lower Chalk was not included due to lateral facies variations, whereas the Danian Chalk generally is absent in his study area. The Chalk in the wells thus selected as references (UK 38/25-1, UK 44/29-1A) is also close to normal compaction relative to V_N. Based on Bulat and Stoker's (1987) assumption of linearity of velocity (not transit time) with depth, Hillis (1995a) found the

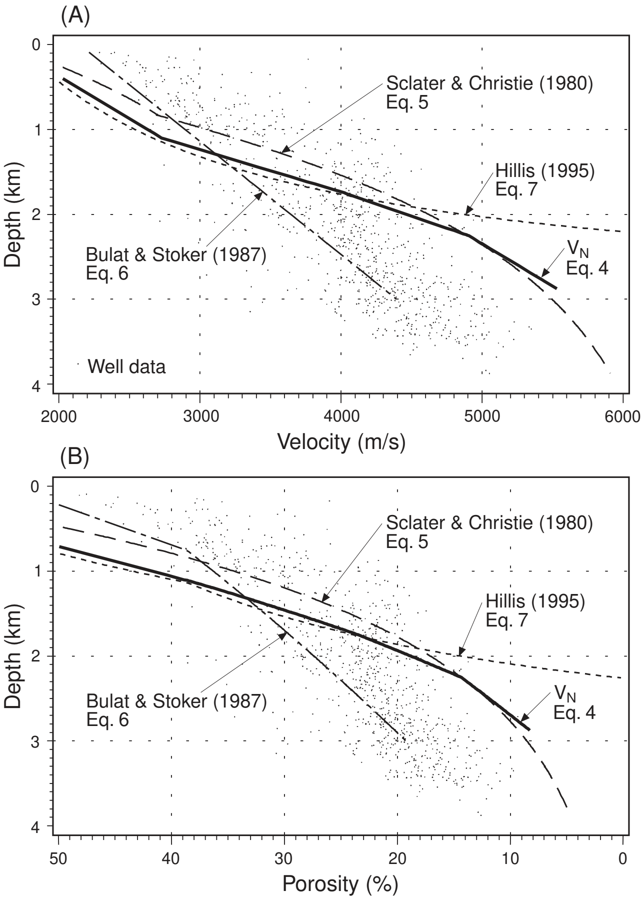

Figure 20—Comparison of normal compaction trends for the North Sea Chalk. V_N matches the general trend of Sclater and Christie's (1980) curve, and the trend of Hillis (1995a) for V < 4250 m/s. (A) Velocity vs. depth. (B) Porosity vs. depth. Conversion between porosities and velocities based on equation 15 (see Appendix 3).

following relation between interval transit time, *itt* (µs/ft), and depth, *z* (m):

$$itt_H = 0.3048 \times 10^6/V_H = 177.5 - 57.5 \times 10^{-3} \times z \quad (11)$$

V_H matches V_N along segments A, B, and a part of C ($V < 4250$ m/s) (Figure 20A). V_H fails, however, to match data from the deeply buried parts of the North Sea (segments C, in parts, and D) because V_N is more than 100 m below V_H for $V > 4250$ m/s. Hillis's (1995a) assumption of linearity between transit time and depth implies that transit time becomes zero and then negative at depth as indicated by the accelerating increase in V_H with z (Figure 20A). The match between the upper parts of V_H and V_N means that the validity of Hillis's argumentation is confirmed for the entire Chalk Group for moderate velocities, and with a larger data set; however, Hillis's trend was based on wells with average depth around 1000 m, and because he has few data points with $V > 4250$ m/s, his conclusions regarding the exhumation of the UK southern North Sea are not disputed.

Hillis et al. (1994) established normal velocity-depth trends for the Upper Cretaceous Hod and Tor chalk in the Inner Moray Firth (quadrants UK 11–13). For each formation, the transit time-depth gradient was taken as the mean sonic gradient, and the well with the lowest velocity for its burial as reference (UK 13/30-1, UK 13/30-2). The problem in their study is whether "the reference wells in quadrant 13/30 themselves are above their maximum burial depth" (Hillis et al., 1994, p. 289). The estimated Hod and Tor trends are well above V_H (Hillis, 1995a) and, respectively, 800 and 500 m above V_N for $V = 4300$ m/s.

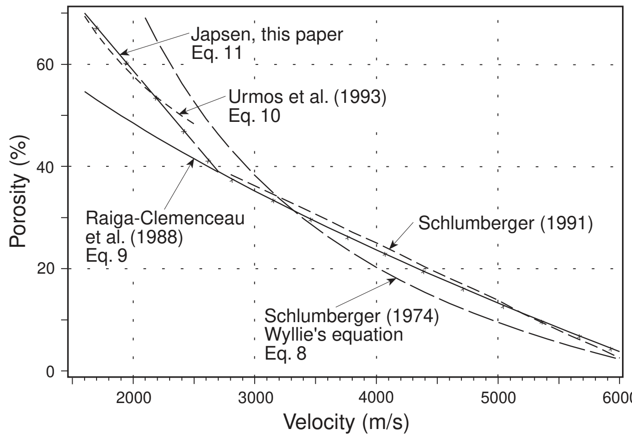

Figure 21—Porosity-velocity relations for chalk. For comparison of normal compaction trends for the North Sea Chalk, the relation of Raiga-Clemenceau et al. (1988) is used for V > 2700 m/s, and for 1600 < V < 2700 m/s, a linear trend matches Ocean-Drilling Program data (Urmos et al., 1993).

APPENDIX 3: VELOCITY-POROSITY CONVERSION FOR CHALK

Wyllie et al. (1956) suggested a general relation between interval transit time, *itt*, and porosity for sedimentary rocks (Figure 21):

$$\phi = (itt - itt_m) / (itt_f - itt_m) \quad (12)$$

where itt_m ($= 1/V_m$) and itt_f ($= 1/V_f$) are the transit times (velocities) for the matrix and the pore fluid, respectively. Schlumberger (1974) applied Wyllie's equation for chalk with ø < 44%, substituting $V_f = 1615$ m/s and $V_m = 6400$ m/s. Raiga-Clemenceau et al. (1988) reported a poor fit between Wyllie's equation and experimental data. They suggested the following alternative relation:

$$\phi = 1 - (V/V_m)^{1/x} \quad (13)$$

where x is an exponent specific to the matrix characteristics. The parameters were estimated from a Chalk data set from the Ekofisk oil field in the central North Sea, and yielded $x = 1.76$ and $V_m = 6403$ m/s. Equation 13 matches within 2 porosity percent the empirical relation for limestones given by Schlumberger (1991) in a revised edition of Schlumberger (1974). Porosities in Raiga-Clemenceau et al.'s (1988) chalk data set were from 10 to 40%, whereas Schlumberger's (1991) chart ranges from 0 to 39%. These porosity-velocity relations are thus not well established for $\phi > 40\%$.

Urmos et al. (1993) found that log data from pelagic carbonate deposits with $48 < \phi < 74\%$ in hole 807 (ODP Leg 130) fitted the empirical relation

$$\phi = (1000/V + 0.1156) / 1.0672 \qquad (14)$$

Urmos et al. (1993) found that this equation did not match deeper water carbonate deposits. Sonic data from hole 807 were used to support the definition of the normal velocity-depth trend for the North Sea Chalk (equation 8).

Normal compaction trends for the North Sea Chalk may be expressed in terms of either porosity-depth (Scholle, 1977; Sclater and Christie, 1980) or velocity-depth relations (Bulat and Stoker, 1987; Hillis, 1995a, and equation 8 in this paper). To enable comparison between this group of trends, a simple relation is developed here to convert porosities to velocities. Raiga-Clemenceau et al.'s (1988) equation 13 provides a relation for the North Sea Chalk matching that of Schlumberger (1991) for $\phi < 40\%$. Above 40% porosity, Raiga-Clemenceau et al.'s (1988) equation is not based on data, contrary to the empirical relation of Urmos et al. (1993) (equation 14). A linear trend matching Urmos et al.'s (1993) observations is suggested here for $1600 < V < 2700$ m/s defined by $V(70\%) = 1600$ m/s and $V(38.9\%) = 2700$ m/s. The latter point corresponds to the prediction of Raiga-Clemenceau et al. (1988). We get the following relationships for comparison of Chalk compaction trends:

$$\begin{aligned} \phi &= 1.15 - 2.83 \times 10^{-4} \times v \qquad 1600 < v < 2700\ m/s \\ \phi &= 1 - (v/6403)^{0.57} \qquad v < 2700\ m/s \end{aligned} \qquad (15)$$

The relatively slow increase in chalk velocity at high porosities (70–40%) indicates that mechanical compaction predominantly takes place, leading to reorganization of the grains. For smaller porosities velocities, increase more rapidly due to stiffer grain contacts.

REFERENCES CITED

Allsop, J. M., and G. A. Kirby, 1985, Estimates of post-Cretaceous uplift in eastern England derived from study of sonic logs, *in* A. Whittaker, D. W. Holliday, and I. E. Penn, eds., Geophysical logs in British stratigraphy: The Geological Society Special Report, p. 17–18.

Andersen, M. A., 1995, Petroleum research in North Sea Chalk: Stavanger, RF-Rogaland Research, 179 p.

Andrews, I. J., et al., 1990, United Kingdom offshore regional report: the geology of the Moray Firth: British Geological Survey, 96 p.

Anselmetti, F. S., and G. P. Eberli, 1997, Sonic velocity in carbonate sediments and rocks, *in* I. Palaz and K. J. Marfurt, eds., Carbonate seismology: Tulsa, Society of Exploration Geophysicists Geophysical Development Series, v. 6, p. 53–74.

Barnard, P. C., and P. S. Cooper, 1983, A review of geochemical data related to the northwest European gas province, *in* J. Brooks, ed., Petroleum geochemistry and exploration of Europe: Geological Society Special Publication, 12, p. 19–33.

Bidstrup, T., 1994, Seismic sequence stratigraphy of the Tertiary in the Danish North Sea. EFP-92 project: basin development of the Tertiary if the Central Trough with emphasis on possible hydrocarbon reservoirs: Copenhagen, Geological Survey of Denmark, v. 5, 25 p.

Boldreel, L. O., and M. S. Andersen, 1993, Late Paleocene to Miocene compression in the Faeroe-Rockall area, *in* J. R. Parker, ed., Petroleum geology of northwest Europe: proceedings of the 4th conference: London, The Geological Society, p. 1025–1034.

Boldreel, L. O., and P. Japsen, eds., (1998), Neogene uplift and tectonics around the North Atlantic: Copenhagen, Geological Survey of Denmark and Greenland, 121 p.

Borre, M., and I. Lind, in press, Chemical and mechanical processes during burial diagenesis of chalk. An interpretation based on specific surface data of deep-sea sediments: Sedimentology, v. 45, no. 4.

Bradley, J. S., and D. E. Powley, 1994, Pressure compartments in sedimentary basins: a review, *in* P. J. Ortoleva, ed., Basin compartments and seals: AAPG Memoir 61, p. 3–26.

Bray, R. J., P. F. Green, and I. R. Duddy, 1992, Thermal history reconstruction using apatite fission track analysis and vitrinite reflectance; a case study from the UK East Midlands and southern North Sea, *in* R. F. P. Hardman, ed., Exploration Britain: geological insights for the next decade: London, Geological Society Special Publication, 67, p. 2–25.

Britze, P., P. Japsen, and C. Andersen, 1995a, Geological map of Denmark; the Danish Central Graben; "Base Chalk" and the Chalk Group (two-way traveltime and depth, interval velocity and isochore): Geological Survey of Denmark Map Series, v. 48, scale 1:200,000, 4 maps, 7 p.

Britze, P., P. Japsen, and C. Andersen, 1995b, Geological map of Denmark; the Danish Central Graben; "Top Chalk" and the Post Chalk Group (two-way traveltime, depth and interval velocity): Geological Survey of Denmark Map Series, v. 47, scale 1:200,000, 3 maps, 7 p.

Buhrig, C., 1989, Geopressured Jurassic reservoirs in the Viking Graben; modelling and geological significance: Marine and Petroleum Geology, v. 6, p. 31–48.

Bulat, J., and S. J. Stoker, 1987, Uplift determination from interval velocity studies, UK, southern North Sea, *in* J. Brooks and K. W. Glennie, eds., Petroleum geology of north-west Europe: London, Graham and Trotman, p. 293–305.

Caillet, G., 1998, Discussion: "Overpressure and hydrocarbon trapping in the Chalk of the Norwegian Central Graben" by G. Caillet et al.: Petroleum Geoscience, p. 182–185.

Caillet, G., N. C. Judge, N. P. Bramwell, L. Meciani, M. Green, and P. Adam, 1997, Overpressure and hydrocarbon trapping in the Chalk of the Norwegian Central Graben: Petroleum Geoscience, v. 3, p. 33–42.

Cameron, T. D. J., J. Bulat, N. Parker, P. Frantsen, C. Laban, and R. T. E. Schüttenheim, 1987, Indefatigable. Solid geology. Sheet 53°N-02°E: Southampton, BGS/RGD, scale 1:250 000, 1 map.

Cameron, T. D. J., A. Crosby, P. S. Balson, D. H. Jeffery, G. K. Lott, J. Bulat, and D. J. Harrison, 1992, United Kingdom offshore regional report: the geology of the southern North Sea: British Geological Survey, 120 p.

Cameron, T. D. J., J. Bulat, and C. S. Mesdag, 1993, High resolution seismic profile through a late Cenozoic delta complex in the southern North Sea: Marine and Petroleum Geology, v. 10, p. 591–599.

Carstens, H., 1978, Origin of abnormal formation pressures in central North Sea Lower Tertiary clastics: The Log Analyst, v. 19, p. 24–28.

Carstens, H., and H. Dypvik, 1981, Abnormal formation pressure and shale porosity: AAPG Bulletin, v. 65, p. 344–350.

Cartwright, J. A., 1994, Episodic basin-wide fluid expulsion from geopressured shale sequences in the North Sea Basin: Geology, v. 22, p. 447–450.

Caston, V. N. D., 1977, Quaternary deposits of the central North Sea: London, Institute of Geological Sciences, v. 77/11, 35 p.

Cayley, G. T., 1987, Hydrocarbon migration in the central North Sea, *in* J. Brooks and K. W. Glennie, eds., Petroleum geology of northwest Europe: London, Graham and Trotman, p. 549–555.

Chalmers, J. A., 1998, Possible Neogene uplift in West Greenland and its relation to sea-floor spreading, *in* L. O. Boldreel and P. Japsen, eds., Neogene uplift and tectonics around the North Atlantic: Copenhagen, Geological Survey of Denmark and Greenland, p. 39.

Chiarelli, A., and F. Duffaud, 1980, Pressure origin and distribution in Jurassic of Viking Basin (United Kingdom–Norway): AAPG Bulletin, v. 64, p. 1245–1250.

Choubert, G., and A. Faure-Murat, 1976, Geological world atlas:

Paris, Unesco, 1:10,000,000, 22 maps.
Christiansen, F. G., H. C. Larsen, C. Marcussen, K. Hansen, H. Krabbe, L. M. Larsen, S. Piasecki, L. Stemmerik, and J. W. Watt, 1992, Uplift study of the Jameson Land basin, East Greenland: Norsk Geologisk Tidsskrift, v. 72, p. 291–294.
Cloetingh, S., F. M. Gradstein, H. Kooi, A. C. Grant, and M. Kaminski, 1990, Plate reorganization; a cause of rapid late Neogene subsidence and sedimentation around the North Atlantic: Journal of the Geological Society, London, v. 147, p. 495–506.
Cope, M. J., 1986, An interpretation of vitrinite reflectance data from the southern North Sea Basin, *in* J. Brooks, J. C. Goff, and B. van Hoorn, eds., Habitat of Palaeozoic gas in N. W. Europe: Geological Society Special Publication, 23, p. 85–98.
Damtoft, K., L. H. Nielsen, P. N. Johannessen, E. Thomsen, and P. R. Andersen, 1992, Hydrocarbon plays of the Danish Central Trough, *in* A. M. Spencer, ed., Generation, accumulation and production of Europe's hydrocarbons; II: Berlin, Springer Verlag, p. 35–58.
Danish Energy Agency, 1996, Oil and gas production in Denmark 1995: Copenhagen, Danish Energy Agency, 64 p.
Darby, D., R. S. Haszeldine, and G. D. Couples, 1996, Pressure cells and pressure seals in the UK Central Graben: Marine and Petroleum Geology, v. 13, p. 865–878.
Davis, B. K., 1987, Velocity changes and burial diagenesis in the chalk of the southern North Sea Basin, *in* J. Brooks and K. W. Glennie, eds., Petroleum geology of north-west Europe: London, Graham and Trotman, p. 307–313.
Day, G. A., B. A. Cooper, C. Andersen, W. F. J. Burgers, H. C. Rønnevik, and H. Schoneich, 1981, Regional seismic structure maps of the North Sea, *in* L. V. Illing and G. D. Hobson, eds., Petroleum geology of the continental shelf of north-west Europe: London, Institute of Petroleum, p. 76–84.
Deegan, C. E., and B. J. Scull, 1977, A standard lithostratigraphic nomenclature from the central and northern North Sea: Institute of Geological Sciences Report, v. 77/25, 36 p.
D'Heur, M., 1986, The Norwegian chalk fields, *in* A. M. Spencer, ed., Habitat of hydrocarbons on the Norwegian continental shelf: London, Graham and Trotman, p. 77–89.
D'Heur, M., 1993, The Chalk as a hydrocarbon reservoir, *in* R. A. Downing, M. Price, and G. P. Jones, eds., The hydrogeology of the Chalk of north-west Europe: Oxford, Claredon Press, p. 250–266.
Dickinson, G., 1953, Geological aspects of abnormal reservoir pressures in Gulf Coast Louisiana: AAPG Bulletin, v. 37, p. 410–432.
Doré, A. G., and L. N. Jensen, 1996, The impact of late Cenozoic uplift and erosion on hydrocarbon exploration: Global and Planetary Change, v. 12, p. 415–436.
England, P., and P. Molnar, 1990, Surface uplift, uplift of rocks, and exhumation of rocks: Geology, v. 18, p. 1173–1177.
Eyles, N., 1996, Passive margin uplift around the North Atlantic region and its role in Northern Hemisphere late Cenozoic glaciation: Geology, v. 24, p. 103–106.
Foged, N., A. Krogsbøll, C. F. Hansen, K. Zinck-Jørgensen, H. F. Christensen, and J. -E. Jepsen, 1995, EFP-93; modelling of stresses and fractures in a reservoir; final report: Copenhagen, Geological Survey of Denmark/Danish Geotechnical Institute, 68 p.
Gaarenstroom, L., R. A. J. Tromp, M. C. de Jong, and A. M. Brandenburg, 1993, Overpressures in the central North Sea: implications for trap integrity and drilling safety, *in* J. R. Parker, ed., Petroleum geology of northwest Europe: proceedings of the 4th conference: London, The Geological Society, p. 1305–1313.
Gatliff, R. W., et al., 1994, United Kingdom offshore regional report: the geology of the central North Sea: British Geological Survey, 114 p.
Glennie, K. W., and P. L. E. Boegner, 1981, Sole pit inversion tectonics, *in* L. V. Illing and G. D. Hobson, eds., Petroleum geology of the continental shelf of north-west Europe: London, Institute of Petroleum, p. 110–120.
Green, P. F., 1986, On the thermo-tectonic evolution of northern England: evidence from fission track analysis: Geological Magazine, v. 123, p. 493–506.
Green, P. F., 1989, Thermal and tectonic history of the East Midlands shelf (onshore UK) and surrounding regions assessed by apatite fission track analysis: Journal of the Geological Society, London, v. 146, p. 755–774.
Green, P. F., I. R. Duddy, R. J. Bray, and C. L. E. Lewis, 1993, Elevated paleotemperatures prior to early Tertiary cooling throughout the UK region: implications for hydrocarbon generation, *in* J. R. Parker, ed., Petroleum geology of northwest Europe: proceedings of the 4th conference: London, The Geological Society, p. 1067–1074.
Håkansson, E., and S. S. Pedersen, 1992, Geologisk kort over den danske undergrund: København, Varv, scale 1:540,000, 1 map.
Hall, P. L., 1993, Mechanisms of overpressuring: an overview, *in* D. A. C. Manning, P. L. Hall, and C. R. Hughes, eds., Geochemistry of clay–pore fluid interactions: London, Chapman and Hall, p. 265–315.
Hall, P. L., 1994, Physical and chemical aspects of the development of overpressuring in sedimentary environments: Clay Minerals, v. 29, p. 425–437.
Hansen, S., 1996, Quantification of net uplift and erosion on the Norwegian Shelf south of 66°N from sonic transit times of shale: Norsk Geologisk Tidsskrift, v. 76, p. 245–252.
Haq, B. U., J. Hardenbol, and P. R. Vail, 1987, Chronology of fluctuating sea levels since the Triassic: Science, v. 235, p. 1156–1167.
Herring, E. A., 1973, North Sea abnormal pressures determined from logs: Petroleum Engineer, p. 72–84.
Hillis, R. R., 1995a, Quantification of Tertiary exhumation in the United Kingdom southern North Sea using sonic velocity data: AAPG Bulletin, v. 79, p. 130–152.
Hillis, R. R., 1995b, Regional Tertiary exhumation in and around the United Kingdom, *in* J. G. Buchanan and P. G. Buchanan, eds., Basin inversion: London, Geological Society Special Publication, 88, p. 167–190.
Hillis, R. R., K. Thomson, and J. R. Underhill, 1994, Quantification of Tertiary erosion in the Inner Moray Firth using sonic velocity data from the Chalk and Kimmeridge Clay: Marine and Petroleum Geology, v. 11, p. 283–293.
Hohn, M. E., 1988, Geostatistics and petroleum geology: New York, van Nostrand Reinhold, 264 p.
Hubbert, M. K., and W. W. Rubey, 1959, Role of fluid pressure in mechanics of overthrust faulting: Geological Society of America Bulletin, v. 70, p. 115–166.
Hunt, J. M., 1990, Generation and migration of petroleum from abnormally pressured fluid compartments: AAPG Bulletin, v. 74, p. 1–12.
Isaksen, D., and K. Tonstad, 1989, A revised Cretaceous and Tertiary lithostratigraphic nomenclature for the Norwegian North Sea: Norwegian Petroleum Directorate Bulletin, v. 5, 59 p.
Japsen, P., 1993a, Influence of lithology and Neogene uplift on seismic velocities in Denmark; implications for depth conversion of maps: AAPG Bulletin, v. 77, p. 194–211.
Japsen, P., 1993b, Outline of the central North Sea overpressured zone based on chalk velocities: Extended Abstracts EAEG 55th Meeting and Technical Exhibition, p. 1–2.
Japsen, P., 1994, Retarded compaction due to overpressure deduced from a seismic velocity/depth conversion study in the Danish Central Trough, North Sea: Marine and Petroleum Geology, v. 11, p. 715–733.
Japsen, P., 1997, Regional Neogene exhumation of Britain and the western North Sea: Journal of the Geological Society, London, v. 154, p. 239–247.
Japsen, P., 1998, Discussion: "Overpressure and hydrocarbon trapping in the Chalk of the Norwegian Central Graben" by G. Caillet et al.: Petroleum Geoscience, p. 184.
Japsen, P., and C. Langtofte, 1991, Geological map of Denmark; the Danish Basin; "Base Chalk" and the Chalk Group; two-way traveltime and depth, thickness and interval velocity: Geological Survey of Denmark Map Series, v. 29, scale 1:400,000, 4 maps and 4 p.
Jensen, L. N., and B. J. Schmidt, 1992, Late Tertiary uplift and erosion

in the Skagerrak area; magnitude and consequences: Norsk Geologisk Tidsskrift, v. 72, p. 275–279.

Jensen, L. N., and B. J. Schmidt, 1993, Neogene uplift and erosion offshore south Norway; magnitude and consequences for hydrocarbon exploration in the Farsund Basin, *in* A. M. Spencer, ed., Generation, accumulation, and production of Europe's hydrocarbons, III: Berlin, Springer Verlag, p. 79–88.

Jensen, L. N., F. Riis, and R. Boyd, 1992, Post-Cretaceous uplift and sedimentation along the western Fennoscandian shield: Norsk Geologisk Tidsskrift, v. 72, 338 p.

Johnson, H., and G. K. Lott, 1993, 2. Cretaceous of the central and northern North Sea: lithostratigraphic nomenclature of the UK North Sea: British Geological Survey, 169 p.

Johnson, H., P. C. Richards, D. Long, and C. C. Graham, 1993, United Kingdom offshore regional report: the geology of the northern North Sea: British Geological Survey, 110 p.

Jordt, H., J. I. Faleide, K. Bjørlykke, and M. T. Ibrahim, 1995, Cenozoic sequence stratigraphy of the central and northern North Sea Basin: tectonic development, sediment distribution and provenance areas: Marine and Petroleum Geology, v. 12, p. 845–879.

Kennedy, W. J., 1987, Sedimentology of Late Cretaceous–Palaeocene chalk reservoirs, North Sea Central Graben, *in* J. Brooks and K. W. Glennie, eds., Petroleum geology of northwest Europe: London, Graham and Trotman, p. 469–481.

Knox, R. W. O., and S. Holloway, 1992, Paleogene of the central and northern North Sea: lithostratigraphic nomenclature of the UK North Sea: British Geological Survey, 133 p.

Knudsen, P., 1993, Integrated inversion of gravity data: National Survey and Cadastre: Denmark, Geodetic Division Technical Teport, v. 7, 52 p.

Kockel, F., 1988a, The NW-European Tertiary basin; base post-Danian Tertiary; structural contour map, 1:2,500,000, *in* R. Vinken, ed., The northwest European Tertiary basin: Geologisches Jahrbuch, Reihe A, v. 100, 1 map.

Kockel, F., 1988b, The NW-European Tertiary basin; base "Middle Miocene;" structural contour map (Reinbek fm. = Base Nordland Group), 1:2,500,000, *in* R. Vinken, ed., The northwest European Tertiary basin: Geologisches Jahrbuch, Reihe A, v. 100, 1 map.

Konradi, P., 1995, Foraminiferal biostratigraphy of the post middle Miocene in two boreholes in the Danish North Sea, *in* O. Michelsen, ed., Proceedings of the 2nd symposium on marine geology: Geological Survey of Denmark Series C, v. 12, p. 101–112.

Kooi, H., M. Hettema, and S. Cloetingh, 1991, Lithospheric dynamics and the rapid Pliocene–Quaternary subsidence phase in the southern North Sea basin: Tectonophysics, v. 192, p. 245–259.

Kreizer, J., and W. J. Letsch, 1963, Geology of the Tertiary in the Netherlands: Transactions of the Jubilee Convention, Part Two, Geologische serie, v. 21-2, p. 147–172.

Laursen, G. V., 1992, Foraminifera of the eastern North Sea, *in* G. V. Laursen, C. Heilmann-Clausen, and E. Thomsen, eds., Cenozoic biostratigraphy of the eastern North Sea based on foraminifera, dinoflagellates, and calcareous nannofossils: Århus, Geologisk Institut, p. 1–68.

Leonard, R. C., 1993, Distribution of sub-surface pressure in the Norwegian Central Graben and applications for exploration, *in* J. R. Parker, ed., Petroleum geology of northwest Europe: proceedings of the 4th conference: London, The Geological Society, p. 1295–1303.

Lewis, C. L. E., P. F. Green, A. Carter, and A. J. Hurford, 1992, Elevated K/T paleotemperatures throughout northwest England; three kilometres of Tertiary erosion?: Earth and Planetary Science Letters, v. 112, p. 131–145.

Lidmar-Bergström, K., 1996, Long term morphotectonic evolution in Sweden: Geomorphology, v. 16, p. 33–59.

Lind, I., 1988, Stylolite formation: Ph.D. dissertation, Danmarks Tekniske Højskole, Denmark, 299 p.

Lind, I., 1993, Stylolites in chalk from Leg 130, Ontong Java Plateau, *in* W. H. Berger et al., eds., Proceedings of the Ocean Drilling Program. scientific results: Ocean Drilling Program, v. 130, p. 445–449.

Magara, K., 1978, Compaction and fluid migration; practical petroleum geology: Amsterdam, Elsevier, 319 p.

Maliva, R. G., and J. A. D. Dickson, 1992, Microfacies and diagenetic controls of porosity in Cretaceous–Tertiary chalks, Eldfisk field, Norwegian North Sea: AAPG Bulletin, v. 76, p. 1825–1838.

Marie, J. P. P., 1975, Rotliegendes stratigraphy and diagenesis, *in* A. W. Woodland, ed., Petroleum and the continental shelf of northwest Europe: London, Applied Science, p. 205–211.

Mathiesen, A., F. G. Christiansen, T. Bidstrup, C. Marcussen, G. Dam, S. Piasecki, and L. Stemmerik, 1995, Modeling of hydrocarbon generation in the Jameson Land basin, East Greenland: First Break, v. 13, p. 329–341.

McKenzie, D. P., 1978, Some remarks on the development of sedimentary basins: Earth and Planetary Science Letters, v. 40, p. 25–32.

Megson, J. B., 1992, The North Sea chalk play; examples from the Danish Central Graben, *in* R. F. P. Hardman, ed., Exploration Britain: geological insights for the next decade: London, Geological Society Special Publication, 67, p. 247–282.

Megson, J. B., 1998, Discussion: "Overpressure and hydrocarbon trapping in the Chalk of the Norwegian Central Graben" by G. Caillet et al.: Petroleum Geoscience, p. 181–182.

Meyer, W., 1983, Pre-Quaternary uplift in the central part of the Rheinish Massif, *in* K. Fuchs, K. von Gehlen, H. Mälzer, H. Murawski, and A. Semmel, eds., Plateau uplift; the Rheihish shield—a case story: Berlin, Springer-Verlag, p. 39–46.

Michelsen, O., 1982, Geology of the Danish Central Graben: Geological Survey of Denmark, Series B, v. 8, 135 p.

Michelsen, O., and L. H. Nielsen, 1993, Structural development of the Fennoscandian border zone, offshore Denmark: Marine and Petroleum Geology, v. 10, p. 124–134.

Michelsen, O., E. Thomsen, M. Danielsen, C. Heilmann-Clausen, H. Jordt, and G. V. Laursen, 1996, Cenozoic sequence stratigraphy in the eastern North Sea, *in* P. C. Graciansky, T. Jaquin, and P. R. Vail, eds., Mesozoic and Cenozoic sequence stratigraphy of the western European basins, 2: Stavanger, NPF Special Publication, 5, p. 415–427.

Nederlandse Aardolie Maatschappij B. V. (NAM) and Rijks Geologische Deinst (RDG), 1980, Stratigraphic nomenclature of the Netherlands: Verhandelingen van het Koninklijk Nederlands Geologisch Mijnbouwkundig Genootschap, v. 32, 77 p.

Nielsen, L. H., and P. Japsen, 1991, Deep wells in Denmark, 1935–1990; lithostratigraphic subdivision: Geological Survey of Denmark, Series A, v. 31, 179 p.

Nielsen, O. B., 1979, A sedimentological mineralogical investigation of the Tertiary sediments from the borehole M-2X in Central Trough, North Sea: Årbog: København, Danmarks Geologiske Undersøgelse, p. 41–50.

Nielsen, O. B., S. Sørensen, J. Thiede, and O. Skarbo, 1986, Cenozoic differential subsidence of North Sea: AAPG Bulletin, v. 70, p. 276–298.

Osborne, M. J., and R. E. Swarbrick, 1997, Mechanisms for generating overpressure in sedimentary basins: a reevaluation: AAPG Bulletin, v. 81, p. 1023–1041.

Penny, B., 1991, The Heather field, block 2/5, UK North Sea, *in* I. L. Abbott, ed., United Kingdom oil and gas fields, 25 years commemorative volume: Geological Society Memoir, p. 127–134.

Petersen, H. I., L. H. Nielsen, T. Bidstrup, and E. Thomsen, in press, A regional coalification curve for the Danish Basin and Fennoscandian border zone, and estimates of burial depth and uplift of Lower–Middle Jurassic strata in the Fennoscandian border zone, *in* J. Ineson and F. Surlyk, eds., The Jurassic of Denmark and Greenland: Copenhagen, Geological Survey of Denmark and Greenland.

Raiga-Clemenceau, J., J. P. Martin, and S. Nicoletis, 1988, The concept of acoustic formation factor for more accurate porosity determination from sonic transit time data: The Log Analyst, v. 29, p. 54–60.

Riis, F., 1996, Quantification of Cenozoic vertical movements of

Scandinavia by correlation of morphological surfaces with offshore data: Global and Planetary Change, v. 12, p. 331–357.
Riis, F., and L. N. Jensen, 1992, Introduction; measuring uplift and erosion; proposal for a terminology: Norsk Geologisk Tidsskrift, v. 72, p. 223–228.
Rohrman, M., and P. van der Beek, 1996, Cenozoic postrift domal uplift of North Atlantic margins: an asthenospheric diapirism model: Geology, v. 24, p. 901–904.
Rohrman, M., P. van der Beek, P. Andriessen, and S. Cloetingh, 1995, Meso–Cenozoic morphotectonic evolution of southern Norway: Neogene domal uplift inferred from apatite fission track thermochronology: Tectonics, v. 14, p. 700–714.
Rubey, W. W., and M. K. Hubbert, 1959, Role of fluid pressure in mechanics of overthrust faulting, II: Geological Society of America Bulletin, v. 70, p. 167–206.
Schlumberger, 1974, Log interpretation, volume II—applications: New York, Schlumberger Ltd., 116 p.
Schlumberger, 1991, Log interpretation charts: Schlumberger Educational Services, 171 p.
Scholle, P. A., 1977, Chalk diagenesis and its relation to petroleum exploration; oil from chalks, a modern miracle?: AAPG Bulletin, v. 61, p. 982–1009.
Sclater, J. G., and P. A. F. Christie, 1980, Continental stretching; an explanation of the post-mid-Cretaceous subsidence of the central North Sea basin: Journal of Geophysical Research, v. 85, p. 3711–3739.
Shipboard Scientific Party, 1991, Site 807, *in* L. W. Kroenke, W. H. Berger, T. R. Janecek, and L. A. Mayer, eds., Proceedings of the Ocean Drilling Program, initial reports: Ocean Drilling Program, v. 130, p. 369–493.
Sigmond, E. M. O., 1993, Bedrock map of Norway and adjacent ocean areas: Oslo, Geological Survey of Norway, scale 1:3,000,000, 1 map.
Slotnick, M. M., 1936, On seismic computations, with applications, II: Geophysics, v. 1, p. 299–305.
Sørensen, J. C., and O. Michelsen, 1995, Upper Cenozoic sequences in the southeastern North Sea Basin: Bulletin of the Geological Society of Denmark, v. 42, p. 74–95.
Sørensen, S., M. Jones, R. F. P. Hardman, W. K. Leutz, and P. H. Schwarz, 1986, Reservoir characteristics of high and low productivity chalks from the central North Sea, *in* A. M. Spencer, ed., Habitat of hydrocarbons on the Norwegian continental shelf; proceedings of an international conference: London, Graham and Trotman, p. 91–110.
Sorgenfrei, T., and A. Buch, 1964, Deep test in Denmark, 1935–1959: Danmarks Geologiske Undersøgelse, III række, v. 36, 146 p.
Spencer, A. M., 1987, Geology of the Norwegian oil and gas fields: London, Graham and Trotman, 360 p.
Spjeldnæs, N., 1975, Palaeogeography and facies distribution in the Tertiary of Denmark and surrounding areas: Norges Geologiske Undersøgelse Bulletin, v. 316, p. 289–311.
Stewart, S. A., and H. W. Bailey, 1996, The Flamborough Tertiary outlier, UK southern North Sea: Journal of the Geological Society, London, v. 153, p. 163–173.
Stuevold, L. M., and O. Eldholm, 1996, Cenozoic uplift of Fennoscandia inferred from a study of the mid-Norwegian margin: Global and Planetary Change, v. 12, p. 359–386.
Surlyk, F., 1997, A cool-water carbonate ramp with bryozoan mounds: Late Cretaceous–Danian of the Danish Basin, *in* N. P. James and J. D. A. Clarke, eds., Cool-water carbonates: SEPM Special Publication, 56, p. 293–307.
Taylor, S. R., and J. F. Lapre, 1987, North Sea chalk diagenesis: its effect on reservoir location and properties, *in* J. Brooks and K. W. Glennie, eds., Petroleum geology of north-west Europe: London, Graham and Trotman, p. 483–495.
Ter-Borch, N., 1990, Geological map of Denmark; structural map of top Chalk Group: Geological Survey of Denmark, Map Series, v. 7, scale 1:500,000, 1 map and 2 p.
Terzaghi, K., and R. P. Peck, 1968, Soil mechanics in engineering practice: New York, John Wiley, 729 p.
Thomson, K., and R. R. Hillis, 1995, Tertiary structuration and erosion of the Inner Moray Firth, *in* R. A. Scrutton, M. S. Stoker, G. B. Shimmield, and T. A. W. Tudhope, eds., The tectonics, sedimentation and paleooceanography of the north Atlantic region: Geological Society Special Publication, 90, p. 167–190.
Thorne, J. A., and A. B. Watts, 1989, Quantitative analysis of North Sea subsidence: AAPG Bulletin, v. 73, p. 88–116.
Urmos, J., R. H. Wilkens, F. Bassinot, M. Lyle, J. C. Marsters, L. A. Mayer, and D. C. Mosher, 1993, Laboratory and well-log velocity and density measurements from the Ontong Java Plateau: new in-situ corrections to laboratory data for pelagic carbonates, *in* W. H. Berger, L. W. Kroenke, L. A. Mayer, and T. R. Janecek, Proceedings of the Ocean Drilling Program, scientific results: Ocean Drilling Program, v. 130, p. 607–622.
van Wees, J.-D. and S. Cloetingh, 1996, 3-D flexure and intraplate compression in the North Sea Basin: Tectonophysics, v. 266, p. 343–359.
van Wijhe, D. H., 1987, Structural evolution of inverted basins in the Dutch offshore: Tectonophysics, v. 137, p. 171–219.
Vejbæk, O. V., 1992, Geodynamic modeling of the Danish Central Trough, *in* R. M. Larsen, H. Brekke, B. T. Larsen, and E. Telleraas, eds., Structural and tectonic modeling and its applications to petroleum geology: NPF Special Publication 1, p. 1–17.
Vinken, R., C. H. von Daniels, F. Gramann, A. Koethe, R. W. O. Knox, F. Kockel, K. J. Meyer, and W. Weiss, 1988, The northwest European Tertiary basin; results of the International Geological Correlation Programme Project No. 124: Geologisches Jahrbuch, v. 100, 1065 p.
Watts, N. L., 1983, Microfractures in chalks of Albuskjell field, Norwegian sector, North Sea: possible origin and distribution: AAPG Bulletin, v. 67, p. 201–234.
Whittaker, R. C., N. E. Hamann, and C. Pulvertaft, 1997, A new frontier province offshore Northwest Greenland: structure, basin development, and petroleum potential of the Melville Bay area: AAPG Bulletin, v. 81, p. 987–998.
Wyllie, M. R. J., A. R. Gregory, and L. W. Gardner, 1956, Elastic wave velocities in heterogeneous and porous media: Geophysics, v. 21, p. 41–70.
Zagwijn, W. H., 1989, The Netherlands during the Tertiary and the Quaternary: a case story of coastal lowland evolution: Geologie en Mijnbouw, v. 68, p. 107–120.
Ziegler, P. A., 1990, Geological atlas of western and central Europe: The Hague, Shell International Petroleum Maatschappij B. V., 239 p.

ABOUT THE AUTHOR

Peter Japsen

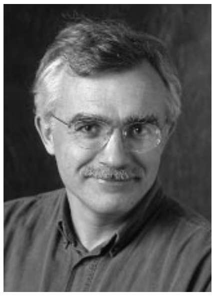

Peter Japsen is a senior research geophysicist at the Geological Survey of Denmark and Greenland, where he has been working with a variety of problems related to exploration and geophysical mapping since 1980. In recent years he has focused on the constraints on basin development that may be drawn from the sonic velocities of sedimentary rocks. He currently is involved in research projects on the rock physics of chalk and on Neogene uplift and tectonics around the North Atlantic.